

#### UNIVERSIDADE FEDERAL DA BAHIA PROGRAMA DE PÓS-GRADUAÇÃO EM ENGENHARIA ELÉTRICA - PPGEE

# A RECEPTANCE-BASED VIBRATION CONTROL WITH DEAD-ZONE COMPENSATION FOR SYSTEMS WITH INPUT DELAY

André Juárez Jaime Duarte

Salvador 2022

#### UNIVERSIDADE FEDERAL DA BAHIA PROGRAMA DE PÓS-GRADUAÇÃO EM ENGENHARIA ELÉTRICA - PPGEE

#### André Juárez Jaime Duarte

# A RECEPTANCE-BASED VIBRATION CONTROL WITH DEAD-ZONE COMPENSATION FOR SYSTEMS WITH INPUT DELAY

MSc dissertation presented to the Graduate Program in Electrical Engineering, Universidade Federal da Bahia, as part of the requirements for obtaining the MSc in Electrical Engineering title.

Advisor: Prof. Dr. José Mário Araújo - IFBA Co-Advisor: Prof. Dr. Tito Luís Maia Santos -UFBA

Salvador 2022

D812 Duarte, André Juárez Jaime.

A receptance-based vibration control with dead-zone compensation for systems with input delay / André Juárez Jaime Duarte. – Salvador, 2022.

102 f.: il. color.

Orientador: Prof. Dr. José Mário Araújo. Coorientador: Prof. Dr. Tito Luís Maia Santos.

Dissertação (mestrado) – Universidade Federal da Bahia. Escola Politécnica, 2022.

1. Vibração - controle. 2. Preditor de Smith. 3. Controle adaptativo. I. Araújo, José Mário. II. Santos, Tito Luís Maia. III. Universidade Federal da Bahia. IV. Título.

CDD: 629.892

#### André Juárez Jaime Duarte

## A RECEPTANCE-BASED VIBRATION CONTROL WITH DEAD-ZONE COMPENSATION FOR SYSTEMS WITH INPUT DELAY

MSc dissertation presented to the Graduate Program in Electrical Engineering, Universidade Federal da Bahia, as part of the requirements for obtaining the MSc in Electrical Engineering title.

**Board of Examiners** 

Prof. Dr. José Mário Araújo
(Advisor - IFBA)

Prof. Dr. Tito Luís Maia Santos (Co-Advisor - UFBA)

Prof. Dr. Acbal Rucas Andrade Achy (UFRB)

Prof. Dr. Thiage Antômo Melo Euzébio (ITV)

Prof. Dr. Tiago Trindade Ribeiro (UFBA)

" Todas as vitórias ocultam uma abdicação." Simone de Beauvoir.

## Dedicatória

Dedico este trabalho a todos aqueles que sempre acreditaram em mim e que de alguma forma me ajudaram ao longo desta caminhada.

### **Agradecimentos**

Agradeço primeiramente a Deus, que nos guia com sabedoria e possibilita alcançar os objetivos e metas que traçamos ao longo da caminhada da vida, nos auxiliando a superar desafios.

À minha família que, de perto ou à distância, me incentiva na busca contínua de conhecimento e crescimento pessoal e profissional. Em especial à minha mãe, que sempre viabilizou esforços para que eu pudesse estudar.

Aos meus orientadores Dr. José Mário Araújo e Dr. Tito Luís Maia Santos, expresso minha gratidão pela disponbilidade de tempo, atenção, dedicação e ensinamentos transmitidos, estando totalmente presentes ao longo desta minha jornada como aluno da Pós-Graduação.

Agradeço aos Professores da banca examinadora, os quais se dispuseram à leitura e avaliação deste trabalho.

Aos professores e colaboradores do Programa de Pós-Graduação em Engenharia Elétrica da Universidade Federal da Bahia, que colocaram à disposição sua atenção e conhecimento, me auxiliando ao longo dessa jornada no decorrer do Programa de Pós-Graduação.

#### Resumo

A presente dissertação apresenta uma nova abordagem para compensação de atraso e de zona morta com parâmetros desconhecidos, ambos na entrada de sistemas de segunda ordem baseados em receptâncias. O modelo de segunda ordem baseado em receptâncias é usado em várias aplicações fundamentais, destacando-se o controle ativo de vibração de sistemas mecânicos vibracionais. A abordagem proposta é baseada em um preditor de Smith filtrado em conjunto com um estimador adaptativo em tempo discreto, ambos modelados em receptâncias, para lidar, respectivamente, com o atraso e zona morta. Através do preditor de Smith filtrado, o erro de predição, relativo às discrepâncias entre modelo nominal e saída futura em regime permanente, tem seu resultado tratado pelo filtro de erro de predição. Este filtro pode ser projetado para atender a um compromisso entre o desempenho de atenuação de perturbações na entrada ou saída do sistema em estudo, bem como atenuar os efeitos oriundos de erros de modelagem e relativos à robustez, além de garantir estabilidade interna para os casos nos quais o modelo é BIBO (bounded-input bounded-output) estável. Dessa forma, o preditor e a compensação de zona morta são usados para permitir que um projeto baseado num sistema linear sem atraso seja usado para controlar um sistema com atraso e zona morta. O tratamento da zona morta é realizado por um algoritmo de estimação adaptativo, que é composto por um observador de perturbação em tempo discreto, que utiliza os sinais de deslocamento, velocidade e esforço de controle para estimar os parâmetros desconhecidos, além da compensação por ação inversa com estratégia anti-chattering. A principal contribuição deste trabalho é combinar um mecanismo adaptativo de zona morta desconhecida e uma compensação de atraso de tempo baseada em receptâncias em um projeto unificado. Alguns exemplos numéricos ilustram a eficácia da abordagem proposta.

**Palavras-chave**: Receptância, Preditor de Smith, Controle de vibrações, atraso no tempo, zona-morta, controle adaptativo.

#### **Abstract**

The present dissertation presents a novel approach for the time delay and the deadzone compensation with unknown parameters, both at the input of second-order systems based on receptances. The second-order model based on receptance is used in several fundamental applications, most notably the active vibration control of mechanical vibrational systems. The proposed approach is based on a filtered Smith predictor in conjunction with a discrete-time adaptive estimator, both modeled on receptances, to deal, respectively, with delay and dead zone. Through the filtered Smith predictor, the prediction error, related to the discrepancies between the nominal model and future steady-state output, has its result treated by the prediction error filter. This filter can be designed to meet a compromise between the attenuation performance disturbances in the input or output of the system under study, as well as to attenuate the effects arising from modeling errors and related to robustness, in addition, to guaranteeing internal stability for cases in which the model is BIBO (bounded-input bounded-output) stable. In this way, predictor and dead-zone compensation are applied to allow a design based on a linear system without delay to be used to control a system with delay and dead zone. The treatment of the dead zone is performed by an adaptive estimation algorithm, which is composed of a disturbance observer in discrete time, which uses the displacement, velocity and the control effort signals to estimate the unknown parameters, in addition to the inverse action compensation, with an anti-chattering strategy. The main contribution of this work is to combine an adaptive unknown dead zone mechanism and a time delay compensation based on receptances in a unified design. Some numerical examples illustrate the effectiveness of the proposed approach.

**Keywords**: Receptance, Smith predictor, Vibration control, Time delay, Dead zone, Adaptive control.

## **Contents**

Su	ımma	ry	ix
Gl	ossar	y	xi
Li	st of S	ymbols	xii
Li	st of l	ligures	xiii
1	Intr	oduction	1
	1.1	Motivations	2
	1.2	Related Works	3
	1.3	Objectives and Contributions	7
	1.4	Master's Dissertation Structure	8
2	Prel	minaries Fundamentals	10
	2.1	Vibrating systems modeled by receptance-based method	10
		2.1.1 Receptance-based formulation	10
		2.1.2 Active vibration control by pole placement methods	14
	2.2	Dead-zone nonlinearity considerations	19
		2.2.1 Limit cycle prediction	22
	2.3	Continuous-time filtered Smith predictor for receptance systems .	23
		2.3.1 Receptance-based filtered Smith predictor	24
	2.4	Discrete-time filtered Smith predictor for receptance systems	27
		2.4.1 Discrete-time prediction based on FSP	27
		2.4.2 State-feedback control law	29
		2.4.3 Considerations about pole placement problem	30
3	Filte	red Smith predictor with dead-zone compensation	31
4	Rec	eptance-based discrete-time observer for adaptive compensation	36
	4.1	Dead-zone adaptation mechanism	38
	4.2	Numerical examples	40
		4.2.1 Test case I: a marginally stable vibrating system	40
		4.2.2 Test case II: a multiple-input marginally stable vibrating	
		system	51

	4.2.3	Test case III: a two-link robot arm	58
	4.2.4	Test case IV: the 3-DoF asymmetric system flutter sup-	
		pression case	64
5	Concludin	g remarks and future works	71
Bi	bliography		74
A	Describing	g function representation	80
В	Continuou	s and discrete-time FSP filters design	82
	B.1 Conti	nuous-time FSP filter design	82
	B.2 Discr	ete-time FSP filter design	83
C	UIO conve	ergence analysis	85

## Glossary

BIBO Bounded-Input Bounded-Output

**DF** Describing Function

**DTC** Dead-Time Compensator

**DoF** Degree-of-Freedom

**FSP** Filtered Smith Predictor

MIMO Multiple-Input Multiple-Output

**PQVEAP** Partial Quadratic Eigenvalue Assignment Problem

**SP** Smith Predictor

UIO Unknown Input-Output Observer

**ZOH** Zero-Order Holder

## **List of Symbols**

```
A \succ 0
           Matrix A is positive-definite.
           Matrix A is positive semi-definite.
A^{T}
           Transpose of a matrix A.
A^{-1}
           Inverse of a matrix A.
||A||
           Euclidian-norm of a matrix A.
||A||_{\infty}
           Infinity norm of a matrix A.
A^{+}
           Moore-Penrose or pseudoinverse of a matrix A.
det(A)
          Determinant of a matrix A.
\{\lambda \mathbf{v}\}\
           Eigenpair for open-loop eigenvalue \lambda and eigenvector \mathbf{v}.
          Eigenpair for closed-loop eigenvalue \lambda and eigenvector w.
\{\mu \ \mathbf{w}\}
\gamma_i(\circ)
           Dead-zone compensation function for i-th element.
           Dead-zone nonlinearity function for i-th element.
\rho_i(\circ)
           Identity matrix.
\mathbb{N}
           Set of natural numbers.
           Set of real numbers.
\mathbb{R}^{n \times m}
           Set of real-valued matrices with n rows and m columns.
           Saturation non-linearity function for i-th element.
sat_i(\circ)
           i-th element of vector x.
x_i
          time derivative \frac{dx}{dt}.
х
\mathbf{x}[k]
           Zero-order hold discretized signal of the continuous-time signal x(t).
\mathbf{X}(s)
          Laplace transform of a continuous-time signal x(t).
\mathbf{X}(z)
           Unilateral Z-transform of a continuous-time signal x(t).
```

Function composition operation.

## **List of Figures**

2.1	Receptance-based system with full-state feedback control representation.	11
2.2	Representation of the dead-zone nonlinearity - single-input case	20
2.3	Input and output signals under dead-zone nonlinearity influence.	21
2.4	Basic schema for describing functions method analysis	21
2.5	Graphical representation for dead-zone describing function	22
2.6	Schematic representation of the closed-loop system with continuous-	
	time FSP.	25
2.7	Schematic representation of the closed-loop system with discrete-	
	time FSP	29
3.1	Schematic description of the dead-zone inverse compensation strat-	
	egy based on saturation nonlinearity	32
3.2	Schematic representation of the FSP approach with dead zone at input of the system	33
3.3	Equivalent schematic representation of the linear delayed system	
	with bounded disturbance and FSP compensation	34
3.4	Equivalent schematic representation of the linear delayed system	
	with bounded disturbance and discrete-time FSP compensation	35
4.1	Receptance-based discrete adaptive estimator scheme	39
4.2	Displacement and velocity responses in the test case I with dead-	
	zone nonlinearity and no time delay	42
4.3	Displacement responses in test case I with dead zone and no time	
	delay: (A) UIO approach dead-zone compensation. (B) Adaptive scheme by [15] for dead-zone compensation	42
4.4	scheme by [15] for dead-zone compensation	42
4.4	delay compensation	43
4.5	Displacement responses in test case I: (A) $\mathbf{F}_2$ and $\mathbf{G}_2$ matrices	13
т.Э	designed for time delay $\tau = 5s$ and adaptive scheme [15]. (B) FSP	
	and adaptive scheme [15]	44
4.6	Displacement responses $x_1$ and $x_2$ for Test case I with the FSP	
	and UIO adaptive dead-zone compensation approach for several	
	dead-zone initial values	44

4.7	Velocity responses $v_1$ and $v_2$ for Test case I with the FSP and UIO adaptive dead-zone compensation approach for several dead-zone	
	initial values.	45
4.8	Dead-zone estimation parameters under UIO approach for several	45
4.0	dead-zone initial values in Test case I	
4.9 4.10	Closed-loop with dead-zone influence. (B) Closed-loop system with FSP and UIO discrete observer dead-zone compensation ap-	46
	proach	47
4.11	Displacement and velocity responses in the test case I with modeling error for receptance matrices and time delay	47
4.12	Displacement responses in the test case I with modeling error for <b>M</b> matrix: (A) For $\alpha_M = -0.20$ ; (B) For $\alpha_M = +0.20$	48
4.13	Displacement responses in the test case I with modeling error for	
4.14	C matrix: (A) For $\alpha_C = -0.25$ ; (B) For $\alpha_C = +0.25$ Displacement responses in the test case I with modeling error for	48
	<b>K</b> matrix: (A) For $\alpha_K = -0.25$ ; (B) For $\alpha_K = +0.25$ Displacement responses in the test case I with modeling error for	49
	time delay $\tau$ : (A) For $\alpha_r = -0.08$ ; (B) For $\alpha_r = +0.08$	49
4.16	Noise signals in the test case I for displacement and velocity measurements	50
4.17		50
4.18	Dead-zone estimation parameters under the proposed approach	
<b>Л</b> 10	and additive noise for the system in Test case I	51
т.17	case II	52
4.20	Phase portrait plane under dead-zone influence, for the system in Test case II	52
4.21	Dead-zone estimation parameters under the proposed approach for the system in Test case II	53
4.22	Time-domain response with FSP and UIO discrete observer ap-	
4.23	proach for the system in Test case II	53
	in Test case II	54
4.24	Closed-loop control effort for the system in Test case II, with FSP and UIO discrete observer dead-zone compensation approach	54
4.25	Estimation signals $\omega_1$ and $\omega_2$ for discrete observer for the system of Test case II	55
4.26	Displacement responses $x_1$ and $x_2$ for Test case II with the FSP	<i>J J</i>
	and UIO adaptive dead-zone compensation approach for several dead-zone initial values	55

4.27	Velocity responses $x_1$ and $x_2$ for Test case II with the FSP and UIO adaptive dead-zone compensation approach for several dead-zone	<b>7.</b> C
4.20	initial values.	56
4.28	Displacement and velocity responses in the test case II with mod-	
	eling error and additive noise	56
4.29	Dead-zone estimation parameters under the proposed approach for the system in Test case II with modeling error and additive	
4.20	noise.	57
4.30	The two-link flexible robot arm and its kinematic scheme [2] for Test case III	58
4.31	Time-domain responses with FSP and UIO discrete observer ap-	
	proach for the system in Test case III: (A) Displacement; (B)	
	Closed-loop control effort	59
4.32	Dead-zone estimation parameters under the proposed approach	
	for the system in Test case III	60
4.33	Dead-zone estimation parameters under the proposed approach	
	and additive signal for the system in Test case III	60
4.34	Time-domain responses with FSP and UIO discrete observer ap-	
	proach for the system in Test case III: (A) Displacement; (B)	
	Closed-loop control effort	61
4.35	Time-domain responses with FSP and UIO discrete observer ap-	
	proach for the system in Test case III: (A) Displacement; (B)	
	Closed-loop control effort	61
4.36	Dead-zone estimation parameters under the proposed approach	
	for the system in test case III	62
4.37	Time-domain responses with FSP and UIO discrete observer ap-	
	proach and modeling error for the system in test case III	62
4.38	Displacement responses with FSP and UIO discrete observer ap-	
	proach and modeling error in the test case III: (A) $\alpha_M = \alpha_C =$	
	$\alpha_K = -0.25$ and $\alpha_r = 0$ ; (B) $\alpha_M = \alpha_C = \alpha_K = +0.25$ and $\alpha_r = 0$ ;	63
4.39	Displacement responses with FSP and UIO discrete observer ap-	
	proach and modeling error in the test case III: (A) $\alpha_M = \alpha_C =$	
	$\alpha_K = 0.0$ and $\alpha_r = -0.19$ ; (B) $\alpha_M = \alpha_C = \alpha_K = +0.0$ and $\alpha_r =$	
	$+0.20; \ldots \ldots$	63
	Nyquist diagram for the system in Test case IV	65
4.41	Dead-zone amplitude analysis for the Test case IV. (A) Control	
	effort $\mathbf{v}(t)$ . (B) Describing function dead-zone curve $N(A)$	66
4.42	Dead-zone estimation parameters under the proposed approach	
	for the system in test case IV	67
4.43	Displacement and velocity responses with the proposed approach	
	for the system in test case IV	67
4.44	Displacement and velocity responses with the proposed approach	
	and modeling error in the test case IV	68

4.45	Time-domain responses with FSP and UIO discrete observer approach for the system with modeling error in Test case IV: (A)	
	Closed-loop control effort; (B) UIO dead-zone estimation signal	68
4.46	Closed-loop control effort responses with FSP and UIO discrete	
	observer approach for the system with modeling error in Test case	
	IV: (A) $\alpha_M = -0.10$ (B) $\alpha_M = +0.20$	69
4.47	Displacement responses with FSP and UIO discrete observer ap-	
	proach for the system with modeling error in Test case IV: (A)	
	$\alpha_C = -0.25$ (B) $\alpha_C = +0.25$	69
4.48	Displacement responses with FSP and UIO discrete observer ap-	
	proach for the system with modeling error in Test case IV: (A)	
	$\alpha_{\nu} = -0.15$ (B) $\alpha_{\nu} = +0.15$	70

## **Chapter 1**

#### Introduction

The closed-loop control of mechanical systems, described by second-order models, which can effectively represent several real control problems, such as the active control of mechanical vibrations, oscillations in electrical networks and vibroacoustic phenomena, among others, has received increasing attention due to its relevance in practice [1], [2]. In this kind of systems, state feedback control is implemented by using state measurements, which provide useful properties for analysis and synthesis purposes [3]. The receptance - also called the frequency response - is the transfer matrix that relates the input and output of a linear mechanical system, which is subject to harmonic forces as input [4]. The secondorder-based approaches' benefits have been reported in remarkable related works [5], [6], in which the design and control of the second-order system based on the receptance approach have been widely used because the receptance model can be obtained experimentally without the necessity of the knowledge of the mass, stiffness and damping matrices in some cases. Besides, it is possible to perform the total or partial allocation of poles and zeros, as shown in [7], including the influence and analysis of the influence of the time delay [5], [8].

As presented in [9], [10] and several related works, time delay introduces adverse effects in control systems, such as the effects of disturbances are not noticed until the delay has elapsed; the effects of the control action take some time to be noticed on manipulated variables of the system and the control action, based on current information, tries to correct a situation that happened in the past. Thus, a solution to deal with the time-delay effect can be obtained through the use of controllers with time-delay compensation (DTC). The first DTC was proposed in [11], known as Smith predictor (SP). However, it should be noted that the SP

cannot be used in open-loop unstable processes, and the disturbance rejection responses depend on the open-loop poles. Thus, a modified structure based on SP is proposed in [9], [10], [12], [13], called filtered Smith predictor (FSP), in which a filter is used in the prediction error, allowing adjustments to provide closed-loop robustness, noise attenuation and disturbance rejection. It can also be used for processes with unstable open-loop poles [5], [12], [14].

In practice, systems present significant nonlinearities, such as the dead zone (also named free-play) and saturation, among others, generally when activated within a control system [15], [16]. The dead-zone nonlinearity can occur in pneumatic, piezoelectric, and hydraulic actuators (robot manipulators [17], fast-tool servos [18], among others), having several unwanted effects on control systems and degrading control accuracy. They can also lead to limit cycles or system instability, even in closed-loop, and may be accompanied by saturation [18], [19]. Besides, it is known that for dynamical systems affected by the dead zone, the stability and control system design in closed-loop control systems are important research topics in control theory. The parameters that describe the characteristics of the dead zone may not be accurately known, and such inaccurate information about the dead zone can lead to undesired dynamic performance or instability of closed-loop dynamic systems [19]–[21]. The study of adaptive control for systems subject to dead-zone nonlinearity in actuators using an inverse function to tackle its effects is addressed in classical works [15], [21], [22]. Several approaches for adaptive control with performance and robustness trade-offs have been reported, including those involving nonlinear systems, with the use of a stability evaluation via Lyapunov sense [22]-[24] to delimit candidate functions which will make the systems under evaluation locally stable. This conception often can increase the complexity in the mathematical treatment of the algorithms for adapting the parameters of the functions and the dead-zone and time-delay uncertainties, combined or not, which can become a challenge for practical applications.

#### 1.1 Motivations

The compensation of nonlinearities, such as the dead zone, has been widely discussed and addressed in applications involving linear and nonlinear systems,

with an approach through adaptive techniques and evaluation regarding stability and robustness [25], [26]. The dead-zone nonlinearity is increasingly present in electrical, hydraulic and pneumatic equipment, among others, due to technological development, offering a great range of resources to end-users, which requires solutions for mathematical treatment, aiming to mitigate its effects [27], [28].

In several works about receptances, a great concern is demonstrated in the improvement of techniques of partial and total allocation of marginally stable or unstable poles and zeros through the state feedback matrices [7], [29], aiming to eliminate the closed-loop instability that can be potentiated in the presence of time delay [5], [8] or even perform the treatment of eigenvalues that represent an unstable behavior of the system [6], [30], along with its frequency response. However, aspects about the presence and influence of dead zones or other associated nonlinearities, as well as time delay, on the systems represented by receptances, are not addressed in numerical simulation works or practical experiments.

Thus, the negative effects of input delay and dead-zone, both at the input of system, motivate the combined development of a filtered Smith predictor [5], [6], [14] and an adaptive nonlinear dead-zone compensator for accurate estimation of the uncertain parameters inherent for unknown dead zone. The main objective is to achieve the performance requirements such as robustness and disturbance rejection based on a project for a linear model without delay.

#### 1.2 Related Works

In continuity with the concepts related to the mathematical theory of vibration absorption presented in [4], Mottershead and Ram presented in [3] the method for pole/zero assignment for state feedback in active vibration suppression based on measured receptance, where the pole or zero assignment problem uses the characteristic polynomial of closed-loop receptance matrix obtained from Sherman-Morrison formula, which gives the inverse of a matrix with a rank-1 modification in terms of the inverse of the original matrix. In [31], [32], the same concepts and formulation are applied for time delay at the input of receptance-based system for partial pole placement, without spillover. The active vibration control for multiple-input multiple-output (MIMO) system by partial pole placement is intro-

duced in [7], where the mathematical formulation considers the quadratic eigenvalue problem based on eigenvalues and eigenvectors of the system, for changing the undesirable open-loop poles to a given new position, keeping unchanged the remaining open-loop poles. An experimental extension related to results obtained from [7] is described in [33] and in [34] is presented a strategy for multi-input control from measurement output feedback (acceleration, velocity and displacement) systems, where control law is composed by gain matrices aiming to obtain realisable control gains. In [35], [36], the partial pole assignment for asymmetric receptance-based systems is presented for a friction-induced vibration problem, also studied in [29], where uncontrollability condition is used. Also, in [37], an output feedback-linearisation theory is presented for the treatment of nonlinear vibration problems (friction-induced vibration system, viscous damping) by a receptance-based approach, investigating the stability of the zero dynamics. In [38], active vibration control by receptance-based method for a nonlinear system (Duffing oscillator) is explained, where an iterative Sherman-Morrison method is used to reassign complex poles. Practical applications for feedback linearisation and receptance method for non-smooth nonlinearity in a lumped mass system with a piece-wise linear spring is described on [1], [39]. In [2], a practical implementation is described based on method for active vibration control, for a two-link flexible robot arm in the presence of time delay, by means of robust pole placement and Nyquist stability criterion for stability margin. Some works address the concepts of sensitiveness and robustness for state and derivative feedback designs for symmetrical [40] and asymmetrical systems [41], whereas in [42] the proposed approach needs only of the system and closed-loop feedback matrices for partial quadratic eigenvalue assignment problem (PQVEAP) in active vibration control.

Related to works about time delay and its compensation (also known dead-time compensation, DTC), two relevant articles about the design of feedback control in second-order symmetric and asymmetric linear involving receptance-based systems under long input time delay are described in [5], [6]. In [5], a filtered Smith predictor (FSP) is applied to compensate time delay by providing a nominal characteristic polynomial without delay. The prediction is obtained by employing the receptance approach in the conception of the predictor, and thus the design is fully made at the frequency domain. The proposal uses a filtered prediction error

which can be applied to attenuate the undesired effect of the poorly damped eigenvalues and ensure the internal stability of the marginally stable case, dealing with the compromise between performance and robustness. In [6], a discrete-time FSP version is proposed for asymmetrical receptance-based systems to deal with unstable second-order systems, an issue in friction-induced vibration and aeroelastic systems. Among the applications of FSP for systems subject to input nonlinearities, in [14], a structure using FSP for inputs represented by nonlinear functions is proposed. The results have demonstrated that the filtered prediction strategy for systems with input nonlinearity and delays can be used to meet a compromise between robustness, internal stability, and perturbation rejection as in the linear FSP presented in [13]. The use of the filtered Smith predictor has been recently addressed, as can be seen in practical applications described in [43], [44], in addition to works that propose modified prediction structures for handling higher time delays [14], [45] and in open-loop unstable plants [46]. The use of the small-gain theorem to evaluate the stability criteria for time delays is described in [47]. The analysis of noise influence in DTCs for unstable processes is described in [48], where the FSP approach is analyzed to consider noise attenuation.

Relevant works deal with dead-zone nonlinearity and its mathematical modeling [49]–[51] by describing functions, highlighting the Nyquist criterion's frequency domain to evaluate the stability of systems under the dead-zone or other nonlinearities, such as friction, backslash phenomena, among others. In [52], [53], a receptance-based limit cycle prediction method based on describing functions (DF) and Sherman-Morison formula is proposed for dealing with nonlinear structures. Also, with representing the nonlinearity via DFs, the nonlinear active control theory using measured receptance is developed without the presence of time delay. In [38], is presented an application of the receptance method to nonlinear systems for active vibration control characterised using DF.

Classical approaches about adaptive control for systems subject to dead-zone actuators, using an adaptive dead-zone inverse function to minimize the effects of dead-zone, both symmetrical or asymmetrical, are presented in [21], [22], where this approach is applied in a model reference adaptive control to include controls of unknown system with an unknown dead zone. Also, in [15], the adaptive dead-zone mitigation is also presented, but is assumed that both the input and

output of the dead zone are available for measurement, which is not always an affordable condition. It is important highlight that, in [15], [21], [22], the chattering mitigation on its solution and also time delay is not considered. Besides, some approaches to reach a compromise between performance and robustness are presented, including those involving nonlinear systems, according to the works recently developed in [17], [23], which use the stability evaluation via Lyapunov sense criterias [54], which is also conceptually applied in [21], [22], to delimit candidate functions which will make the systems under evaluation stable in certain convergence regions, where this conception increases at great amount the complexity in the mathematical treatment of the algorithms for adapting the parameters of the functions and the dead-zone and time delay uncertainties, combined or not. In a similar way, in [26], an active disturbance rejection control by an extended state observer is designed for nonlinear systems to estimate deadzone input and external disturbances, by using of an output feedback linearization control, where its stabilty proof is also performed by Lyapunov theory. It is also important to highlight that in [17], [20] and [55], techniques for estimating the parameters of the dead-zone, the nonlinear systems under study, and the uncertainties in the perturbations on the systems are also used, but focused on deadzone nonlinearity. In [27], an adaptive control to deal with the dead-zone and time delay issues in actuators was proposed, based on a type-2 fuzzy neural network integrating using a Riccati-like equation. In [56], an adaptive fuzzy neural network was proposed for electric-hydraulic systems, also considering a nonlinear system and with the asymmetric dead-zone, in order to solve the reference tracking problem [55]. In [20], an adaptive controller approach for flutter and free-play suppression in an aeroservoelastic system modeled by receptance representation, is presented, but no time delay is considered. In [23], results for nonlinear systems defined via Lyapunov-Krasovskii sense are presented, considering the dead-zone as asymmetric and variable time delay in the reference tracking situation, but not dealing with the performances in the transient regime and delay mitigation, establishing on its analysis only boundary conditions for time delay. In a recent work, [18], a practical application is presented using a proposal with the Smith predictor and anti-windup mechanism, for saturation compensation with inverse dead-zone and time delay uncertainties, for high-speed servo-mechanical systems represented by modeling second-order linear. In [28], an adaptive approach based on an output tracking problem is considered for a class of uncertain nonlinear systems but only considering non-symmetric unknown dead-zone input. In [24] (and the references therein), an adaptive control scheme is applied to uncertain time-delay systems with non-symmetric dead-zone input and any information on the dead-zone input is not required to be known. Hence, it is possible to consider that, as also highlighted in [18], the adaptive methods proposed in the control literature on dynamical systems with uncertain input dead-zone (with or without delays) are not as simple as the control strategies for undelayed linear systems.

#### 1.3 Objectives and Contributions

This work aims to propose an approach to deal with time delay and unknown asymmetric dead-zone at the input of receptance-based systems for active vibration control, where is considered, in the same design, the identification and dealing of unknown dead-zone nonlinearity and mitigation of long time delay, both for receptance-based systems, which is a benchmark for mechanical vibrating second-order systems.

In this way, the main control challenges can be summarized as follows: (i) The active vibration control should be performed by a typical receptance-based pole placement, where the control law is obtained from a linear combination of the displacement and velocity of the system (state feedback control) (ii) The filtered Smith predictor should be used in order to preserve closed-loop stability in the presence of delay despite the pole placement based on an undelayed model and the infinity dimensional nature of the closed-loop characteristic polynomial. The main benefit of the receptance-based filtered Smith predictor comes from the fact that the feedback gains can be designed to control a delayed second-order system based on a delay-free receptance model. This simplifying concept is now explored in the presence of uncertain input dead-zones combined with delays; (iii) The unknown dead-zone nonlinearity at the input of the system should be compensated based on two estimated break-point parameters in order to achieve steady-state convergence.

In this dissertation, the main contributions are: (i) the use of filtered Smith predictor approach proposed in [5], [6], which is modeled by receptance, which

considers active vibration control and long time delay compensation; (ii) associated with this FSP approach, an adaptive inverse dead-zone compensation scheme is added, whose unknown dead-zone bounds parameters will be dynamically estimated through a discrete-time unknown input observer - UIO - based on state vector from the system (displacement and velocity) and the feedback control law signal, calculated directly from state vector; (iii) the dead-zone inverse compensation strategy to be proposed provides chattering mitigation; (iv) the BIBO stability is addressed, where an equivalent linear bounded signal disturbance can represent the approximated dead-zone nonlinear compensation. Simulation test cases are presented to illustrate the benefits of the proposed strategy.

#### 1.4 Master's Dissertation Structure

This dissertation is organized as follows:

- Chapter 2 is dedicated to the presentation of theoretical concepts. In item 2.1 addresses relevant aspects of the representation of vibrating systems by receptance matrix and partial pole assignment for active control vibration in single-input and multi-input systems. In item 2.2, the main theoretical concepts about dead-zone nonlinearity in control systems are presented, concerning its modeling and stability analysis through describing function method. In item 2.3, the relevant considerations about receptance-based symmetric linear systems time-delay compensation using the filtered Smith predictor approach is presented. In item 2.4, the considerations about the sampled-data version approach using filtered Smith predictor to control second-order receptance-based asymmetrical systems are presented, where the approach to dealing with unstable eigenvalues and time delay is high-lighted.
- On Chapter 3, is presented the conceptual aspects of receptance-based filtered Smith predictor with the dead-zone compensation approach to jointly dead with time delay and dead-zone nonlinearity, extending its application for both continuous and discrete time domain. Here are presented considerations about BIBO stability for the proposed approach.

- On Chapter 4, the receptance-based discrete-time unknown input observer
   UIO for adaptive dead-zone compensation approach is presented, where its mathematical formulation about adaption mechanism is detailed. Simulation case studies are presented to illustrate the benefits of the proposed strategy.
- On Chapter 5, is presented the concluding remarks conclusion of the proposed approach in this work for the mitigation of long time delay and unknown dead-zone nonlinearity. Some suggestions for future work related to the topic are also presented in this chapter.
- Appendix A contains the general mathematical description for describing function representation. Appendix B details the computation of continuoustime and discrete-time domain error prediction scalar filters, respectively. Appendix C contains the convergence analysis for unknown input observer for adaptive dead-zone compensation illustrated in Chapter 4.

### Chapter 2

#### **Preliminaries Fundamentals**

This chapter presents the preliminary concepts used in the proposed approach. Initially, the background to define receptance-based models is presented. Later, topics about dead-zone nonlinearity and its describing functions are presented. Finally, the filtered Smith predictor in the continue and discrete-time domain modeled by receptance-based systems is presented.

## 2.1 Vibrating systems modeled by receptance-based method

#### 2.1.1 Receptance-based formulation

Consider second-order linear systems in the form:

$$\mathbf{M}\ddot{\mathbf{x}}(t) + \mathbf{C}\dot{\mathbf{x}}(t) + \mathbf{K}\mathbf{x}(t) = \mathbf{f}(t), \tag{2.1}$$

where  $\mathbf{M}$ ,  $\mathbf{C}$ ,  $\mathbf{K} \in \mathbb{R}^{n \times n}$  are, respectively, the mass, damping and stiffness matrices,  $\mathbf{M} \succ 0$ ,  $\mathbf{C} \succeq 0$ ,  $\mathbf{K} \succ 0$ ,  $\mathbf{x}(t) \in \mathbb{R}^n$  is the displacement vector and  $\mathbf{f}(t) \in \mathbb{R}^n$  is an external vector force. A matrix  $\mathbf{B} \in \mathbb{R}^{n \times m}$  is defined as the influence matrix that represents the actuator configuration, where  $\mathbf{f}(t)$  is given then as follows:

$$\mathbf{f}(t) = \mathbf{B}\mathbf{u}(t - \tau) + \mathbf{d}(t). \tag{2.2}$$

The full-state feedback control law  $\mathbf{u}(t-\tau) \in \mathbb{R}^m$ , considering time delay  $\tau > 0$  at the input of the system, is typically defined by:

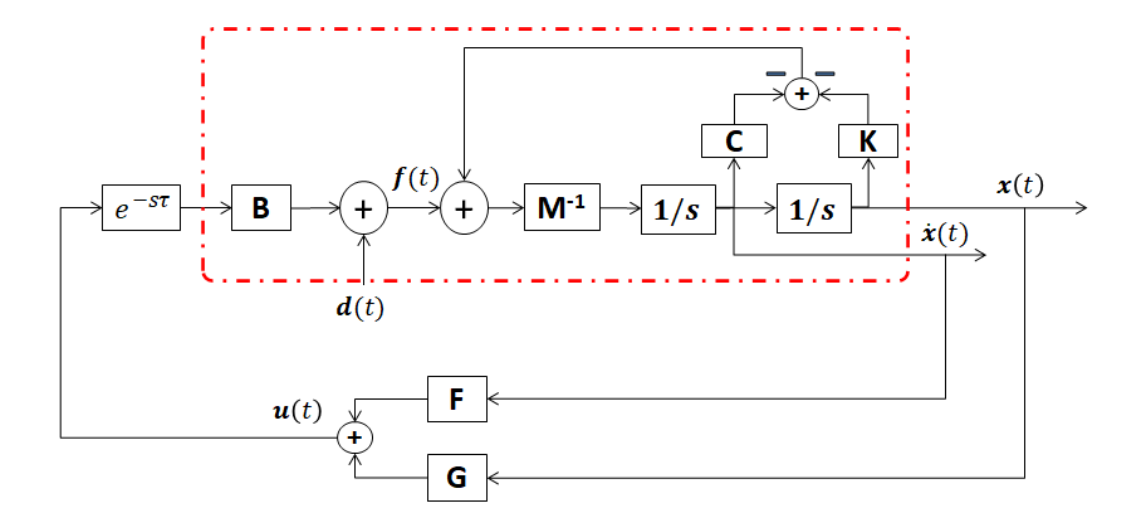


Figure 2.1: Receptance-based system with full-state feedback control representation.

$$\mathbf{u}(t-\tau) = \mathbf{F}\dot{\mathbf{x}}(t-\tau) + \mathbf{G}\mathbf{x}(t-\tau), \tag{2.3}$$

where  $\mathbf{F} \in \mathbb{R}^{m \times n}$  and  $\mathbf{G} \in \mathbb{R}^{m \times n}$  are the feedback gain matrices, designed to provide a specific closed-loop performance. The control law is obtained from a linear combination of the state of the system, i.e., the position and the velocity of the various degrees of freedom,  $\mathbf{d}(t) \in \mathbb{R}^{n \times m}$  is a bounded external disturbance. The receptance-based system with full-state feedback control representation is displayed in Fig.2.1. It should be noted that each nonzero term in  $\mathbf{B}$  implies the use of an actuator and each nonzero term in  $\mathbf{F}$  or  $\mathbf{G}$  implies the use of a sensor [3], [57]. Combining (2.1), (2.2), (2.3) and taking its unilateral Laplace Transform, the closed-loop dynamical law, for  $\mathbf{d}(t) = 0$  is given by:

$$[\mathbf{M}s^2 + (\mathbf{C} - \mathbf{B}\mathbf{F}e^{-s\tau})s + (\mathbf{K} - \mathbf{B}\mathbf{G}e^{-s\tau})]\mathbf{X}(s) = 0$$
 (2.4)

The open-loop receptance or simply receptance  $\mathbf{H}(s)$  is defined by:

$$\mathbf{H}(s) = (\mathbf{M}s^2 + \mathbf{C}s + \mathbf{K})^{-1}.$$
 (2.5)

where this type of representation is relevant because the second-order linear model can be directly obtained from an experimental data-set (so called modal test), that is, it is not necessary to evaluate or to know the structural, **M**, **C**, **K** matrices. Besides, as highlighted in [7], there is no requirements for model reduction and for the using of an observer to achieve state variables. Also, it is important to note that [7]: (i) it is not needed to place a sensor at each degree of freedom of the system, where the number of sensors can be defined by the number of pairs of complex-conjugated poles to be exactly assigned; (ii) in principle, all the poles of the system can be assigned using a single actuator [31]; (iii) this description is useful for high-dimension systems [3], [4] and it can be directly used to derive the control law.

The closed-loop receptance matrix of a system under full state feedback control law described in 2.4 can be expressed in terms of the original open-loop receptance  $\mathbf{H}(s)$ , by using the Matrix Inversion Lemma as follows:

$$\hat{\mathbf{H}}(s) = \{\mathbf{H}(s)^{-1} - \mathbf{B}[s\mathbf{F} + \mathbf{G}]e^{-s\tau}\}^{-1} 
= \mathbf{H}(s) + \mathbf{H}(s)\mathbf{B}\{\mathbf{I} - [s\mathbf{F} + \mathbf{G}]e^{-s\tau}\mathbf{H}(s)\mathbf{B}\}^{-1}[s\mathbf{F} + \mathbf{G}]e^{-s\tau}\mathbf{H}(s)$$
(2.6)

where  $\mathbf{I} \in \mathbb{R}^{n \times n}$  is the identity matrix. The  $\hat{\mathbf{H}}(s)$  representation is equivalent to the Sherman-Morrison formula [3], [57] with multiple inputs and without delay and  $\{\mathbf{I} - [s\mathbf{F} + \mathbf{G}]\mathbf{H}(s)\mathbf{B}e^{-s\tau}\}^{-1}$  is the closed-loop characteristic equation, whose dimension is defined by the number of inputs m instead of the state dimension n, which may be relevantly smaller than the system dimension [6].

Additionally, the unilateral Laplace Transform for the displacement vector can be expressed by:

$$\mathbf{X}(s) = \mathbf{e}^{-s\tau}\mathbf{H}(s)\mathbf{B}\mathbf{U}(s) + \mathbf{W}(s)$$
 (2.7)

The effect of the initial conditions and external disturbances  $\mathbf{W}(s)$  is described as:

$$\mathbf{W}(s) = \mathbf{H}(s)[(\mathbf{M}s + \mathbf{C})\mathbf{x}(0) + \mathbf{M}s\dot{\mathbf{x}}(0)] + \mathbf{H}(s)\mathbf{D}(s)$$
(2.8)

In the next subsection, the receptance-based representation for asymmetrical systems will be presented.

#### 2.1.1.1 Receptance-based representation for asymmetrical systems

In general, the equations of motion of discretized linear vibration systems under conventional loads have symmetric mass, stiffness, and damping matrices. However, when some internal forces are presented, such as friction and aerodynamic load, these system matrices can be asymmetric. Examples can be found in [6], [41]. In a dynamics context, they are self-excited vibrations and susceptible, for example, to flutter instability. The flutter is a class of vibrations induced by non-conservative forces when occurs relative motion between flexible structures and air [58]. Besides, for the system in which the vibration is generated by friction force, the symmetry of the stiffness matrix or damping matrix, or both, are violated. These asymmetric systems are prone to dynamic instability as a result of some of the eigenvalues being on the right-half-side of the complex plane [29], [41].

For asymmetrical receptance-based systems, the **K** and **C** symmetrical matrices can be rewritten by  $\mathbf{K} = \mathbf{K}_s + \mathbf{K}_{as}$  and  $\mathbf{C} = \mathbf{C}_s + \mathbf{C}_{as}$ , where  $\mathbf{C}_s = \mathbf{C}_s^T$  and  $\mathbf{K}_s = \mathbf{K}_s^T$  are, respectively, the damping and stiffness matrices that contain symmetrical components and  $\mathbf{C}_{as} \neq \mathbf{C}_{as}^T$  and  $\mathbf{K}_{as} \neq \mathbf{K}_{as}^T$  are the asymmetrical components for damping and stiffness, respectively. Considering that at least the asymmetrical parts  $\mathbf{C}_{as}$  and  $\mathbf{K}_{as}$  are known, then the full system open-loop receptance  $\mathbf{H}(s)$  with the asymmetrical parts, is given by [59]:

$$\mathbf{H}(s) = (\mathbf{M}s^2 + \mathbf{C}_s s + \mathbf{K}_s + \mathbf{C}_{as} s + \mathbf{K}_{as})^{-1}$$
(2.9)

and applying the inversion lemma in  $\mathbf{H}(s)$ :

$$\mathbf{H}(s) = [\mathbf{I} + \mathbf{H}_s(s)(\mathbf{C}_{as}s + \mathbf{K}_{as})^{-1}]\mathbf{H}_s(s)$$
 (2.10)

where the  $\mathbf{H}_s(s)$  is the open-loop receptance for the symmetrical term. It is relevant to point out that  $\mathbf{H}(s)$  is difficult to measure in practice. So, the representation of  $\mathbf{H}(s)$  in terms of  $\mathbf{H}_s(s)$  is valid, such that  $\mathbf{H}_s(s)$  is easier to measure.

In a similar way to symmetrical case, the closed-loop receptance  $\hat{\mathbf{H}}(s)$  for asymmetrical system, including the time delay, can be expressed by 2.6, where it is possible to note that the characteristic equation in the last equation presents a similar formulation, compared to the symmetrical case, which allows applying pole placement techniques based on symmetrical matrices that composes the receptance  $\mathbf{H}_s(s)$ . In this dissertation, the asymmetrical representation will be applied in a discrete-time filtered Smith predictor, described in a subsequent chapter.

In the next subsection, it will be presented the pole placement methods for single and multiple input systems based on state feedback control.

#### 2.1.2 Active vibration control by pole placement methods

The dynamics of the vibrating systems are naturally governed by second-order differential equations. In practice, the vibration control problems are formulated in a state-space form leading to systems of second-order differential equations, and several pole assignment techniques exist to achieve pole placement in state-space setting [60]. Besides, undesirable vibration generated from machines and natural sources may lead to degradation of machine performances, failure of structures, among others. It can be reduced in many ways. One of them, the active pole assignment based on receptance modeling, is to shift natural frequencies away from the excitation frequencies to avoid resonances and/or to add damping to prevent excessive vibration, as presented in [32], [57] and references therein.

#### 2.1.2.1 Full pole placement method

The full pole placement method based on receptance representation, where the all eigenvalues need to be reassigned to predetermined values, was presented in [3], [57]. For this, considering the eq.(2.6), the characteristic polynomial of the closed-loop system can be rewritten by  $\mathbf{I} - (\mathbf{G} + \mathbf{F}s)\mathbf{H}(s)\mathbf{B}e^{-s\tau}$ , and the problem of assigning the poles of the system to predetermined values  $\mu_1$ ,  $\mu_2$ , ...,  $\mu_{2n}$  may be expressed as follows: given  $\mathbf{M}$ ,  $\mathbf{C}$ ,  $\mathbf{K}$ ,  $\mathbf{B}$ , and 2n required eigenvalues  $\mu_k$ , k = 1, 2, ..., 2n, where  $n \in \mathbb{N}^*$  is the order of the system, find the control vectors  $\mathbf{F}$  and  $\mathbf{G}$  such that the 2n given values  $\mu_k$  are eigenvalues of the closed-loop system, i.e.:

$$[\mathbf{H}(s)\mathbf{B}]^T(\mathbf{G}^T + \mathbf{F}^T s) = \mathbf{I}e^{s\tau}$$
 (2.11)

where, to solve this problem, is possible to define:

$$\mathbf{r}_k^T = [\mathbf{H}(s_k)\mathbf{B}]^T \tag{2.12}$$

and eq.(2.11) can be defined by:

$$\begin{bmatrix} \mathbf{r}_{1}^{T} & s_{1}\mathbf{r}_{1}^{T} \\ \mathbf{r}_{2}^{T} & s_{2}\mathbf{r}_{2}^{T} \\ \vdots & \vdots \\ \mathbf{r}_{2n}^{T} & s_{2n}\mathbf{r}_{2n}^{T} \end{bmatrix} \begin{bmatrix} \mathbf{G}^{T} \\ \mathbf{F}^{T} \end{bmatrix} = \mathbf{I} \begin{bmatrix} e^{s_{1}\tau} \\ e^{s_{2}\tau} \\ \vdots \\ e^{s_{2n}\tau} \end{bmatrix}$$
(2.13)

and the control vectors  $\mathbf{F}$  and  $\mathbf{G}$  are obtained by the solution of the set of  $2n \times 2n$  linear equations, where this solution is expressed in terms of measured receptances, so in practice there is no need to know or to evaluate the system matrices  $\mathbf{M}$ ,  $\mathbf{C}$  and  $\mathbf{K}$ . Furthermore, as described in [3], [57], the assignment is possible whenever the matrix on the left-hand side of eq.(2.13) is invertible, which, in turn, the system is controllable and  $\mu_k$ , k = 1, 2, ..., 2n are distinct. Due to the presence of the time delay, the closed-loop characteristic equation has generally an infinite number of roots over the complex plane. Hence, assigning 2n eigenvalues in such a system does not guarantee that the dynamics of the system are under control. In [8], based on the ideas dealt in [57], an analysis is presented, based on concepts of classical control theory, as system margins, Nyquist plots and Padé approximations for time-delay effects can be used to carry out *a posteriori* analysis of the closed-loop characteristic equation.

#### 2.1.2.2 Partial pole placement method considerations

Based on full assignment pole theory, in the partial pole placement issue, the main objective is to reassign a subset with the p first eigenvalues/poles of the full set 2n of open-loop poles, keeping the remaining poles constant. The development of this method for single-input receptance-based systems and considering time delay at the input was detailed on [32], for single-input systems. In [7], the multi-input receptance-based systems partial pole assignment is detailed, where the method considers in its formulation the assignment of eigenvalues and corresponding eigenvectors. Attempting to assign only part of the spectrum to given eigenvalues may result in spillover, a phenomenon of destabilization of the system where poles that are not intended to be changed are relocated to undesired locations, which could increase the vibration level or even destabilize the system. The pole placement with no spillover strategy is detailed in several relevant works [7], [32], where some poles in the open and closed-loop system are common.

In practice, only a few eigenvalues are undesirable and need to be reassigned, which it is not a computationally expensive and time-consuming task. In this dissertation, the partial pole placement for single and multiple inputs, with no spillover, will be applied in the overall approach proposed.

#### 2.1.2.3 Partial pole placement for single input systems

For better understanding about the partial pole placement method, let consider the eigenvalue problems associated with the open-loop and closed-loop system, with no time delay, respectively given by:

$$(\lambda_k^2 \mathbf{M} + \lambda_k \mathbf{C} + \mathbf{K}) \mathbf{v}_k = \mathbf{0}, \quad k = 1, 2, ..., 2n$$
(2.14)

$$(\mu_k^2 \mathbf{M} + \mu_k \mathbf{C} + \mathbf{K}) \mathbf{w}_k = \mathbf{B} (\mathbf{G} + \mu_k \mathbf{F}) \mathbf{w}_k, \quad k = 1, 2, ..., 2n$$
 (2.15)

where  $\{\lambda_k \ \mathbf{v}_k\}$  is an eigenpair associated for open-loop eigenvalue  $\lambda_k$  and eigenvector  $\mathbf{v}_k$  and  $\{\mu_k \ \mathbf{w}_k\}$  is an eigenpair associated for closed-loop eigenvalue  $\lambda_k$  and eigenvector  $\mathbf{w}_k$ . Assuming that each closed-loop eigenvalue in  $\{\mu_k\}_{k=1}^p$  is distinct from eigenvalues  $\{\lambda_k\}_{k=1}^{2n}$  of the open-loop system, the poles not modified by the pole placement can be defined by:

$$\mu_k = \lambda_k, \quad k = p + 1, p + 2, ..., 2n$$
 (2.16)

Substituting eq.(2.16) in eq.(2.15), the closed-loop control law is given by:

$$(\lambda_k^2 \mathbf{M} + \lambda_k \mathbf{C} + \mathbf{K}) \mathbf{w}_k = \mathbf{B} (\mathbf{G} + \lambda_k \mathbf{F}) \mathbf{w}_k, \quad k = p + 1, p + 2, ..., 2n$$
 (2.17)

where a non-trivial solution to eq.(2.17) is:

$$\mathbf{w}_k = \mathbf{v}_k, \quad k = p + 1, p + 2, ..., 2n$$
 (2.18)

and:

$$\mathbf{B}(\mathbf{G} + \lambda_k \mathbf{F}) \mathbf{v}_k = \mathbf{0}, \quad k = p + 1, p + 2, ..., 2n$$
 (2.19)

based on eq.(2.14). Since  $\mathbf{B} \neq \mathbf{0}$  implies that:

$$\mathbf{v}_k^T(\mathbf{G} + \lambda_k \mathbf{F})^T = \mathbf{0}, \quad k = p + 1, p + 2, ..., 2n$$
(2.20)

The first p equations of eq.(2.15) give:

$$\mathbf{w}_k = (\mu_k^2 \mathbf{M} + \mu_k \mathbf{C} + \mathbf{K})^{-1} \mathbf{B} (\mathbf{G} + \mu_k \mathbf{F}) \mathbf{w}_k, \quad k = 1, 2, ..., p.$$
 (2.21)

Note that the dynamic stiffness matrix in eq.(2.21) is invertible since that eigenvalues in  $\{\mu_k\}_{k=1}^p$  are distinct from eigenvalues in  $\{\lambda_k\}_{k=1}^{2n}$ . Considering that receptance matrix is  $\mathbf{H}(s) = (\mathbf{M}s^2 + \mathbf{C}s + \mathbf{K})^{-1}$  and use the notation  $\mathbf{r}_s = \mathbf{H}(s)\mathbf{B}$ , then eq.(2.21) takes the form:

$$\mathbf{w}_k = \mathbf{r}_{\mu_k} (\mathbf{G} + \mu_k \mathbf{F}) \mathbf{w}_k \tag{2.22}$$

Since  $\mathbf{w}_k$  may be scaled arbitrarily,  $\mathbf{w}_k$  can be defined such that:

$$(\mathbf{G} + \mu_k \mathbf{F}) \mathbf{w}_k = 1, \quad k = 1, 2, ..., p.$$
 (2.23)

From eq.(2.22):

$$\mathbf{w}_k = \mathbf{r}_k, \quad k = 1, 2, \dots, p \tag{2.24}$$

where, substituting eq.(2.24) in eq.(2.23):

$$\mathbf{r}_{\mu_k}^T(\mathbf{G}^T + \mu_k \mathbf{F}^T) = 1, \quad k = 1, 2, ..., p.$$
 (2.25)

Besides, considering the following notation:

$$\mathbf{P} = \begin{bmatrix} \mathbf{r}_{\mu_1}^T & \mu_1 \mathbf{r}_{\mu_1}^T \\ \vdots & \vdots \\ \mathbf{r}_{\mu_p}^T & \mu_p \mathbf{r}_{\mu_p}^T \end{bmatrix}, \quad \mathbf{Q} = \begin{bmatrix} \mathbf{v}_{p+1}^T & \mu_{p+1} \mathbf{v}_{p+1}^T \\ \vdots & \vdots \\ \mathbf{v}_{2n}^T & \mu_{2n} \mathbf{v}_{2n}^T \end{bmatrix}, \quad (2.26)$$

where the 2n equations based on eq.(2.25) and eq.(2.20) can assume the form:

$$\begin{bmatrix} \mathbf{P} \\ \mathbf{Q} \end{bmatrix} \begin{bmatrix} \mathbf{G}^T \\ \mathbf{F}^T \end{bmatrix} = \begin{bmatrix} \mathbf{d} \\ \mathbf{0} \end{bmatrix} \tag{2.27}$$

where  $\mathbf{d} = (1 \dots 1)^T \in \mathbb{R}^p$ . Note that the vectors  $\mathbf{F}$  and  $\mathbf{G}$  are real vectors and that the partial assignment of eigenvalues is achieved with no spillover, based on only a small set of eigenvalues which are required to be changed, being a practical engineering problem for pole placement concept [32].

To validate the F and G matrices, obtained by the partial allocation method, the determinant of the closed-loop characteristic equation can be calculated:

$$det[\mathbf{M}\mu_k^2 + (\mathbf{C} - \mathbf{BF})\mu_k + (\mathbf{K} - \mathbf{BG})] = \mathbf{0}$$
 (2.28)

where the roots will correspond to the closed-loop poles, including those reassigned.

#### 2.1.2.4 Partial pole placement for multiple input systems

Similar to the single input partial pole placement approach presented above, based on the development described in [7], for the partial pole placement for m multiple inputs, the matrices  $\mathbf{F}$  and  $\mathbf{G}$  can be found by solving the following linear system:

$$\begin{bmatrix} \mathbf{P}_k \\ \mathbf{Q}_k \end{bmatrix} \begin{bmatrix} \mathbf{G}^T \\ \mathbf{F}^T \end{bmatrix} = \begin{bmatrix} \alpha_m \\ \mathbf{0} \end{bmatrix}$$
 (2.29)

In this linear system, the matrix  $P_k$ , associated for the p poles to be reassigned, for k = 1, 2, ..., p is given by:

$$\mathbf{P}_{k} = \begin{bmatrix} \mathbf{w}_{k}^{T} & 0 & \dots & 0 & \mu_{k} \mathbf{w}_{k}^{T} & 0 & \dots & 0 \\ 0 & \mathbf{w}_{k}^{T} & \dots & 0 & 0 & \mu_{k} \mathbf{w}_{k}^{T} & \dots & 0 \\ \vdots & \vdots \\ 0 & 0 & \dots & \mathbf{w}_{k}^{T} & 0 & 0 & \dots & \mu_{k} \mathbf{w}_{k}^{T} \end{bmatrix}$$
(2.30)

where the eigenvectors  $\mathbf{w}_k$  of the closed-loop is defined as a linear combination of  $\mathbf{r}_{\mu_k,j} = \mathbf{H}(\mu_k)\mathbf{B}_j, k = 1, 2, \dots, p, j = 1, 2, \dots, m$ :

$$\mathbf{w}_{k} = \alpha_{\mu_{k},1} \mathbf{r}_{\mu_{k},1} + \alpha_{\mu_{k},2} \mathbf{r}_{\mu_{k},2} + \ldots + \alpha_{\mu_{k},m} \mathbf{r}_{\mu_{k},m}$$
(2.31)

and  $\alpha_{\mu_k,j}$ , k = 1, 2, ..., p, j = 1, 2, ..., m is a matrix that can be choosed for modal constraints for  $\mathbf{w}_k$ , as described in [7].

The matrix  $\mathbf{Q}_k$ , for the remaining poles not modified by the pole placement (invariant poles), can be defined by, for k = p + 1, p + 2, ..., 2n:

$$\mathbf{Q}_{k} = \begin{bmatrix} \mathbf{v}_{k}^{T} & 0 & \dots & 0 & \lambda_{k} \mathbf{v}_{k}^{T} & 0 & \dots & 0 \\ 0 & \mathbf{v}_{k}^{T} & \dots & 0 & 0 & \lambda_{k} \mathbf{v}_{k}^{T} & \dots & 0 \\ \vdots & \vdots \\ 0 & 0 & \dots & \mathbf{v}_{k}^{T} & 0 & 0 & \dots & \lambda_{k} \mathbf{v}_{k}^{T} \end{bmatrix}$$
(2.32)

where it is possible to see that the **F** and **G** matrices may be determined from measured receptances  $\mathbf{H}(s)$  at the desired poles  $s = \mu_k$ , k = 1, 2, ..., p, without the need to know or evaluate the  $\mathbf{M}, \mathbf{C}, \mathbf{K}$  matrices of the system.

#### 2.2 Dead-zone nonlinearity considerations

The dead-zone function  $\rho(\circ): \mathbb{R}^m \to \mathbb{R}^m$  is assumed to be a static and memoryless input nonlinearity, as illustrated in Fig. 2.2 for single input systems, that can described by

$$\overline{u}_{j}(t) = \begin{cases}
\widehat{u}_{j}(t) - b_{r,j}, & \text{if } \widehat{u}_{j}(t) > b_{r,j} & \text{(or } \overline{u}_{j}(t) > 0), \\
0, & \text{if } -b_{l,j} \leq \widehat{u}_{j}(t) \leq b_{r,j} & \text{(or } \overline{u}_{j}(t) = 0), \\
\widehat{u}_{j}(t) + b_{l,j}, & \text{if } \widehat{u}_{j}(t) < -b_{l,j} & \text{(or } \overline{u}_{j}(t) < 0),
\end{cases} (2.33)$$

where  $\widehat{\mathbf{u}}(t) = [\widehat{u}_1(t) \ \widehat{u}_2(t) \ ... \ \widehat{u}_m(t)]^{\top}$  is the control signal before dead zone,  $\overline{\mathbf{u}}(t) = [\overline{u}_1(t) \ \overline{u}_2(t) \ ... \ \overline{u}_m(t)]^{\top}$  is the dead-zone output signal,  $b_{l,j}$  and  $b_{r,j}$  are the dead-zone break points and  $\overline{\mathbf{u}}(t) = \rho(\widehat{\mathbf{u}}(t))$ .

Consider the dead-zone characteristics shown in Fig.2.2, with a symmetrical dead zone  $|b_{r,j}| = |b_{l,j}| = \delta_j$ , for simplicity purposes and its slope constant and equals to 1 (this is the typical case, without loss of generality, since the slope different from 1 can be represented by a constant gain). The output waveform of dead-zone nonlinearity with a sinusoidal input  $\hat{u}_j(t) = A_j sin(\omega t)$  is illustrated on Fig.2.3, where the mathematical expression of  $\bar{u}_j(t)$  is as follows:

$$\overline{u}_{j}(t) = \begin{cases} 0, & 0 \le \omega t < \varphi_{j} \\ A_{j}sin(\omega t) - \delta_{j}, & \varphi_{j} \le \omega t \le \pi/2 \end{cases}$$
 (2.34)

where  $\varphi_j = arcsin(\frac{\delta_j}{A_j})$ . In Fig.2.3, note that the dead-zone break-point limits directly influences on output signal amplitude, which decreases with  $\delta_j$  value, and

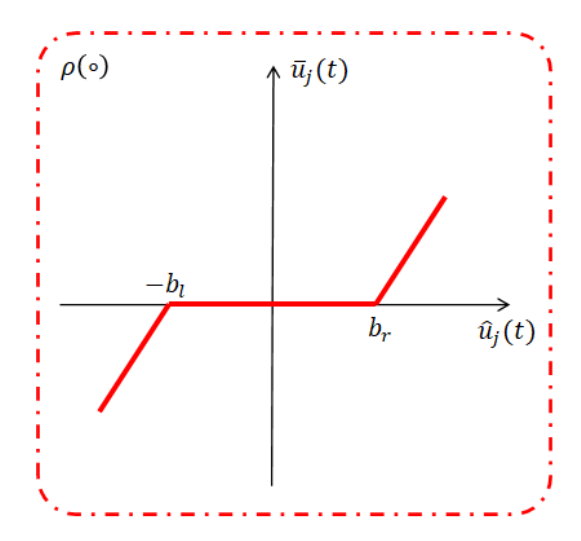


Figure 2.2: Representation of the dead-zone nonlinearity - single-input case.

at the intersection points with the *x* axis, which is affected by  $\varphi_j$ , due to nonlinear characteristic present in dead zone.

For evaluating the existence of self-sustaining oscillations or limit cycles in control loops for nonlinear systems, also to verify their stability and estimate their amplitudes and frequency based on the frequency-domain approach, such as dead-zone nonlinearity influence, the DF method is a useful operator that associates the nonlinearity with a complex function that generalizes the frequency response of transfer functions [49]–[53]. In order to be able to use describing functions method, consider a control system like the one represented by the block diagram of Fig.2.4, in which C(s) and H(s) denote the transfer functions of the controller and the process, respectively, and N the nonlinearity, that is, an nonlinear operator that transforms the  $\widehat{\mathbf{u}}_i(t)$  sign in the  $\overline{\mathbf{u}}_i(t)$  sign.

Thus, the describing function of the nonlinear element is defined by the complex ratio of the fundamental component of the nonlinear element by the sinusoidal input, given by:

$$N(A, \omega) = \frac{Me^{j(\omega t + \phi)}}{Ae^{j\omega t}} = \frac{1}{A}(b_1 + ja_1)$$
 (2.35)

where its mathematical proof is described in Appendix A.

For the dead-zone nonlinearity represented in Fig.2.2, because of the odd sym-

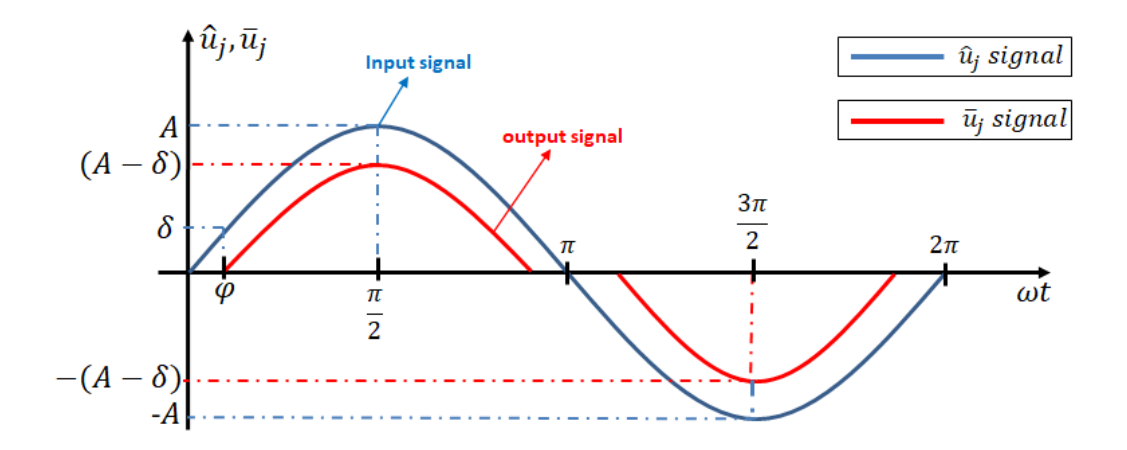


Figure 2.3: Input and output signals under dead-zone nonlinearity influence.

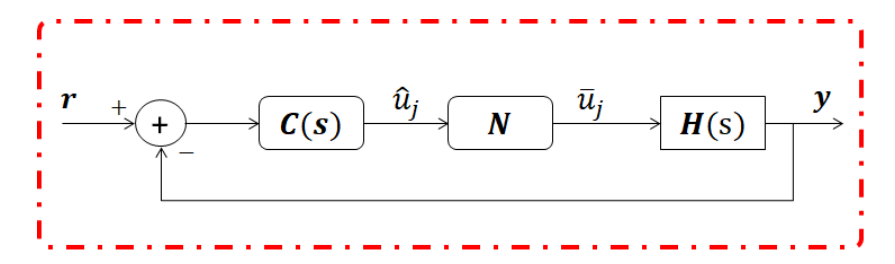


Figure 2.4: Basic schema for describing functions method analysis

metry,  $a_0 = 0$  and  $a_1 = 0$ . Then,  $b_1$  is given by:

$$b_{1} = \frac{1}{\pi} \int_{0}^{2\pi} \widehat{\mathbf{u}}(t) \sin(\omega t) d(\omega t)$$

$$= \frac{4}{\pi} \int_{0}^{\pi/2} [A \sin(\omega t) - \delta] \sin(\omega t) d(\omega t)$$

$$= \frac{2A}{\pi} (\frac{\pi}{2} - \arcsin(\frac{\delta}{A}) - \frac{\delta}{A} \sqrt{1 - (\frac{\delta}{A})^{2}})$$
(2.36)

Thus, the describing function N(A) for the dead zone is given by:

$$N(A) = \frac{b_1}{A} = 1 - \frac{2}{\pi} \left[ \arcsin\left(\frac{\delta}{A}\right) + \frac{\delta}{A} \sqrt{1 - \left(\frac{\delta}{A}\right)^2} \right]$$
 (2.37)

where the expression obtained above is a real function and frequency independent (phase angle lag equals to zero), i.e,  $N(A, \omega) = N(A)$ . Also note that N(A) = 0 when  $\frac{A}{\delta} < 1$  and increases as the effect of the dead zone diminishes as the amplitude A is increased, as displayed in Fig.2.5.

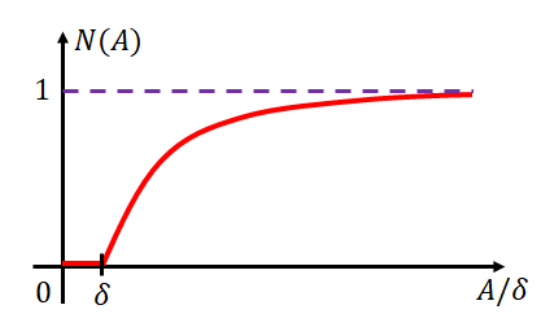


Figure 2.5: Graphical representation for dead-zone describing function.

### 2.2.1 Limit cycle prediction

Consider the system of Fig.2.4 and assume, for simplicity, that the reference signal  $\mathbf{r}$  is null, since want to analyze the oscillation inherent in the closed loop, and that  $N(A, \omega)$  is the DF of the nonlinearity  $\mathbf{N}$ . The linear part is denoted by G(s), which is defined by G(s) = C(s)H(s). According to the DF method, if the system of Fig.2.4 sustains a limit cycle with the control signal u having an amplitude  $A_0$  and a frequency  $\omega_0$ , then the pair  $(A_0, \omega_0)$  is a solution of the Harmonic Balance Equation [49], [50]:

$$G(j\omega) = -\frac{1}{N(A,\omega)} \tag{2.38}$$

Under general conditions, it is verified whether the harmonic balance equation admits solutions in  $(A, \omega)$  to predict the existence of limit cycles and estimate their amplitudes and frequencies. From the harmonic balance equation, a graphical method is obtained to predict limit cycles in the system when the describing function of the nonlinearity in question depends only on the amplitude  $(N(A, \omega) = N(A))$ , which is also the case for several nonlinearities, including dead zone, Coloumb friction, among others [50], for the most common case where the oddity property is considered. For this purpose, this analysis considers the Nyquist plot of both the frequency response function  $G(j\omega)$ , varying  $\omega$ , and the negative inverse describing function -1/N(A), varying A, in the complex plane. If these curves intersect at some point  $z_0$ , then the system admits a limit cycle, and the values of the parameters of the curves  $A_0$  and  $\omega_0$  for which the intersection are solutions of that equation and, therefore, correspond to the frequency and amplitude

of the limit cycle found. For dead-zone describing function, note that its plot lies on the real axis and tends to point (-1,0) in Nyquist plot when  $A \to \infty$ .

For receptance-based systems, with no time delay, considering the system in Fig.2.4, in comparison with closed-loop receptance given by Eq.(2.6), which is possible to define that the harmonic balance equation can be described by:

$$-(\mathbf{G} + j\omega\mathbf{F})\mathbf{H}(j\omega)\mathbf{B} = -\frac{1}{N(A,\omega)}$$
(2.39)

where, if there is an intersection between the open-loop transfer function based on receptance and the negative reciprocal expression for nonlinearity, the procedure gives a prediction of the existence of limit cycles, i.e., when then the pair  $(A_0, \omega_0)$  will be a solution of the Harmonic Balance Equation.

At the same method, the limit cycles can be stable or unstable. To determine the stability of a limit cycle, is used, as described in [49], [50] and references therein, the Nyquist criterion for stability analysis, where the closed-loop system is stable if the open-loop frequency response in the complex plane circulates the point (-1,0) in a positive direction for frequency changes from  $-\infty$  to  $+\infty$  as many times as the number of open-loop poles lies in the right half of the plane  $j\omega$ . In other words, the stability condition is respected if the number of turns in the positive direction coincides with the number of open-loop unstable poles. Otherwise, the limit cycle is unstable.

## 2.3 Continuous-time filtered Smith predictor for receptance systems

In this section, the filtered Smith predictor for second-order receptance-based systems is presented, based on the theory developed in [5]. For presentation simplicity purpose and based on Eq.(2.7) and Eq.(2.8), the nominal prediction, considering that the system is initially relaxed, i.e,  $\mathbf{x}(0) = \dot{\mathbf{x}}(0) = 0$ , and the external disturbance  $\mathbf{d}(t) = 0$ , can be given by:

$$\hat{\mathbf{X}}(s) = \mathbf{H}(s)\mathbf{B}\mathbf{U}(s) \tag{2.40}$$

where  $\mathbf{W}(s) = 0$  and  $\hat{\mathbf{X}}(s)$  can be given by 2.40, the nominal prediction of  $\mathbf{X}(s)$ ,

since  $\mathbf{x}(t)$  could be expressed by:

$$\mathbf{x}(t) = \hat{\mathbf{x}}(t - \tau) + \mathbf{w}(t) \tag{2.41}$$

Then, the compensated prediction will be given by:

$$\mathbf{X}_{p}(s) = \hat{\mathbf{X}}(s) + [\mathbf{X}(s) - \hat{\mathbf{X}}(s)e^{-s\tau}]$$
(2.42)

where  $\hat{\mathbf{X}}(s)$  is defined in Eq.(2.40) and  $\mathbf{E}(s) = \hat{\mathbf{X}}(s) + [\mathbf{X}(s) - \hat{\mathbf{X}}(s)e^{-s\tau}]$  is defined as the prediction error used for correction purposes and can be used for an estimator for  $\mathbf{w}(t)$ . Two important properties can be defined for Smith predictor in second-order systems based on receptance representation: (i)  $\lim_{t\to\infty} x_p(t) = \lim_{t\to\infty} x(t)$ , due to  $e^{-s\tau}|_{s=0} = 1$ , confirming exact convergence in the presence of constant disturbances; (ii) Considering that w(t) = 0, then  $\mathbf{X}(s) = \hat{\mathbf{X}}(s)e^{-s\tau}$ , that implies in  $\mathbf{x}_p(t) = \hat{\mathbf{x}}(t) = \mathbf{x}(t+\tau)$ , ensuring exact prediction in the absence of disturbances, where  $\mathbf{x}_p(t)$  is considered as a future measurement  $\mathbf{x}(t+\tau)$  so the delay influence can be removed from the nominal closed-loop representation. Then, control law is defined for a system without time delay controlling a system with delay.

Based on nominal prediction for Smith predictor given by Eq.(2.40), if the system is not Bounded-Input Bounded-Output (BIBO) stable,  $\hat{\mathbf{X}}(s)$  can have a divergent behavior even if the input is bounded. Then, the Smith predictor is not internally stable if the receptance has any pole which is not strictly inside the left-half plane. This is a relevant consideration, because some applications have poles over the imaginary axis, such as, for example, a friction-induced mechanical systems [30] and a vibration absorber of a machine [42], which including active vibration for receptance-based systems.

### 2.3.1 Receptance-based filtered Smith predictor

Now, consider the following version for the receptance matrix  $\mathbf{H}(s)$  for second-order systems, given by:

$$\mathbf{H}_{\Delta}(s) = [\mathbf{M}s^2 + (\delta \mathbf{I} + \mathbf{C})s + \mathbf{K}]^{-1}$$
 (2.43)

where  $\delta > 0$  is a positive and arbitrarily small scalar, such as  $\delta \ll ||\mathbf{C}||$ , and  $\mathbf{I}$  the identity matrix. The objective is, with the insertion of  $\delta$  and considering that

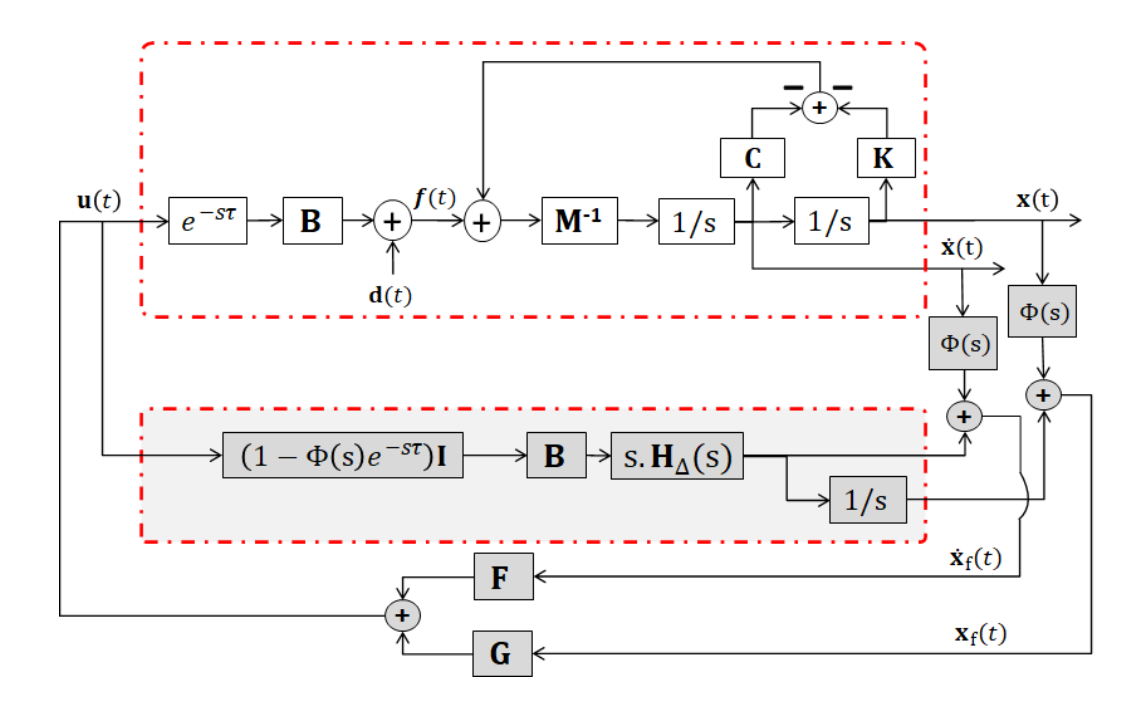


Figure 2.6: Schematic representation of the closed-loop system with continuous-time FSP.

 $C \succeq 0$ , make the adjusted term  $(\delta I + C) \succ 0$  so that the poles of  $H_{\Delta}(s)$  lie at the left half-plane and out of imaginary axis. The numerical uncertainty  $\delta$  is defined in such a way as to provide a small variation in the original matrix of the defined system by Eq.(2.1) and, within the context presented, allows the application of filtered Smith's predictor for marginally stable systems, thus guaranteeing BIBO stability. In this way, the new nominal prediction is defined as:

$$\hat{\mathbf{X}}_{\Delta}(s) = \mathbf{H}_{\Delta}(s)\mathbf{B}\mathbf{U}(s) \tag{2.44}$$

where the perturbed version of  $\mathbf{H}(s)$ , based on matrix lemma, can be rewritten by:

$$\mathbf{H}_{\Delta}(s) = [(\mathbf{M}s^2 + (\delta \mathbf{I} + \mathbf{C})s + \mathbf{K})^{-1}] = \mathbf{H}(s) - s\delta \mathbf{H}(s)[\mathbf{I} + s\delta \mathbf{H}(s)]^{-1}\mathbf{H}(s)$$
 (2.45)

and only the structural, open-loop receptance is needed in the modified Smith Predictor. That is, there is no need to know the system matrices M, C, K. Then, the filtered Smith predictor is defined by:

$$\mathbf{X}_f(s) = \hat{\mathbf{X}}_{\Delta}(s) + \Phi(s)[\mathbf{X}(s) - \hat{\mathbf{X}}_{\Delta}(s)e^{-s\tau}]$$
 (2.46)

where  $\Phi(s) = \phi(s)\mathbf{I}$ ,  $\phi(s)$  is a scalar stable filter given by:

$$\phi(s) = \frac{1 + a_1 s + a_2 s^2 + \dots + a_k s^k}{(\tau_f s + 1)^{k+1}}$$
 (2.47)

where: (i)  $\tau_f > 0$  is a free tuning parameter; (ii)  $a_l, l = 1, \ldots, k$  are defined in order to guarantee  $[1 - \phi(s)e^{-s\tau}]|_{s=j\omega_i} = 0$  and (iii)  $i = 1, \ldots, v$ , v is the total number of undesirable resonance peaks. This filter has two relevant properties: (i) attenuating the undesired difference between  $\mathbf{X}(s)$  and  $\hat{\mathbf{X}}_{\Delta}(s)$  due to modeling errors and (ii) filtering resonant frequencies carried into control signal  $\mathbf{U}(s)$ . The filter  $\phi(s)$  designing rules are described in Appendix B.

The prediction  $\mathbf{X}_f(s)$  can be alternatively given by:

$$\mathbf{X}_f(s) = \mathbf{H}_{\Delta}(s)\mathbf{B}[1 - \phi(s)e^{-s\tau}]\mathbf{IU}(s) + \Phi(s)\mathbf{X}(s)$$
 (2.48)

where this result implies that:(i) $\phi(s)$  can be defined in order to  $[1 - \phi(s)e^{-s\tau}]|_{s=j\omega_i}$ = 0,  $\omega_i$  are the frequencies related for undamped or poorly undamped undesirable poles; (ii) The  $\tau_f$  parameter can be defined for dealing with the trade-off between disturbance rejection performance and robustness.

Thus, considering the proposed predictor, the control law U(s), illustrated in Fig.(2.6), can be given by:

$$\mathbf{U}(s) = (s\mathbf{F} + \mathbf{G})\mathbf{X}_f(s) = (s\mathbf{F} + \mathbf{G})\{[\mathbf{I} - e^{-s\tau}\Phi(s)]\hat{\mathbf{X}}_{\Delta}(s) + \Phi(s)\mathbf{X}(s)\}$$
(2.49)

where  $\mathbf{U}(s)$  is used for obtaining the prediction  $\mathbf{X}_f(s)$  in a causal implementation loop.

Then, the filtered Smith predictor approach has the following benefits [5], if compared with related strategies [32], [57], [61] for receptance-based second-order systems with input delay: (i) can be used to stabilize marginally stable systems with long input delays; (ii) the prediction is obtained from the receptance matrix; (iii) the strategy can be applied to attenuate the undesired effect of poorly damped poles; (iv) the delay compensation does not require the augmented description.

Thus, the ideal closed-loop dynamics, without time delay  $(\tau=0)$  is defined by:

$$\mathbf{M}\ddot{\mathbf{x}}(t) + (\mathbf{C} - \mathbf{BF})\dot{\mathbf{x}}(t) + (\mathbf{K} - \mathbf{BG})\mathbf{x}(t) = 0$$
 (2.50)

where the proposed prediction based control provides an equivalent nominal closed-loop approach, when compared with the ideal case without delay and disturbances.

## 2.4 Discrete-time filtered Smith predictor for receptance systems

On the FSP prediction for continuous-time, given by  $\hat{\mathbf{X}}(s) = \mathbf{H}(s)\mathbf{B}\mathbf{U}(s)$ , the internal stability cannot be guaranteed by a standard continuous-time structure. Based on the results detailed in [6], the discrete-time FSP structure for receptance-based systems will be presented, considering the delay at the input of system.

### 2.4.1 Discrete-time prediction based on FSP

The nominal prediction for the discrete-time version is given by 1:

$$\overline{\mathbf{X}}(z) = \mathbf{H}(z)\mathbf{B}\mathbf{U}(z) \tag{2.51}$$

 $where^2$ 

$$\mathbf{H}(z) = \frac{z - 1}{z} Z \left\{ \frac{\mathbf{H}(s)}{s} \right\} \tag{2.52}$$

Considering that  $T_s$  is defined such that the discrete-time delay  $\tau = \ell T_s$ ,  $\ell \in \mathbb{N}^*$ . Then, the discrete-time temporal evolution of system, with null conditions and  $\mathbf{d}(t) = 0$ , can be defined as:

$$\mathcal{Z}\{\mathbf{x}(t)|_{t=nT_c}\} = z^{-\ell}\mathbf{H}(z)\mathbf{B}\mathbf{U}(z)$$
(2.53)

Based on [5], the discrete-time filtered Smith prediction is defined by:

<sup>&</sup>lt;sup>1</sup>The unilateral  $\mathbb{Z}$ -Transform is given by  $\mathbf{X}(z) = \sum_{n=0}^{\infty} \mathbf{x}(nT_s)z^{-n}$ , where: (i)  $T_s$  is the sampling interval and (ii)  $t = nT_s$ , for  $t \in (nT_s, (n+1)T_s]$ , is the Zero-Order Hold for discrete-time implementation.

<sup>&</sup>lt;sup>2</sup>For simplicity purposes, the  $\mathbb{Z}$ -Transform of a Laplace representation is defined by  $\mathbb{Z}\{L^{-1}\{\mathbf{X}(s)|_{t=nT}\}.$ 

$$\hat{\mathbf{X}}(z) = \overline{\mathbf{X}}(z) + \Phi(z)[\mathbf{X}(z) - z^{-\ell}\overline{\mathbf{X}}(z)]$$
 (2.54)

where the filter  $\Phi(z) = \phi(z)\mathbf{I}$  and  $\phi(z)$  is a scalar transfer function with unitary gain, having the following objectives: (i) provides predictor stability which is a requirement for aiming internal stability; (ii) deal with the trade-off between robustness and disturbance rejection performance. It is relevant to point out that  $\hat{\mathbf{X}}(z)$  prediction has an unstable response due to unstable open-loop poles. They can be found due to asymmetrical receptance-based representation. Then, the prediction can be alternatively given by:

$$\hat{\mathbf{X}}(z) = [1 - z^{-\ell}\phi(z)]\mathbf{H}(z)\mathbf{B}\mathbf{U}(z) + \Phi(z)\mathbf{X}(z)$$
(2.55)

To deal with unstable open-loop poles, consider a receptance matrix  $\mathbf{H}(z)$  in a factorized representation:

$$\mathbf{H}(z) = \frac{1}{\beta(z)}\mathbf{S}(z) \tag{2.56}$$

where  $\beta(z)$  is a polynomial expression whose roots are the unstable modes of  $\mathbf{H}(z)$  and  $\mathbf{S}(z)$  will contain only stable poles. Then, for aiming internal stability, a filter  $\phi(z)$  can be designed such that the zeros of  $1-z^{-\ell}\phi(z)$  are equal to the roots of  $\beta(z)$  (unstable poles of  $\mathbf{H}(z)$ ). Thus,  $\phi(z)$  is defined such that  $[1-z^{-\ell}\phi(z)] = \beta(z)\phi_s(z)$ , where  $\phi_s(z)$  is given by:

$$\phi_s(z) = \frac{1 - z^{-\ell}\phi(z)}{\beta(z)} \tag{2.57}$$

where the  $\phi_s(z)$  design rules are detailed on Appendix B. Thus, the stable filtered prediction is defined as follows:

$$\hat{\mathbf{X}}(z) = \phi_s(z)\mathbf{S}(z)\mathbf{B}\mathbf{U}(z) + \phi(z)\mathbf{X}(z)$$
 (2.58)

Note that, if Eq.(2.55) is used, bounded inputs could cause a divergent behavior at the output of the system. Then, this consequence can be avoided using Eq.(2.58), based on  $\phi_s(z)$ .

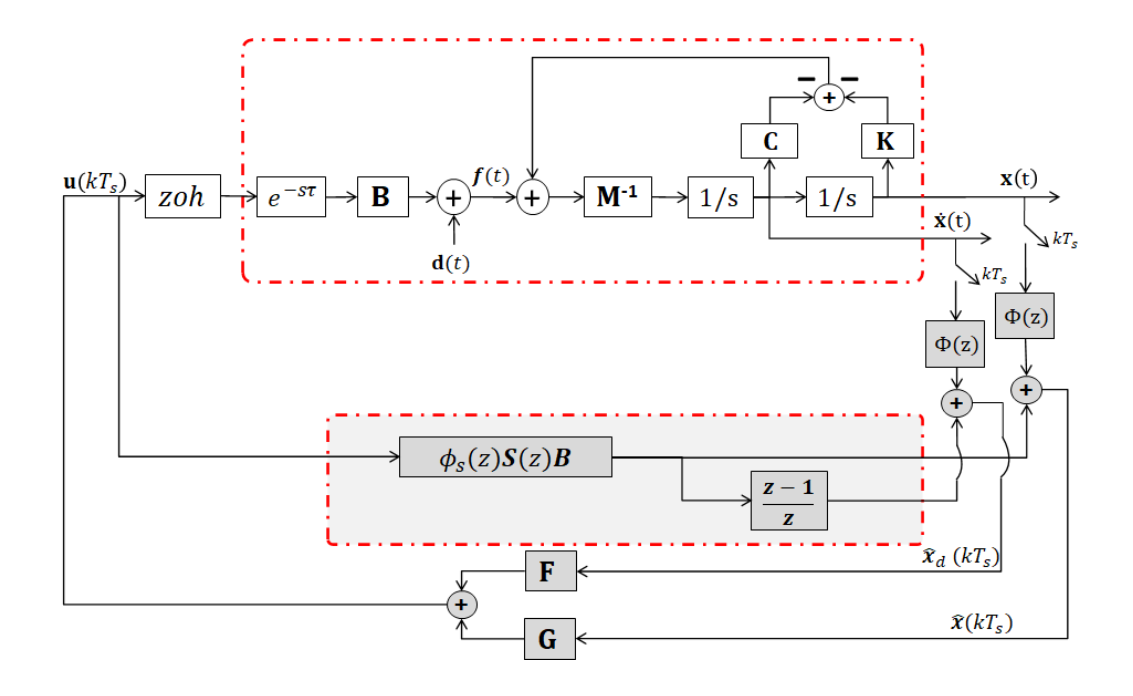


Figure 2.7: Schematic representation of the closed-loop system with discrete-time FSP.

#### 2.4.2 State-feedback control law

Now, consider the standard state-feedback control law given by Eq.(2.3), with time delay at the input of the receptance-based system. The delay induces an undesirable effect, as seen in the closed-loop control law described by Eq.(2.4). Then, based on discrete-time FSP for avoiding this undesirable effect, the sampled-data control signal is described by:

$$\mathbf{u}(t) = \mathbf{F}\hat{\mathbf{x}}(nT_s) + \mathbf{G}\hat{\mathbf{x}}(nT_s), \tag{2.59}$$

where  $\hat{\mathbf{x}}(nT_s) = Z^{-1}\{\hat{\mathbf{X}}(z)\}$  and  $\hat{\mathbf{x}}_d(nT_s) = \hat{\mathbf{x}}(nT_s) = Z^{-1}\{\hat{\mathbf{X}}_d(z)\}$ . The prediction  $\hat{\mathbf{X}}_d$ , relative to velocity prediction, is given by:

$$\hat{\mathbf{X}}_d(z) = [1 - z^{-\ell} \phi(z)] \mathbf{H}_d(z) \mathbf{B} \mathbf{U}(z) + \Phi(z) \mathbf{X}_d(z)$$
 (2.60)

where  $\mathbf{H}_d(z) = \frac{z-1}{z} \mathcal{Z}{\{\mathbf{H}(s)\}}$ .

Then, substituting the Eq.(2.55) and Eq.(2.60) in Eq.(2.59), the state-feedback

closed-loop law, illustrated on the Fig.(2.7), can be described as follows:

$$\mathbf{U}(z) = \mathbf{F}\{[\mathbf{I} - z^{-l}\Phi(z)]\mathbf{H}_d\mathbf{B}\mathbf{U}(z) + \Phi(z)\mathbf{X}_d(z)\}$$

$$+ \mathbf{G}\{[\mathbf{I} - z^{-l}\Phi(z)]\mathbf{H}\mathbf{B}\mathbf{U}(z) + \Phi(z)\mathbf{X}(z)\}$$
(2.61)

Note that, similar to the control law for continuous-time FSP,  $\mathbf{U}(z)$  is used for computing  $\hat{\mathbf{X}}(z)$  and  $\hat{\mathbf{X}}_d(z)$  in a causal implementation loop. Besides, the control law  $\mathbf{U}(z)$ , considering that the delay is mitigated for prediction filter  $\Phi(z)$ , can be rewritten by:

$$\mathbf{U}(z) = [\mathbf{I} - \mathbf{G}\mathbf{H}(z)\mathbf{B} - \mathbf{F}\mathbf{H}_d(z)\mathbf{B}]^{-1}[\mathbf{F}\Phi(z)\mathbf{X}_d(z) + \mathbf{G}\Phi(z)\mathbf{X}(z)]$$
(2.62)

where the transfer matrix from the each state (displacement and velocity) has a delay free characteristic equation is given by [6]:

$$det([\mathbf{I} - \mathbf{GH}(z)\mathbf{B} - \mathbf{FH}_d(z)\mathbf{B}]) = 0$$
(2.63)

#### 2.4.3 Considerations about pole placement problem

The full or partial pole placement for receptance-based systems used for **F** and **G** matrices without input delay, as discussed in this chapter by methods described in [3], [7], can be solved similarly for the continuous-time domain. In this case, considering a single-input system, the reassign of p eigenvalues (poles) of a full set of 2n open-loop poles  $\{e^{\lambda_1 T_s}, \ldots, e^{\lambda_{2n} T_s}\}$ , which implies in a set of p linear equations:

$$\begin{bmatrix} \mathbf{H}_d(e^{\lambda_k T_s}) \mathbf{B} \\ \mathbf{H}(e^{\lambda_k T_s}) \mathbf{B} \end{bmatrix}^T \begin{bmatrix} \mathbf{F} \\ \mathbf{G} \end{bmatrix} = 1 \qquad k = 1, \dots, p.$$
 (2.64)

For the no spillover property, based on the remaining 2n - p poles, the following linear equations can be solved:

$$\begin{bmatrix} \mathbf{y}_k \\ \lambda_k \mathbf{y}_k \end{bmatrix}^T \begin{bmatrix} \mathbf{F} \\ \mathbf{G} \end{bmatrix} = 0 \qquad k = p + 1, \dots, 2n.$$
 (2.65)

where the  $\mathbf{y}_k$  is the eigenvector associated with the eigenvalue  $\lambda_k$ . These same considerations are applicable for partial pole placement for multiple input systems [7].

### Chapter 3

# Filtered Smith predictor with dead-zone compensation

In general, a state feedback control law is considered for second-order linear systems. The desired theoretical control law is typically defined by

$$\mathbf{v}(t) = \mathbf{F}\dot{\mathbf{x}}(t) + \mathbf{G}\mathbf{x}(t), \tag{3.1}$$

where  $\mathbf{F} \in \mathbb{R}^{mxn}$  and  $\mathbf{G} \in \mathbb{R}^{mxn}$  are the well-known feedback gain matrices designed to provide a specific closed-loop performance. The control challenge comes from the fact that  $\mathbf{v}(t)$  is defined from the state feedback control law, but  $\overline{\mathbf{u}}(t-\tau)$  is the effective manipulated input in Eq. (2.2). The idea of the dead-zone compensation is to provide a modified control action such that  $\overline{\mathbf{u}}(t) = \mathbf{v}(t)$ . The filtered Smith predictor is used to design  $\mathbf{F}$  and  $\mathbf{G}$  based on the model without delay.

A typical dead-zone compensation strategy is used in related works [15], [20]–[22], where  $\tilde{\Gamma}(\circ): \mathbb{R}^m \to \mathbb{R}^m$  represents the dead-zone inverse compensation function, i.e.  $\mathbf{v}(t) = [v_1(t) \ v_2(t) \ ... \ v_m(t)]^{\top}, \ \widehat{\mathbf{u}}(t) = \tilde{\Gamma}(\mathbf{v}(t)), \ \widehat{u}_i(t) = \tilde{\gamma}_i(v_i(t)), \ i = 1, 2, ..., m$ . This compensation can be represented by

$$\tilde{\gamma}_{i}(v_{i}(t)) = \begin{cases}
v_{i}(t) + b_{r,i}, & \text{if } v_{i}(t) > 0, \\
0, & \text{if } v_{i}(t) = 0, \\
v_{i}(t) - b_{l,i}, & \text{if } v_{i}(t) < 0.
\end{cases}$$
(3.2)

Hence, as  $\overline{\mathbf{u}}(t) = \rho(\widehat{\mathbf{u}}(t))$ , if  $\widehat{\mathbf{u}}(t) = \widetilde{\gamma}(\mathbf{v}(t))$ , then  $\overline{\mathbf{u}}(t) = \mathbf{v}(t)$  such that the virtual desired control before the dead-zone compensation correspond to the effective control after the dead zone. In other words,  $\rho(\widetilde{\Gamma}(\mathbf{v}(t))) = \mathbf{v}(t)$ .

In practice, this solution provides a chattering effect when  $v_i(t)$  is around the origin. Then, an approximated approach can be defined as depicted in Fig. 3.1 to mitigate the chattering effect. The approximated dead-zone compensation is simply given by

$$\gamma_i(v_i(t)) = v_i(t) + sat_i(\beta v_i(t)), \tag{3.3}$$

where  $\beta \gg 1$ ,  $sat_i(\circ)$  defines a saturation nonlinearity,  $\mathbf{sat}(\circ) : \mathbb{R}^m \to \mathbb{R}^m$  is the generalized saturation version for the case with multiple inputs, and  $\Gamma(\mathbf{v}(t)) = \mathbf{v}(t) + \mathbf{sat}(\mathbf{v}(t))$ . Each saturation function is defined as

$$sat_{i}(\beta v_{i}(t)) = \begin{cases} b_{r,i}, & \text{if } \beta v_{i}(t) > b_{r,i}, \\ \beta v_{i}(t), & \text{if } -b_{l,i} \leq \beta v_{i}(t) \leq b_{r,i}, \\ -b_{l,i}, & \text{if } \beta v_{i}(t) < -b_{l,i}. \end{cases}$$
(3.4)

Notice that the difference between  $\Gamma(\mathbf{v}(t))$  and  $\tilde{\Gamma}(\mathbf{v}(t))$  is negligible for a sufficient high value of the free parameter  $\beta$  because  $\gamma_i(\mathbf{v}(t)) - \tilde{\gamma}_i(\mathbf{v}(t)) = 0$  either if  $\beta v_i(t) > b_{r,i}$  or if  $\beta v_i(t) < -b_{l,i}$ . Moreover,  $\gamma_i(\mathbf{v}(t)) - \tilde{\gamma}_i(\mathbf{v}(t)) = \varepsilon_i(t)$  is bounded by  $|\varepsilon_i(t)| < |\beta v_i(t) - b_{r,i}|$  if  $b_{r,i} > \beta v_i(t) > 0$  and  $|\varepsilon_i(t)| < |b_{l,i} - \beta v_i(t)|$  if  $0 > \beta v_i(t) > -b_{l,i}$ . In summary, the exact condition  $(\gamma_i(\mathbf{v}(t)) - \tilde{\gamma}_i(\mathbf{v}(t)) = 0)$  is easily achieved by increasing  $\beta$ . Then,  $\beta$  is used to deal with the compromise between chattering mitigation and exact dead-zone compensation condition.

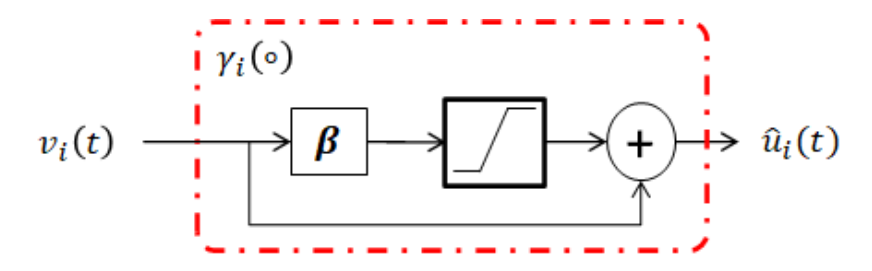


Figure 3.1: Schematic description of the dead-zone inverse compensation strategy based on saturation nonlinearity.

The proposed dead-time compensation strategy can be combined with the filtered Smith predictor to jointly deal with delay and dead zone. A receptance-based filtered Smith predictor with dead-zone compensation is illustrated in Fig. 3.2. In this work, similarly to the approach presented in [5], a perturbed open-loop receptance transfer matrix  $\mathbf{H}_{\Delta}(s)$  is used in the presence of undamped poles. Moreover,

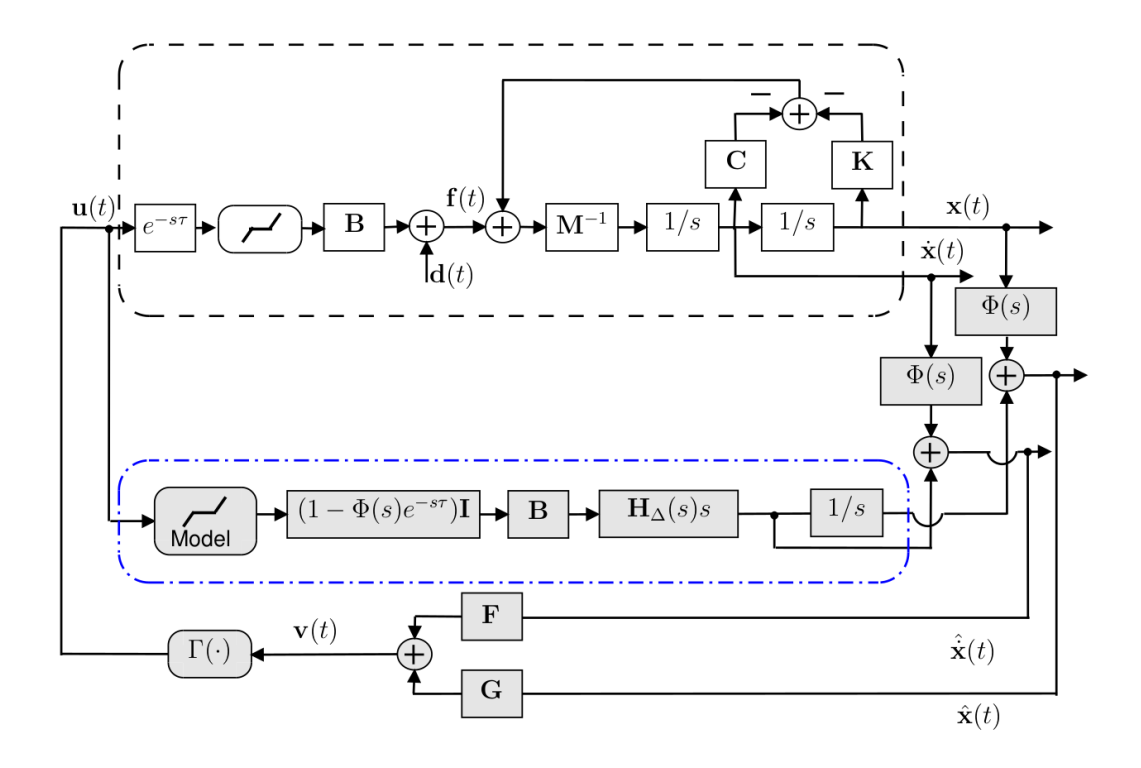


Figure 3.2: Schematic representation of the FSP approach with dead zone at input of the system.

for the open-loop unstable case, the approach given in [6] can be used to implementation of a discrete-time filtered Smith predictor. In both cases, internal stability is assured to the prediction.

The external signal  $\mathbf{f}(t)$  can be redefined as follows to consider the effect of the approximated dead-zone compensation

$$\mathbf{f}(t) = \mathbf{B}\rho(\Gamma(\mathbf{v}(t-\tau))) + \mathbf{d}(t). \tag{3.5}$$

Alternatively, the approximated dead-zone compensation can be described by

$$\mathbf{f(t)} = \mathbf{B}[\mathbf{v}(t-\tau) + \mathbf{\varepsilon}(t-\tau)] + \mathbf{d}(t), \tag{3.6}$$

where  $\varepsilon(t-\tau)$  is a bounded disturbance that comes from the approximated deadtime compensation with chattering mitigation. Due to the fact that  $\varepsilon(t-\tau)$  represent a bounded external disturbance from control perspective, then  $\mathbf{q}(t) = \mathbf{B}\varepsilon(t-\tau)$  is defined in order to simplify the BIBO stability analysis as follows

$$\mathbf{f}(t) = \mathbf{B}\mathbf{v}(t-\tau) + \mathbf{q}(t) + \mathbf{d}(t), \tag{3.7}$$

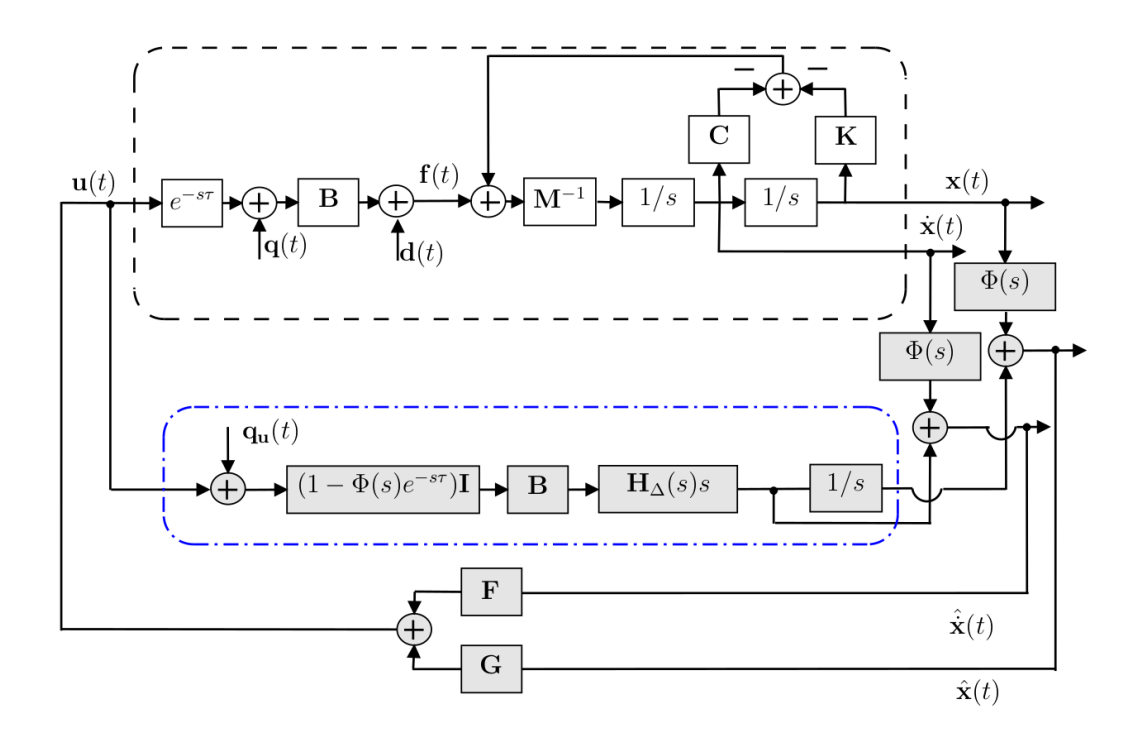


Figure 3.3: Equivalent schematic representation of the linear delayed system with bounded disturbance and FSP compensation.

where  $\mathbf{q}(t) = \mathbf{B}\mathbf{\epsilon}(t-\tau)$  due to the definition of the approximated dead-zone compensation. This result is important once the approximated nonlinear compensation can be represented by an equivalent linear system with bounded disturbance, as illustrated in Fig. 3.3, where the virtual control  $\mathbf{v}(t)$  can be depicted as a typical linear control  $\mathbf{u}(t)$  due to the bounded disturbance description. In a similar way, based on the discrete-time FSP approach for receptance-based asymmetric systems, on Fig. 3.4 is depicted the equivalent schematic of the linear delayed system with bounded disturbance.

**Remark 1.** As discussed in [5], as long the receptance-based filtered Smith Predictor is designed with a stable  $\mathbf{H}_{\Delta}(s)$  receptance representative of the system, internal stability is then guaranteed. Then, the bounded disturbance on the system, including  $\mathbf{d}(t)$ , the exogenous perturbations, and  $\mathbf{q}(t)$ , a bounded disturbance due to the non-chattering approximation of the inverse for dead zone, and deviations from the estimated to the actual dead-zone limits, lead to bounded outputs as the effect.

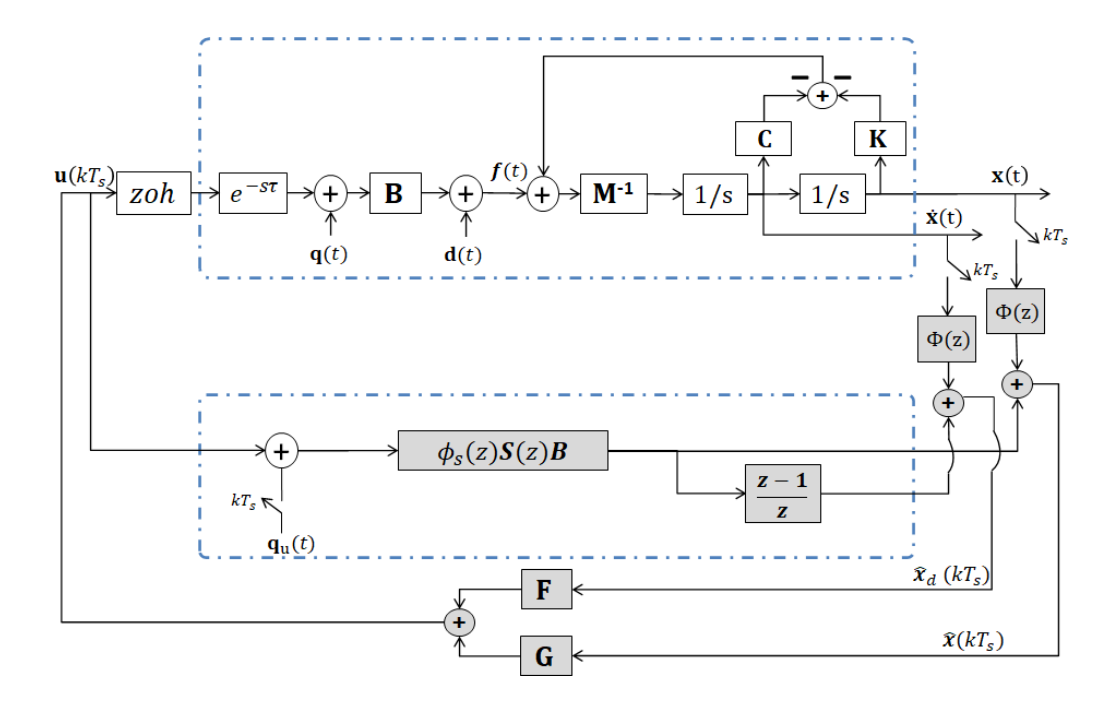


Figure 3.4: Equivalent schematic representation of the linear delayed system with bounded disturbance and discrete-time FSP compensation.

Notice that the unknown dead-zone effect may be described as a bounded disturbance as the difference between the desired control signal and the effective control due to the dead-zone input is limited.

### Chapter 4

# Receptance-based discrete-time observer for adaptive compensation

For presentation purposes, the receptance-based second-order model without delay can be alternatively described by:

$$\mathbf{P}(s) = \begin{bmatrix} \mathbf{H}(s)\mathbf{B} \\ s\mathbf{H}(s)\mathbf{B} \end{bmatrix}. \tag{4.1}$$

The following augmented state description is also considered

$$\boldsymbol{\xi}(t) = \begin{bmatrix} \mathbf{x}(t) \\ \dot{\mathbf{x}}(t) \end{bmatrix},\tag{4.2}$$

where  $\xi(t)$  is augmented description based on the displacement  $\mathbf{x}(t)$  and velocity  $\dot{\mathbf{x}}(t)$ . Now, consider a continuous-time minimal state-space realization of  $\mathbf{P}(s)$ , with state vector given by  $\boldsymbol{\mu}(t) \in \mathbb{R}^{2n}$  such that the following description holds

$$\begin{cases} \dot{\boldsymbol{\mu}}(t) = \mathbf{A}_{s}\boldsymbol{\mu}(t) + \mathbf{B}_{s}\overline{\mathbf{u}}(t-\tau) \\ \boldsymbol{\xi}(t) = \mathbf{C}_{s}\boldsymbol{\mu}(t) + \mathbf{D}_{s}\mathbf{u}(t-\tau) \end{cases}$$
(4.3)

where  $\mathbf{A}_s \in \mathbb{R}^{2n \times 2n}$ ,  $\mathbf{B}_s \in \mathbb{R}^{2n \times m}$ ,  $\mathbf{C}_s \in \mathbb{R}^{2n \times 2n}$  and  $\mathbf{D}_s \in \mathbb{R}^{2n \times m}$ .

For the purpose of defining a transformed state-space realization based on the vector given by  $\xi(t) = [\mathbf{x}(t)^T \ \dot{\mathbf{x}}(t)^T]^T$ , a similarity transformation will be employed such that  $\xi(t)$  is the effective state vector. Therefore, the following equivalent input-output representation is considered

$$\boldsymbol{\mu}(t) = \mathbf{T}_l \boldsymbol{\xi}(t), \tag{4.4}$$

where  $\mathbf{T}_l \in \mathbb{R}^{2n \times 2n}$  represents the similarity transformation. In this problem, this matrix can be obtained as follows

$$\mathbf{T}_l = \mathbf{C}_s^{-1},\tag{4.5}$$

because  $\mathbf{P}_s = \mathbf{0}$ , because  $\mathbf{P}(s)$  is a strictly proper transfer matrix. Then, the alternative representation is given by:

$$\mathbf{A}_t = \mathbf{T}_l^{-1} \mathbf{A}_s \mathbf{T}_l, \ \mathbf{B}_t = \mathbf{T}_l^{-1} \mathbf{B}_s, \ \mathbf{C}_t = \mathbf{C}_s \mathbf{T}_l = \mathbf{I}. \tag{4.6}$$

Consequently, the continuous-time state-space model can be defined as follows:

$$\dot{\mathbf{\xi}}(t) = \mathbf{A}_t \mathbf{\xi}(t) + \mathbf{B}_t \overline{\mathbf{u}}(t - \tau). \tag{4.7}$$

The adaptive dead-zone compensation strategy is based on a discrete-time control with a Zero-Order hold actuation with a sampling period  $T_s$ . From now on, the discrete virtual control is defined by  $\mathbf{v}(t) = \mathbf{F}\dot{\mathbf{x}}(kT_s) + \mathbf{G}\mathbf{x}(kT_s)$  for  $t \in (kT_s, (k+1)T_s]$ , where  $\mathbf{v}(kT_s) = \mathbf{v}[k]$ . Then, the discrete-time model is given by

$$\boldsymbol{\xi}[k+1] = \mathbf{A}_d \boldsymbol{\xi}[k] + \mathbf{B}_d \overline{\mathbf{u}}[k-d], \tag{4.8}$$

where  $\xi[k] = \xi(kT_s)$ ,  $\mathbf{u}[k] = \mathbf{u}(kT_s)$ ,  $\mathbf{A}_d \in \mathbb{R}^{2n \times 2n}$ ,  $\mathbf{B}_d \in \mathbb{R}^{2n \times m}$  are obtained from the zero-order hold discretization of the continuous-time equation, and delay in discrete-time  $d \in \mathbb{N}^*$  is assumed to be defined such that  $\tau = dT_s$ . Hence, the discrete-time matrices are given by

$$\mathbf{A}_d = e^{\mathbf{A}_t T_s}, \ \mathbf{B}_d = \left( \int_0^{T_s} e^{\mathbf{A}_t \tau} d\tau \right) \mathbf{B}_t. \tag{4.9}$$

It is assumed that  $\mathbf{B}_t$  is full column rank, i.e., the actuation effects are not redundant.

The discrete-time equation can be rewritten by

$$\boldsymbol{\xi}[k+1] = \mathbf{A}_d \boldsymbol{\xi}[k] + \mathbf{B}_d \mathbf{v}[k-d] + \mathbf{B}_d (\overline{\mathbf{u}}[k-d] - \mathbf{v}[k-d]), \tag{4.10}$$

where: (i)  $\mathbf{v}[\mathbf{k}]$  is the discrete-time desired control signal; (ii)  $\overline{\mathbf{u}}[k] = \overline{\mathbf{u}}(kT_s)$  is the sampled signal of the control action subject to the dead zone, (iii) and  $\overline{\mathbf{u}}[k-d] - \mathbf{v}[k-d]$  represents the difference between a desired virtual control and the effective control subject to the dead zone. In the absence of disturbances or modeling errors,  $\mathbf{\omega}[k-d-1] = \overline{\mathbf{u}}[k-d-1] - \mathbf{v}[k-d-1]$  can be computed as follows

$$\mathbf{\omega}[k-d-1] = \mathbf{B}_{d}^{+}(\mathbf{\xi}[k] - \mathbf{A}_{d}\mathbf{\xi}[k-1] + \mathbf{B}_{d}\mathbf{v}[k-d-1])$$
(4.11)

where  $\mathbf{B}_d^+ \in \mathbb{R}^{m \times 2n}$  is the Moore-Penrose or pseudoinverse of the influence matrix.

Notice that in the absence of disturbances and modeling errors, as  $\mathbf{B}_d$  is full column rank, then the following relationship holds

$$\mathbf{\omega}[k-d-1] = \mathbf{B}_d^+(\mathbf{\xi}[k] - \mathbf{A}_d\mathbf{\xi}[k-1]) + \mathbf{v}[k-d-1]$$
$$= \overline{\mathbf{u}}[k-d-1] - \mathbf{v}[k-d-1]. \tag{4.12}$$

This observer is useful because  $b_{r,i}$  and  $b_{l,i}$ , i = 1, 2, ..., m may not be exactly known. Fortunately, based on  $\mathbf{\omega}[k-d-1]$ , the compensation parameters can be adapted to track the correct dead-zone parameters. Notice that if the proposed dead-zone compensation strategy is used in the undisturbed nominal case, then

$$\mathbf{\omega}[k-d-1] = \overline{\mathbf{u}}[k-d-1] - \mathbf{v}[k-d-1]$$

$$= \rho(\Gamma(\mathbf{v}[k-d-1])) - \mathbf{v}[k-d-1]. \tag{4.13}$$

### 4.1 Dead-zone adaptation mechanism

The observed signal is defined by the following vector  $\mathbf{\omega}[k-d-1] = [\omega_1[k-d-1] \dots \omega_m[k-d-1]]^{\top}$ . However, either the information of  $b_{r,i}$  or  $b_{l,i}$  can be provided by  $\omega_i[k-d-1]$ , depending on the value of  $\overline{u}_i[k-d-1]$ . If  $\overline{u}_i[k-d-1] > 0$ , then  $\omega_i[k-d-1]$  depends on  $b_{r,i}$ , while  $\overline{u}_i[k-d-1] < 0$  is such that  $\omega_i[k-d-1]$  depends on  $b_{l,i}$ . The adaptive estimation of  $\hat{b}_{r,i}[k]$  and  $\hat{b}_{l,i}[k]$  are defined from a discrete-time integration of  $\hat{b}_{r,i}[0]$  and  $\hat{b}_{l,i}[0]$  based on Euler's approximation method. Thus, the adaptive mechanism can be defined by

$$\hat{b}_{r,i}[k] = \hat{b}_{r,i}[k-1] - K_{r,i}T_s\omega_i[k-d-1], \text{ if } v_i[k-d-1] > 0, \quad (4.14)$$

$$\hat{b}_{r,i}[k] = \hat{b}_{r,i}[k-1],$$
 if  $v_i[k-d-1] \le 0,$  (4.15)

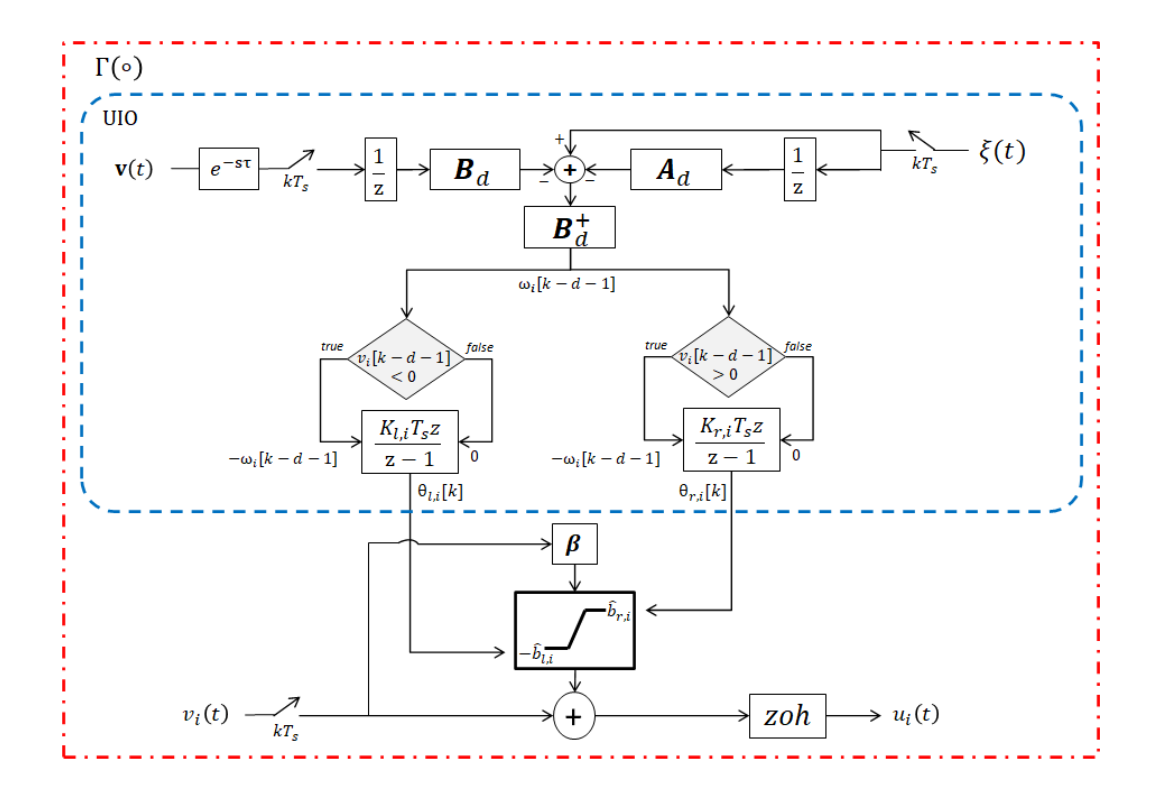


Figure 4.1: Receptance-based discrete adaptive estimator scheme.

in which  $K_{r,i}$  is a gain parameter defined to the computation  $\hat{b}_{r,i}[k]$  if  $v_i[k-d-1] > 0$ . The estimation of  $\hat{b}_{l,i}[k]$  is given by:

$$\hat{b}_{l,i}[k] = \hat{b}_{l,i}[k-1] + K_{l,i}T_s\omega_i[k-d-1], \text{ if } v_i[k-d-1] < 0, \quad (4.16)$$

$$\hat{b}_{l,i}[k] = \hat{b}_{l,i}[k-1],$$
 if  $v_i[k-d-1] \ge 0.$  (4.17)

where  $K_{l,i}$  is also design parameter. The proposed adaptation loop is presented in Fig. 4.1 where  $\theta_{r,i}[k] = \hat{b}_{r,i}[k]$ , and  $\theta_{l,i}[k] = -\hat{b}_{l,i}[k]$ . Notice that in the nominal case without disturbances, if  $\hat{b}_{l,i}[k] = b_{l,i}$ ,  $\hat{b}_{r,i}[k] = b_{r,i}$ , and  $|\beta v_i(k-d)| > \max(|b_{l,i}|,|b_{r,i}|)$ , then  $\omega_i[k-d-1] = 0$ . The main objective is to adapt  $\hat{b}_{l,i}[k]$  and  $\hat{b}_{r,i}[k]$  with an integration loop in order that the integration loop converges if and only of  $\hat{b}_{l,i}[k] \to b_{l,i}$  and  $\hat{b}_{r,i}[k] \to b_{r,i}$ .

Note that, in the proposed scheme represented in Fig. 4.1, there are two inequality blocks that perform the comparison between the virtual control effort signal  $v_i[k-d-1]$  and the estimation error  $\omega_i[k-d-1]$ , to update the  $\hat{b}_{r,i}[k]$  and  $\hat{b}_{l,i}[k]$  signals. For example, for the update of  $\hat{b}_{r,i}[k]$ , whenever the virtual control effort  $v_i[k-d-1]$  is greater than zero, this block performs the update of the

 $\theta_{r,i}[k]$  signal (in this situation, the comparison block will activate the *true* state). Otherwise, the  $\hat{b}_{r,i}[k]$  signal remains with the same value calculated in the previous instant (the comparison block will have a *false* state). The similar conception is applied to the update of  $\hat{b}_{l,i}[k]$ . Besides, the  $sat_i(\beta v_i(t))$  block in dead-zone inverse compensation illustrated in Fig. 4.1 is updated by the  $\hat{b}_{r,i}[k]$  and  $\hat{b}_{l,i}[k]$ , which in turn is based in the adaptive estimation loop.

In this problem, if  $\hat{b}_{l,i}[k]$ ,  $\hat{b}_{r,i}[k]$  are bounded signals, then  $\omega[k]$  is a bounded disturbance, as previously discussed, such that the BIBO stability is respected. The sufficient convergence analysis for  $\hat{b}_{l,i}[k]$  and  $\hat{b}_{r,i}[k]$  at the effective adaptation instants is presented in Appendix C for simplicity.

It is important to highlight that the UIO and the FSP can be designed in a modular way, that is, the design for each approach can be implemented individually, each one based on the specifications of time delay and dead zone to be mitigated.

**Remark 2.** The overall control approach is defined such that any receptance-based design strategy for delay-free models can be applied for second-order systems with input delay and an uncertain input dead zone.

### 4.2 Numerical examples

In this section, the simulation case studies will be presented to illustrate the benefits of the proposed strategy for deal with dead zone and time delay. For that, the  $Simulink^{\mathbb{R}}$  and  $Matlab^{\mathbb{R}}$  environments were used with the purpose of obtaining the results.

### **4.2.1** Test case I: a marginally stable vibrating system

This test case is based on the example presented by [32] and discussed in [5] for a receptance-based FSP approach. The system matrices are the

$$\mathbf{M} = \begin{bmatrix} 1 & 0 \\ 0 & 1 \end{bmatrix}, \quad \mathbf{C} = \begin{bmatrix} 1 & -1 \\ -1 & 1 \end{bmatrix}, \quad \mathbf{K} = \begin{bmatrix} 3 & -2 \\ -2 & 3 \end{bmatrix}$$

and a influence matrix  $\mathbf{B} = \begin{bmatrix} 1 & 0 \end{bmatrix}^T$ . In this problem, open-loop eigenpairs are  $\lambda_{1,2} = \pm i$  and  $\lambda_{3,4} = -1 \pm 2i$ . The method presented on [32] is applied to reassign

the first eigenpair to the position  $\mu_{1,2} = -1 \pm i$  (inside of left-half complex plan), while the second eigenpair is not modified. The original gains, defined for the system without delay, designed in [31] by partial pole placement are given by  $\mathbf{F}_1 = [-2 \quad -2]$  and  $\mathbf{G}_1 = [-1 \quad -1]$ . The time delay is setting as  $\tau = 5s$  and the feedback matrices designed to this time delay using the approach of [32] are  $\mathbf{F}_2 = [-0.0103 \quad -0.0103]$  and  $\mathbf{G}_2 = [-0.0213 \quad -0.0213]$ . The filter applied in FSP receptance-based method described on [5] was implemented for  $\tau_f = 0.5$  (free tuning filter parameter, based on [5]) and considering the resonant frequency  $\omega_r = 1 rad/s$ , resulting in

$$\phi(s) = \frac{-0.3894s^2 + 0.1503s + 1}{(0.5s + 1)^3}$$

where filter  $\phi(s)$  designing can be found in the Appendix B, and  $\delta=10^{-5}$  to obtain a perturbed open-loop receptance transfer matrix  $\mathbf{H}_{\Delta}(s)$  [5] and allow the application of the BIBO stability for open-loop stable marginally systems. The initial conditions for displacement and velocity are, respectively,  $\mathbf{x}(0)=[3\ 1]^T m$  and  $\dot{\mathbf{x}}(0)=[0.2\ 0.1]^T m/s$ . The  $Simulink^{(\mathbb{R})}$  default ode45 integration method ordinary differential equation (ODE) solver was chosen for simulation model. Throughout the test case I, for discrete UIO adaptive scheme, an asymmetrical dead zone is considered with the actual dead-zone limits  $b_{r,1}=+0.9$  and  $b_{l,1}=-0.75$ ; the initial value of estimated dead-zone limits for adaptive algorithms was defined as +1.4 and -1.4 to  $b_{r,1}$  and  $b_{l,1}$ , respectively. The sample time was defined as  $T_s=0.1s$  (value smaller than the Nyquist sampling time criteria, based on fastest dynamics of the system);  $\beta=10^6$  ( $\beta\gg1$  to mitigate chattering); and the adaptive constant gains were  $K_{l,1}=K_{r,1}=0.15$ . For UIO discrete observer approach, the discrete-system augmented state observer matrices  $\mathbf{A}_d$ ,  $\mathbf{B}_d$  and  $\mathbf{B}_d^+$  obtained are given by:

$$\mathbf{A}_{d} = \begin{bmatrix} 0.9858 & 0.0092 & 0.0949 & 0.0050 \\ 0.0092 & 0.9858 & 0.0050 & 0.0949 \\ -0.2746 & 0.1748 & 0.8960 & 0.0990 \\ 0.1748 & -0.2746 & 0.0990 & 0.8960 \end{bmatrix}, \quad \mathbf{B}_{d} = \begin{bmatrix} 0.0048 \\ 0.00016 \\ 0.0949 \\ 0.0050 \end{bmatrix},$$

$$\mathbf{B}_{d}^{+} = \begin{bmatrix} 0.5339 & 0.0184 & 10.4861 & 0.5501 \end{bmatrix}$$

For the sake of comparison and to illustrate the relevance of the proposed approach, an adaptive scheme proposed by [15] for an unknown dead zone also will

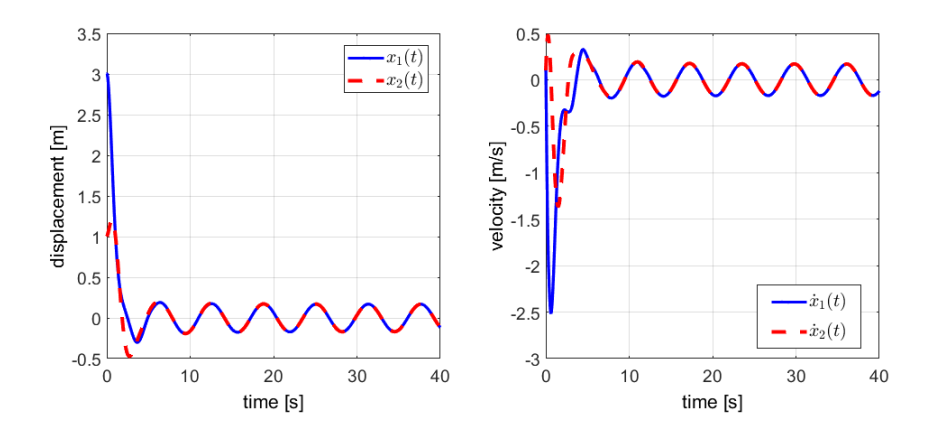


Figure 4.2: Displacement and velocity responses in the test case I with dead-zone nonlinearity and no time delay.

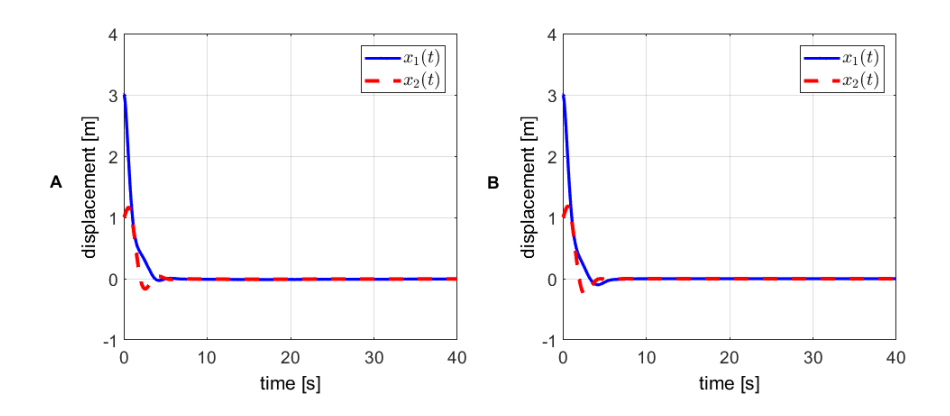


Figure 4.3: Displacement responses in test case I with dead zone and no time delay: (A) UIO approach dead-zone compensation. (B) Adaptive scheme by [15] for dead-zone compensation.

be simulated. This approach takes the  $\mathbf{v}(t)$  and the modified or known effective control signal  $\overline{\mathbf{u}}(t)$  for estimating the unknown dead-zone parameters, with integral action update law on the adaptive scheme. In the approach proposed in this work, the UIO adaptive scheme is based on state vector  $\xi(t)$  and  $\mathbf{v}(t)$  control signal, both accessible for measuring, which can be considered an advantage in terms of practical applications.

Thus, the dead-zone effect on displacement and velocity signals with no time delay is depicted in Fig.4.2. A bounded disturbance is observed in steady-state and

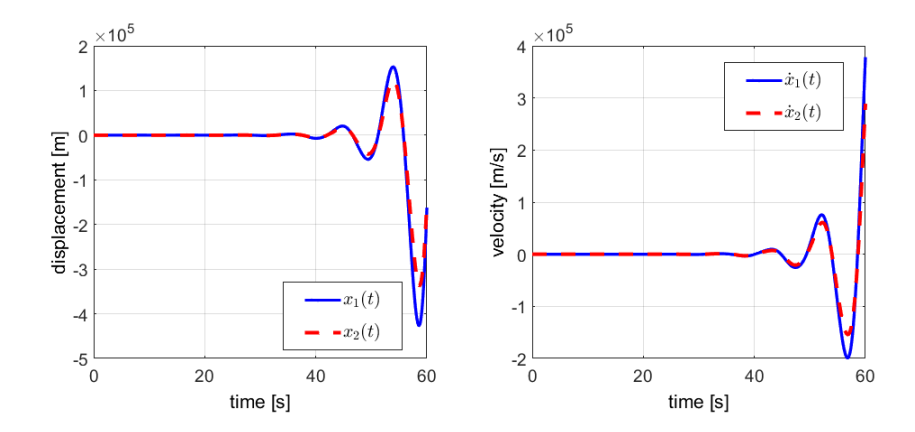


Figure 4.4: Displacement and velocity responses in test case I with no time-delay compensation.

in Fig.4.3 the adaptive methods - the proposed and that in [15] - are applied to the system with an asymmetrical dead zone; both the schemes mitigate the dead-zone effect, illustrating the effectiveness of discrete-time UIO adaptive approach.

The time-domain performances for displacement and velocity under time-delay  $\tau = 5s$  influence, without dead zone, are displayed in Fig.4.4, where it verifies an unstable behavior due to delay presence. Thus, for dealing with time-delay compensation, the  $\mathbf{F}_2$  and  $\mathbf{G}_2$  matrices were applied with a dead-zone adaptive scheme [15], where the displacement response is displayed in Fig.4.5(A), which is possible to verify that the approach [32] degrades the time-domain performance, in comparison with displacement time response in Fig.4.5(B), which the FSP with dead-zone adaptive scheme [15] is applied for  $b_{r,1}$  and  $b_{l,1}$  defined above. As expected, the FSP mitigates the time-delay negative effect. These results are very important to show the main advantage of the proposed approach as the controller gains of the main control law are not delay-dependent. In contrast to [32], for instance, the nominal closed-loop poles are not modified. The main consequence of the new design required in related works is the closed-loop response degradation due to the new pole placement.

In Fig.4.6 and Fig.4.7, the displacement and velocity with FSP and discrete-time UIO adaptive scheme are depicted, respectively, for several dead-zone break-points initial values set,  $b_{r,1} = \{0, +1.4, +2\}$  and  $b_{l,1} = \{0, -1.4, -2\}$ . Note that the steady-state responses are not affected by the choice of the different dead-

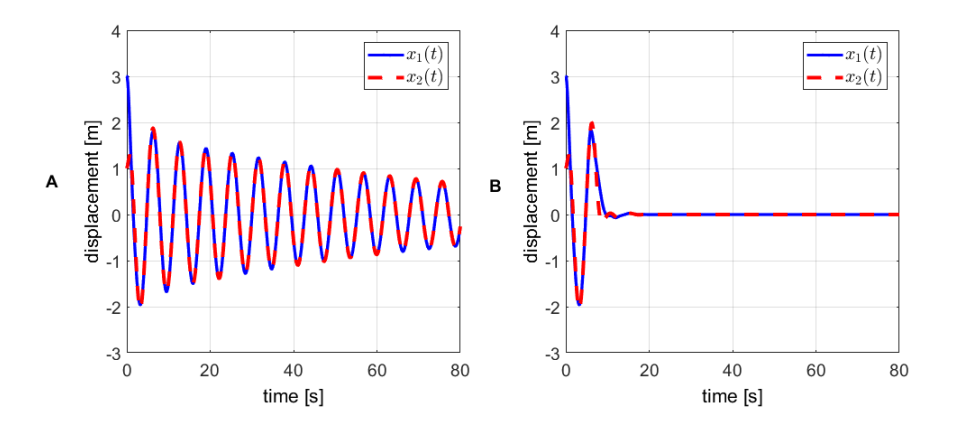


Figure 4.5: Displacement responses in test case I: (A)  $\mathbf{F}_2$  and  $\mathbf{G}_2$  matrices designed for time delay  $\tau = 5s$  and adaptive scheme [15]. (B) FSP and adaptive scheme [15].

zone initial guess limits, considering the approach proposed, including time-delay presence, which is mitigated by FSP.

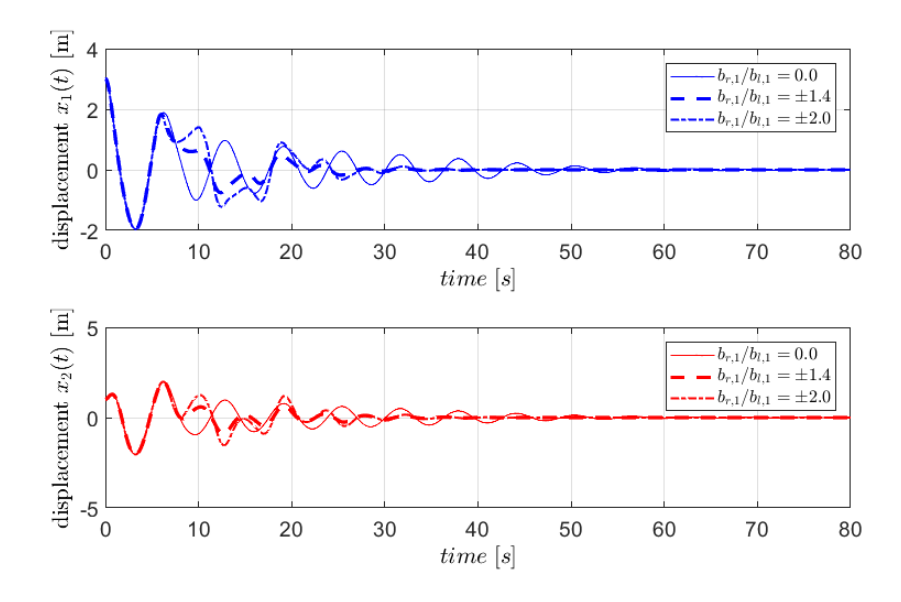


Figure 4.6: Displacement responses  $x_1$  and  $x_2$  for Test case I with the FSP and UIO adaptive dead-zone compensation approach for several dead-zone initial values.

It is important to note that, as previously discussed in [5], the FSP was effective to keep closed-loop stability as expected from the system without delay. Also, it is possible to verify that the dead-zone effect is mitigated without affecting closed-

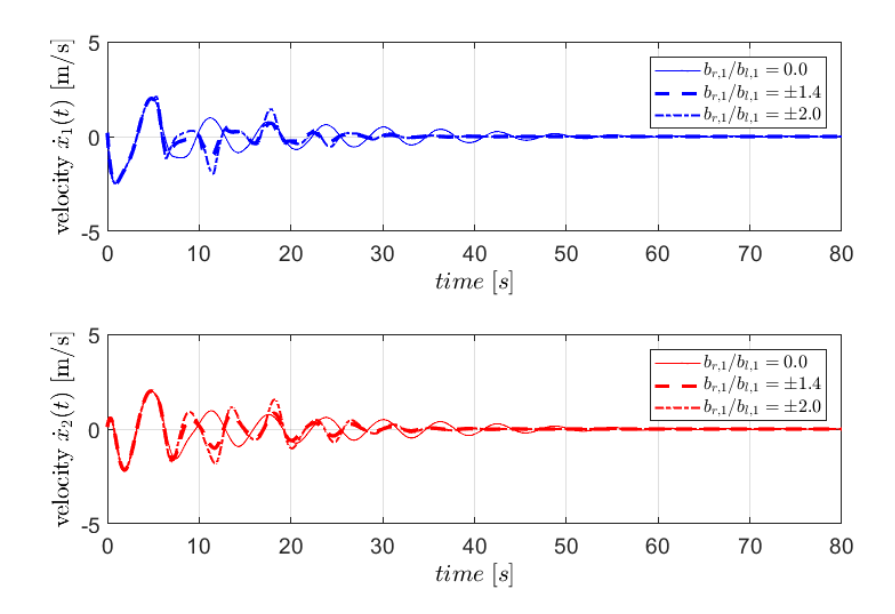


Figure 4.7: Velocity responses  $v_1$  and  $v_2$  for Test case I with the FSP and UIO adaptive dead-zone compensation approach for several dead-zone initial values.

loop stability as seen expected, as a consequence of accurate estimation related to asymmetrical dead-zone break-points  $b_{r,1}$  and  $b_{l,1}$  displayed in Fig.4.8, that illustrate dead-zone estimations for several initial dead-zone values.

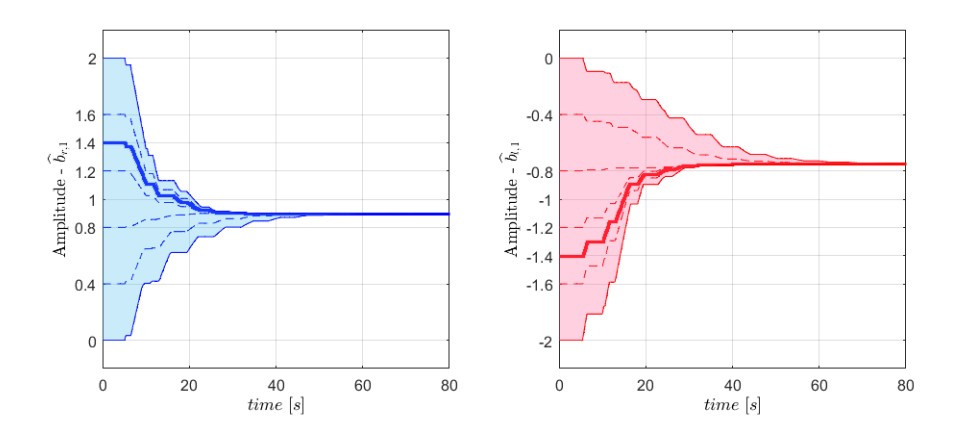


Figure 4.8: Dead-zone estimation parameters under UIO approach for several dead-zone initial values in Test case I.

The convergence related to FSP and UIO approaches can also be seen through discretized estimation error signal  $\omega_i[k]$ , presented in Fig. 4.9. Note that there is

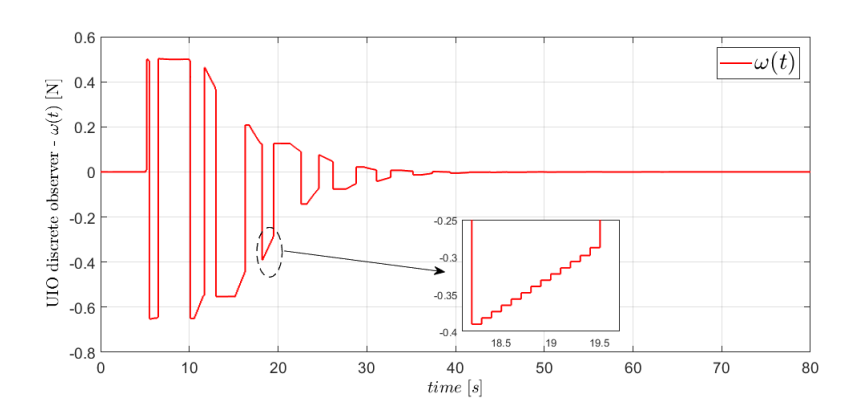


Figure 4.9: Estimation signal for discrete observer for the system of Test case I.

a switching behavior along the signal  $\omega_i[k]$  until the dead-zone influence is not mitigated, which directly implies on  $\omega_i[k] \to 0$  if that disturbance is mitigated from state vector  $\xi(t)$ .

In Fig.4.10 is presented a comparison between closed-loop control effort signals  $\mathbf{v}(t)$  and  $\overline{\mathbf{u}}(t)$ , considering the dead-zone presence and the complete approach (FSP and discrete observer UIO dead-zone compensation), where it verifies that  $[\overline{\mathbf{u}}(k-d-1)-\mathbf{v}(k-d-1)] \to 0$  when dead-zone break-points  $\widehat{b}_{r,1}[k] \to b_{r,1}$  and  $\widehat{b}_{l,1}[k] \to b_{l,1}$ . As also explained in [5], [6], the transient performance of the time-domain responses (displacement, velocity, control effort, etc.) can be adjusted by the  $\tau_f$  free parameter, handling the trade-off between this transient and steady-state attenuation. The smaller the value of  $\tau_f$ , the greater will be the amplitude of the time responses on transient performance and vice versa.

To evaluate the robustness of the proposed approach, consider a modified version to  $\mathbf{M}$ ,  $\mathbf{C}$  and  $\mathbf{K}$  presented in [2.1], given by, respectively,  $\mathbf{M}_r = \mathbf{M} \pm \alpha_M \mathbf{M}$ ,  $\mathbf{C}_r = \mathbf{C} \pm \alpha_C \mathbf{C}$ ,  $\mathbf{K}_r = \mathbf{K} \pm \alpha_K \mathbf{K}$ ,  $\alpha_M$ ,  $\alpha_C$ ,  $\alpha_K \in \mathbb{R}$  and  $|\alpha_M|$ ,  $|\alpha_C|$ ,  $|\alpha_K| \ll 1$ . Besides, also considering a modified time delay  $\tau_r = \tau \pm \alpha_r \tau$ ,  $\alpha_r \in \mathbb{R}$  and  $|\alpha_r| \ll 1$ . These proposed modifications will represent the modeling error related to  $\mathbf{M}$ ,  $\mathbf{C}$ ,  $\mathbf{K}$ , and  $\tau$ , different from those used for both the UIO and predictor design. In Fig.4.11, is depicted the time-domain response to displacement and velocity, considering  $\alpha_M = \alpha_C = \alpha_K = \alpha_r = +0.05$ , illustrating that the mechanism approach (despite being designed for the case without modeling error) has a robustness margin to allow the convergence of states to the origin even with modeling error.

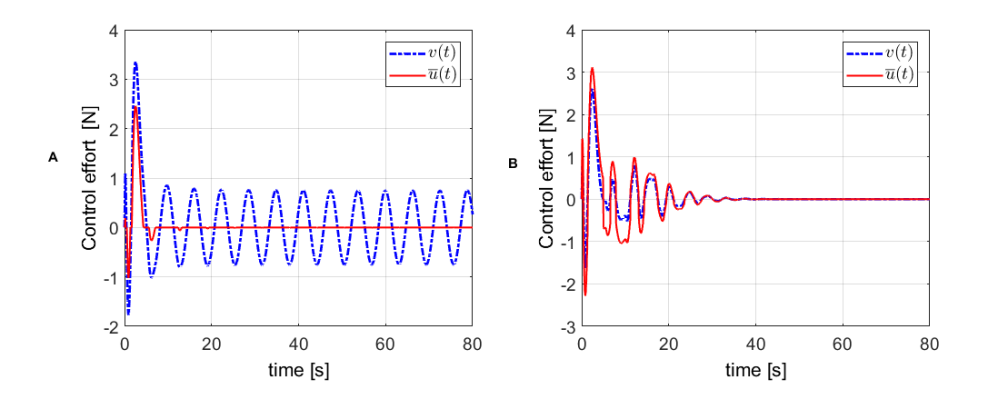


Figure 4.10: Comparison of control effort for the system in Test case I: (A) Closed-loop with dead-zone influence. (B) Closed-loop system with FSP and UIO discrete observer dead-zone compensation approach.

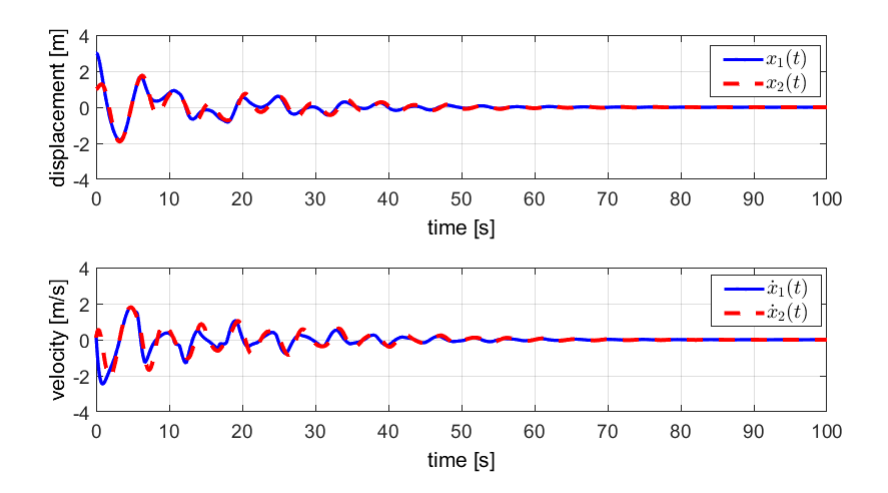


Figure 4.11: Displacement and velocity responses in the test case I with modeling error for receptance matrices and time delay.

Besides, to better illustrate the modeling error influence over the approach, in Fig.4.12, Fig.4.13 ,Fig.4.14 and Fig.4.15, are displayed the displacement time-responses considering the modeling error for a symmetric range of values, respectively: (i) the matrix M, for  $\alpha_M = -0.20$  and  $\alpha_M = +0.20$ ; (ii) the matrix C, for limit values  $\alpha_C = -0.25$  and  $\alpha_C = +0.25$ ; (ii) the matrix K, for  $\alpha_K = -0.25$  and  $\alpha_K = +0.25$ ; (iv)  $\tau$ , for  $\alpha_r = -0.08$  and  $\alpha_r = +0.08$ . The main purpose is to evaluate the modeling error contribution for each variable from receptance ma-

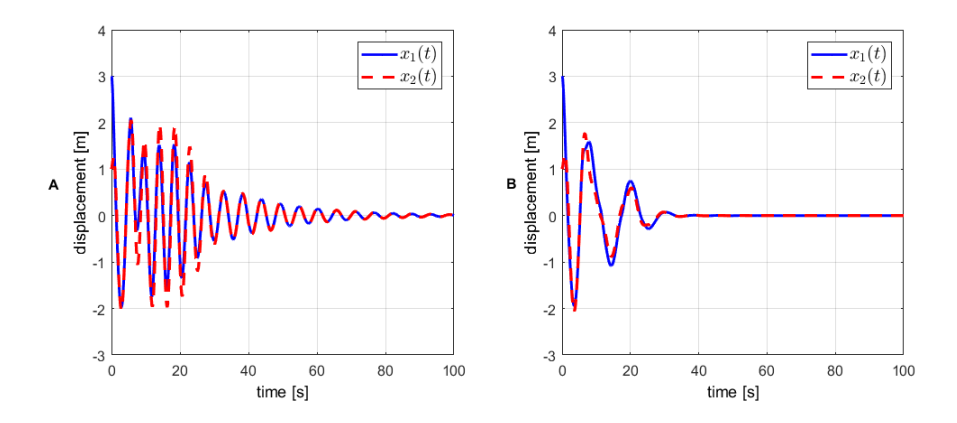


Figure 4.12: Displacement responses in the test case I with modeling error for M matrix: (A) For  $\alpha_M = -0.20$ ; (B) For  $\alpha_M = +0.20$ .

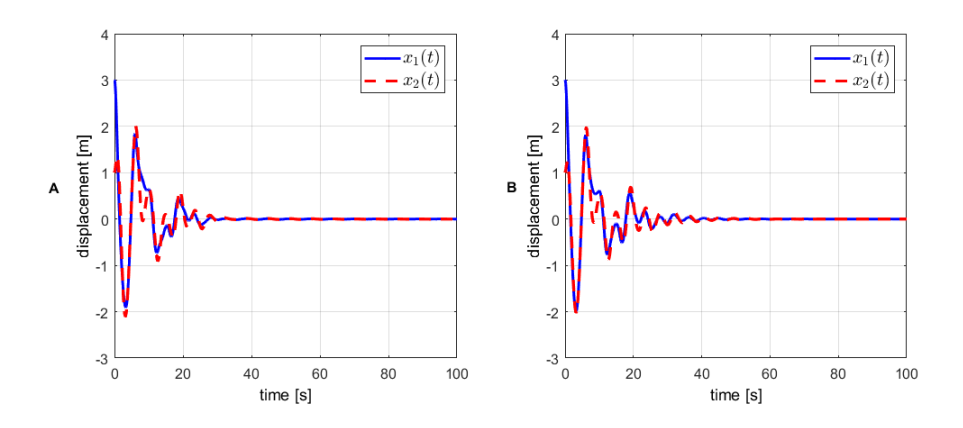


Figure 4.13: Displacement responses in the test case I with modeling error for C matrix: (A) For  $\alpha_C = -0.25$ ; (B) For  $\alpha_C = +0.25$ .

trix (**M**, **C** and **K**) and relative to the time delay, also considering that these limit values described above can represent estimating errors related to the real systems under study, from a practical point of view. Note that, similar to the results in Fig.4.11, the approach presents a good margin of robustness, allowing significant variations in the **M**, **C**, **K** matrices and in time delay  $\tau$ . It is important to emphasize that values outside the analyzed limit values for  $\alpha_M$ ,  $\alpha_C$ ,  $\alpha_K$  and  $\alpha_r$  can lead to a greater transient than the depicted, for example, in Fig.4.12(A) and Fig.4.15, as expected.

To verify, via simulation, the effect of additive noise on the proposed approach, it was considered the use of the white noise block, in the  $Simulink^{\mathbb{R}}$  environment,

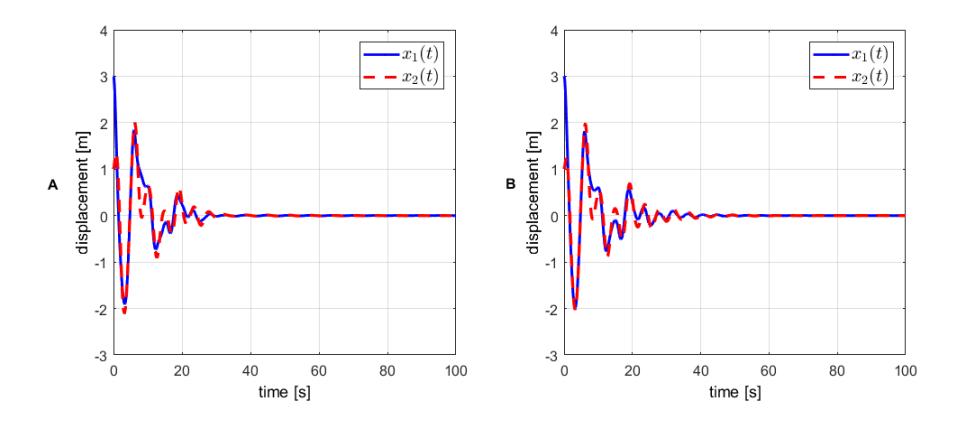


Figure 4.14: Displacement responses in the test case I with modeling error for **K** matrix: (A) For  $\alpha_K = -0.25$ ; (B) For  $\alpha_K = +0.25$ .

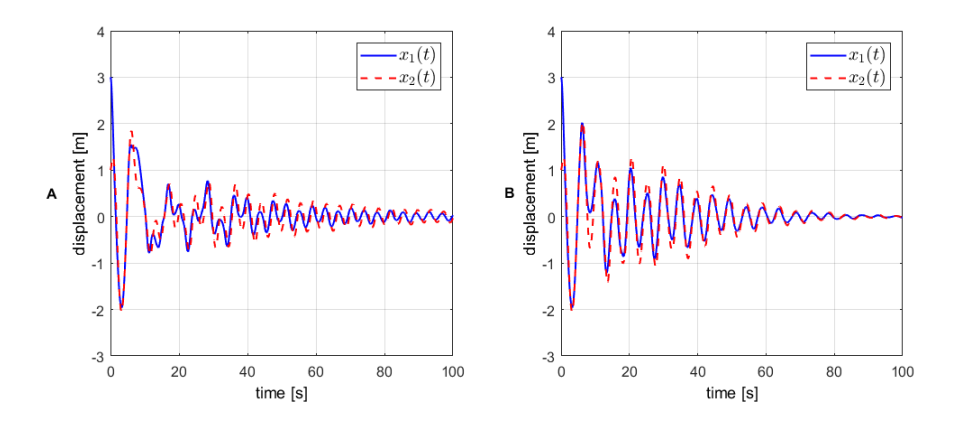


Figure 4.15: Displacement responses in the test case I with modeling error for time delay  $\tau$ : (A) For  $\alpha_r = -0.08$ ; (B) For  $\alpha_r = +0.08$ .

associated individually for each displacement and velocity signals measured at output of the system. The additive noise was configured as follows: (i) noise power on  $10^{-3}W$ , chosen in such as to allow a quantitative evaluation of the influence of noise on the effective measurement of state vector, in closed-loop analysis; (ii) sample time equals 0.1s (value smaller than the Nyquist sampling time criteria, based on fastest dynamics of the system); (iii) the starting seed for the random number generator in this block was defined with distinct seed parameters values for each displacement and velocity signals, for representation of sensors with uncorrelated noises. Fig.4.16 illustrates the noise signals additive used for each effective position signal and system speed. In Fig.4.17, the displacement and

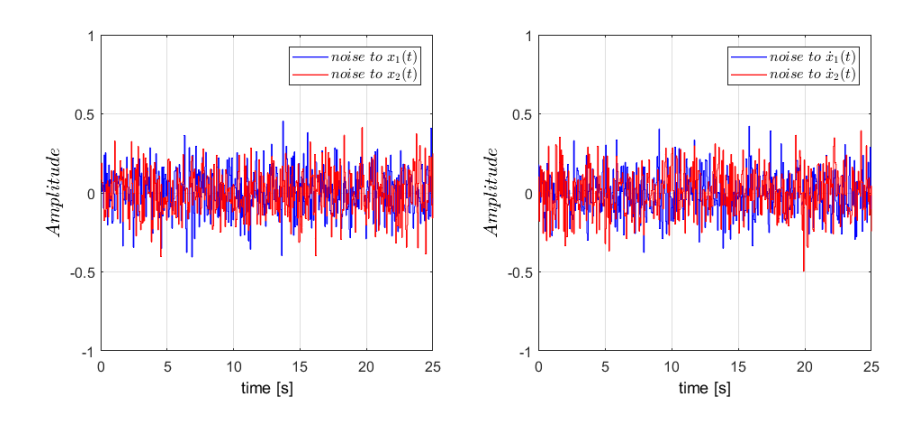


Figure 4.16: Noise signals in the test case I for displacement and velocity measurements.

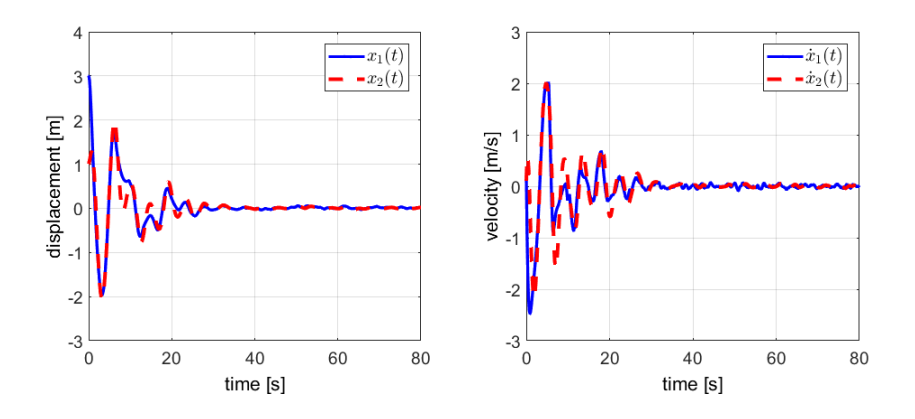


Figure 4.17: Displacement and velocity responses in the test case I under influence of additive noise.

velocity responses are illustrated, including the additive noise, whose signals are minimally affected by the presence of noise, compared with the dynamics shown in Fig.4.11, due to the closed-loop low-pass filtering behavior between the noise and the effective values of displacement and velocity. Besides, the dead-zone estimation is displayed in Fig.4.18, where the proposed approach minimizes the influence of measurement noise in the steady-state, giving a good estimation for  $b_{r,1}$  and  $b_{l,1}$ . In short, the proposed strategy behaves as expected in the presence of measurement noise.

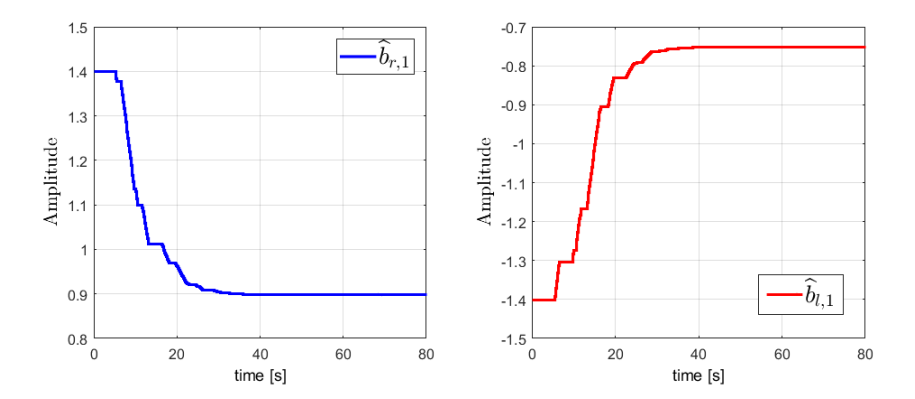


Figure 4.18: Dead-zone estimation parameters under the proposed approach and additive noise for the system in Test case I.

## **4.2.2** Test case II: a multiple-input marginally stable vibrating system

This test case is based on the same system presented in the test case I, where open-loop eigenpairs are  $\lambda_{1,2} = \pm i$  and  $\lambda_{3,4} = -1 \pm 2i$ . The influence matrix **B** is now defined to consider the existence of two actuators in the system whose distribution is given by

$$\mathbf{B} = \left[ \begin{array}{cc} 1 & 1 \\ 2 & 0 \end{array} \right]$$

and the partial pole placement for multiple input systems based on the receptance matrix system is applied to reassign the first eigenpair to the position  $\mu_{1,2} = -1 \pm i$ , while the second eigenpair is not modified, similar to test case I, considering that  $\alpha_{\mu_k,1} = \alpha_{\mu_k,2} = \begin{bmatrix} 1 & 0.5 \end{bmatrix}^T$ , resulting in:

$$\mathbf{F} = \begin{bmatrix} -0.5714 & -0.5714 \\ -0.2857 & -0.2857 \end{bmatrix}, \quad \mathbf{G} = \begin{bmatrix} -0.2857 & -0.2857 \\ -0.1429 & -0.1429 \end{bmatrix}$$

where the time delay is set as  $\tau = 5s$ ,  $\delta = 10^{-6}$  to obtain a perturbed open-loop receptance transfer matrix  $\mathbf{H}_{\Delta}(s)$  and the filter applied is the same as the test case I. To evaluate the UIO discrete adaptive scheme proposed, were considered an asymmetrical dead zone as follows: (i)  $b_{r,1} = +1.1$  and  $b_{l,1} = -0.7$  to first input; (ii)  $b_{r,2} = +0.9$  and  $b_{l,2} = -0.6$  to second input; (iii) the initial value to adaptive dead-zone algorithm was defined as +1.5 to  $b_{r,1}$  and  $b_{r,2}$ , respectively, and -1.5

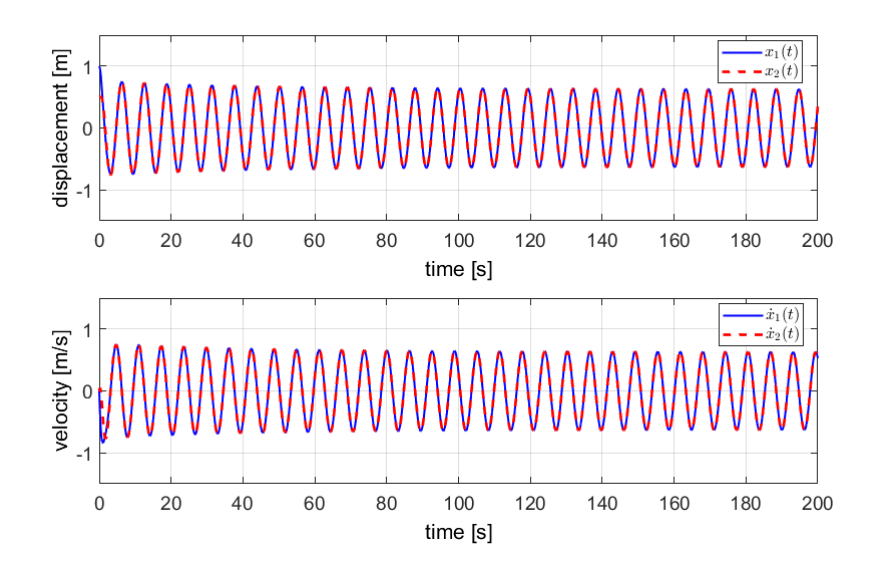


Figure 4.19: Dead-zone effect on time-domain response for the system in Test case II.

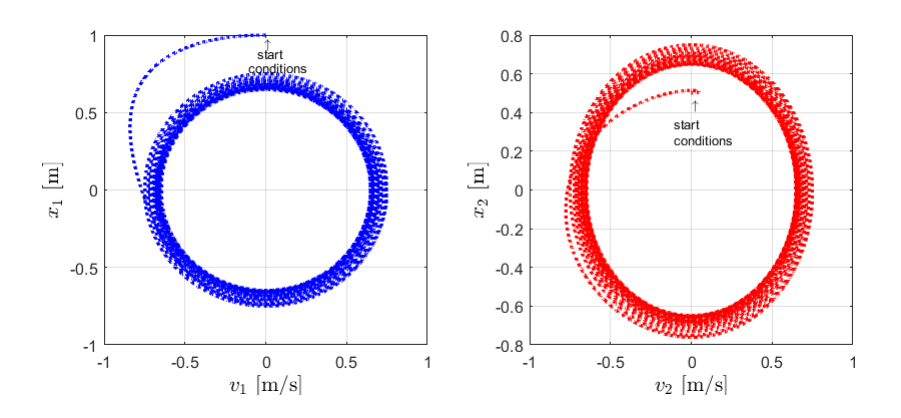


Figure 4.20: Phase portrait plane under dead-zone influence, for the system in Test case II.

to  $b_{l,1}$  and  $b_{l,2}$ , respectively. The *Simulink*<sup>®</sup> default ode45 integration method also was applied for this test case, similar to test case I. For the discrete-time UIO, the sample time was defined  $T_s = 0.1s$  (similar to test case I),  $\beta = 10^6$  ( $\beta \gg 1$  to mitigate chattering), the adaptive constant gains  $K_{l,i} = K_{r,i} = 0.15$  and initial conditions for displacement and velocity are, respectively,  $\mathbf{x}(0) = \begin{bmatrix} 1 & 0.5 \end{bmatrix}^T m$  and  $\dot{\mathbf{x}}(0) = \begin{bmatrix} 0 & 0 \end{bmatrix}^T m/s$ .

In Fig.4.19, the time-domain performances for the displacement and velocity

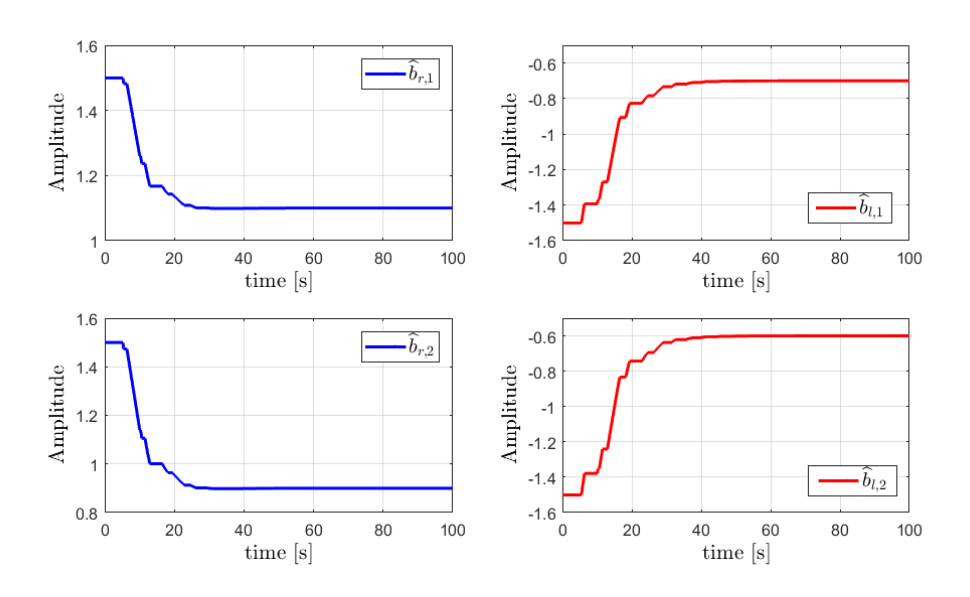


Figure 4.21: Dead-zone estimation parameters under the proposed approach for the system in Test case II.

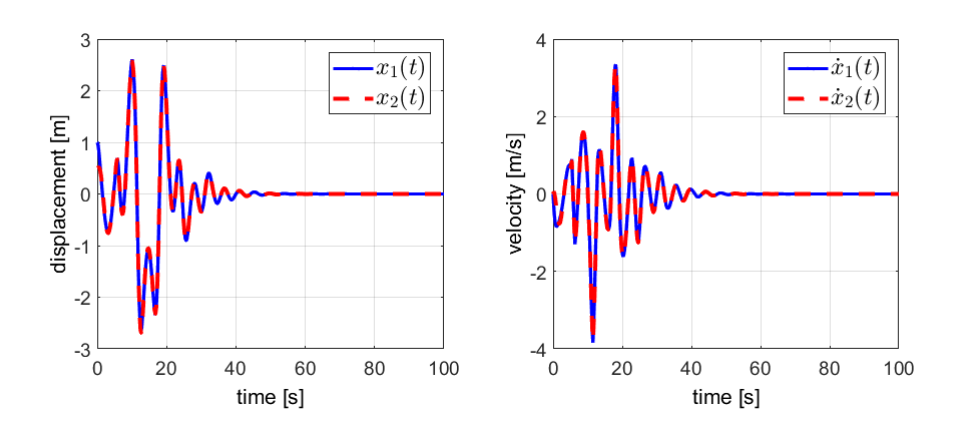


Figure 4.22: Time-domain response with FSP and UIO discrete observer approach for the system in Test case II.

under the dead-zone influence are displayed, also considering time-delay and FSP approach compensation. The dead-zone influence also can be seen in Fig.4.20, where the cyclic steady-state for displacement and velocity, with initial conditions, are displayed by the phase portrait.

The dead-zone break-points estimation for the first input ( $b_{r,1}$  and  $b_{l,1}$ ) and the second input ( $b_{r,2}$  and  $b_{l,2}$ ) is displayed in Fig. 4.21. Based on accurate time es-

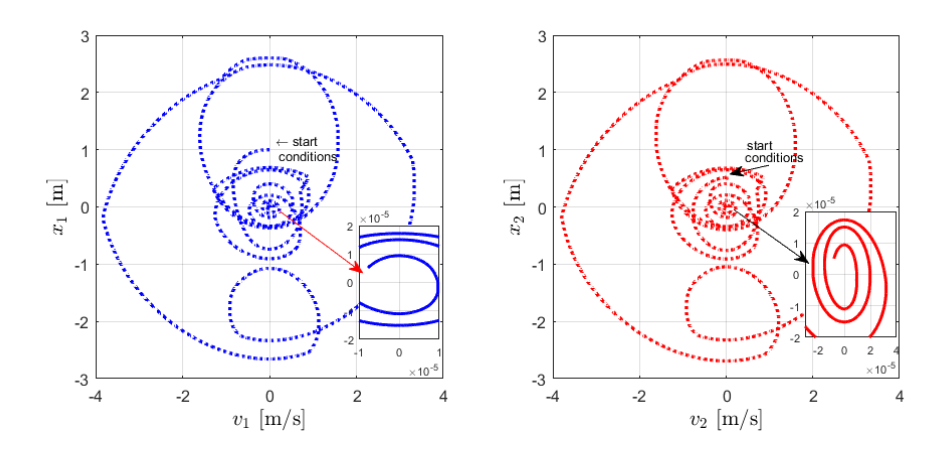


Figure 4.23: Phase-portrait plane under the proposed approach for the system in Test case II.

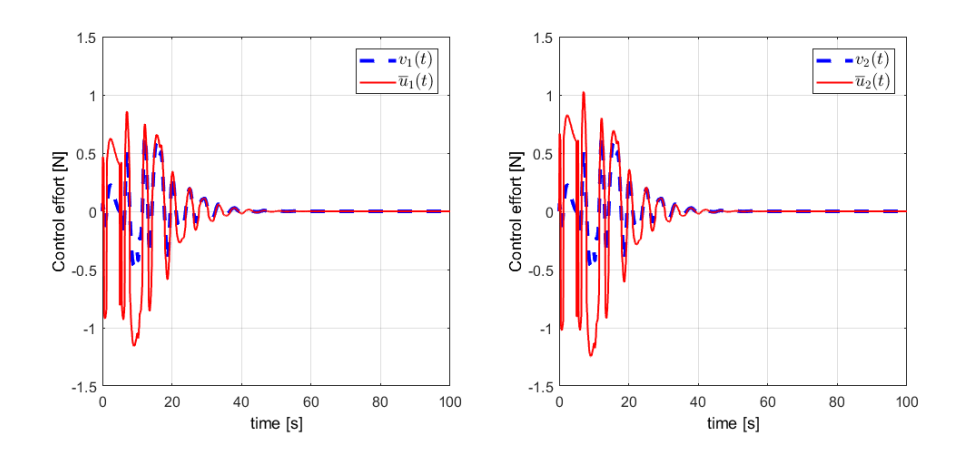


Figure 4.24: Closed-loop control effort for the system in Test case II, with FSP and UIO discrete observer dead-zone compensation approach.

timation responses for dead-zone break-points calculation, it is important to highlight that the discrete observer approach also can be applied for multi-input systems, keeping stability and convergence characteristics predicted in the proposed approach.

In Fig. 4.22, time-domain performance under the asymmetrical dead-zone inverse compensation approach is displayed, as it is possible to verify that dead-zone effects for both inputs are mitigated, without affecting closed-loop stability, as seen expected, as a consequence of accurate estimation for dead-zone break-

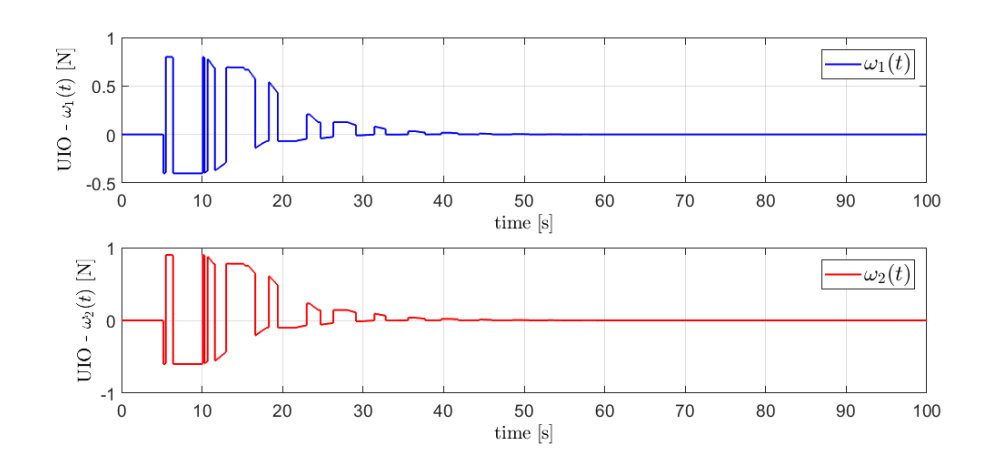


Figure 4.25: Estimation signals  $\omega_1$  and  $\omega_2$  for discrete observer for the system of Test case II.

points  $b_{r,1}$ ,  $b_{l,1}$ ,  $b_{r,2}$  and  $b_{l,2}$ . In Fig.4.23, the phase portrait, under the proposed approach, is displayed, where the trajectories converge for an equilibrium point, near the origin of the plane, also verifying the accurate estimation for the dead-zone break-points parameters.

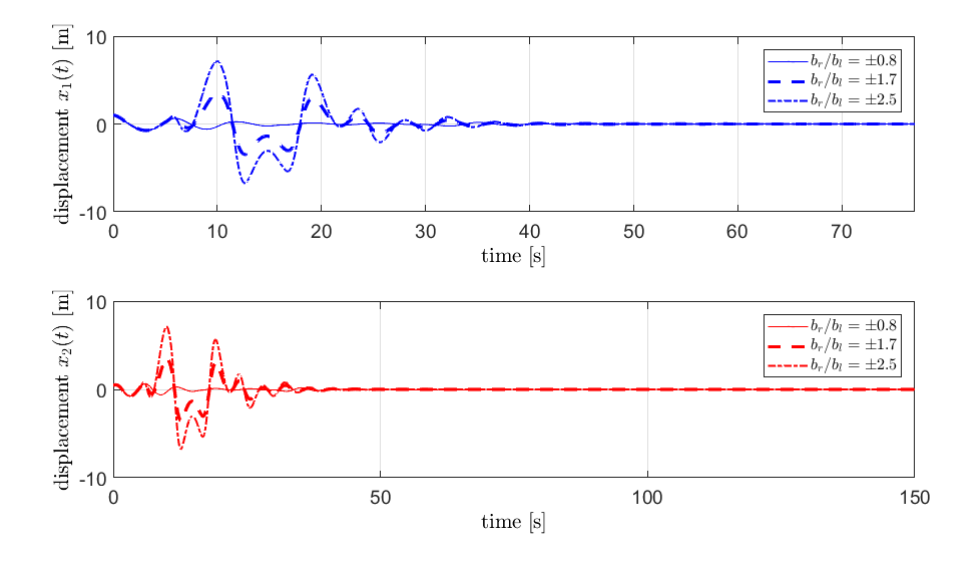


Figure 4.26: Displacement responses  $x_1$  and  $x_2$  for Test case II with the FSP and UIO adaptive dead-zone compensation approach for several dead-zone initial values.

In Fig. 4.24 is illustrated closed-loop control effort for the complete approach

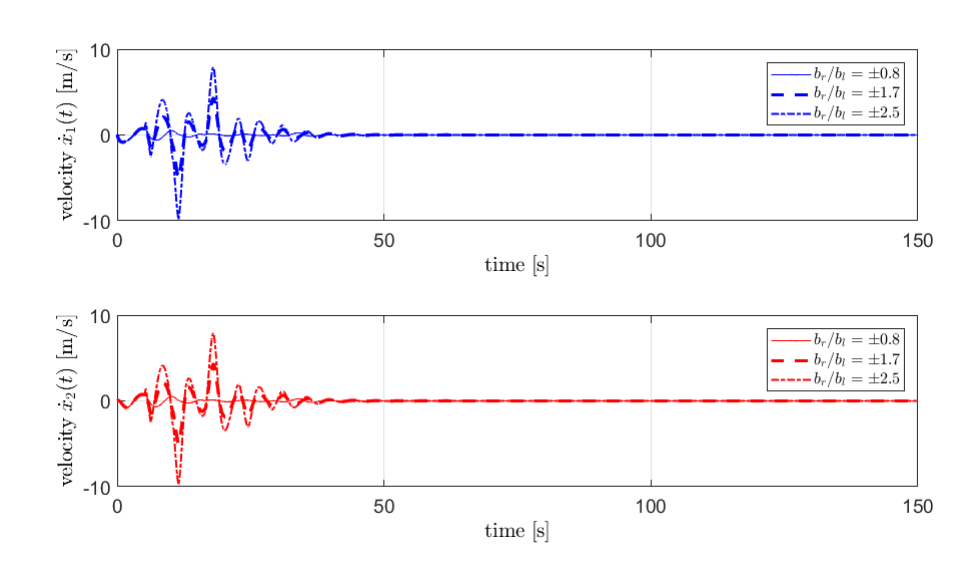


Figure 4.27: Velocity responses  $x_1$  and  $x_2$  for Test case II with the FSP and UIO adaptive dead-zone compensation approach for several dead-zone initial values.

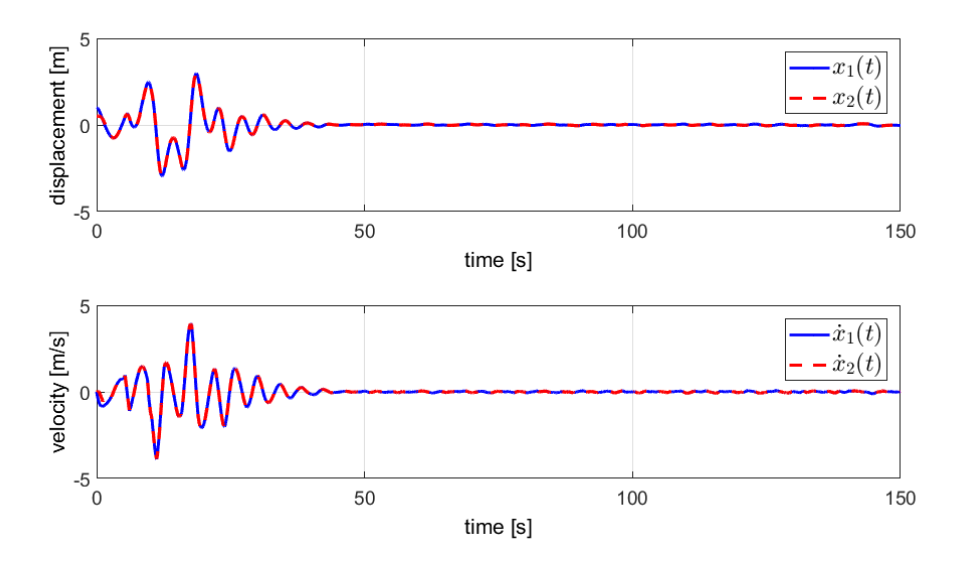


Figure 4.28: Displacement and velocity responses in the test case II with modeling error and additive noise.

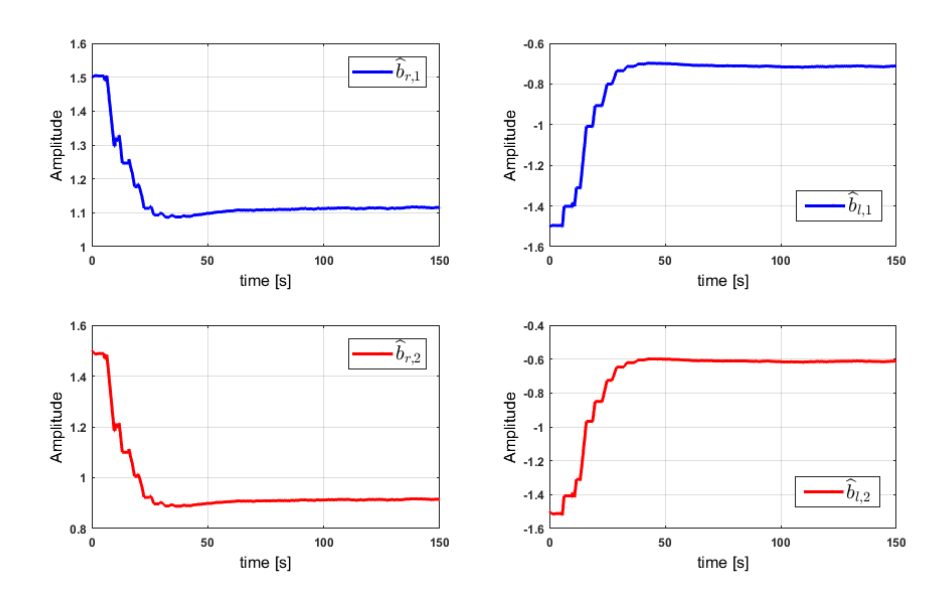


Figure 4.29: Dead-zone estimation parameters under the proposed approach for the system in Test case II with modeling error and additive noise.

(FSP and discrete observer dead-zone compensation), where it verifies, for both inputs, that signals  $\mathbf{v}(t)$  and  $\overline{\mathbf{u}}(t)$  tend to zero, as a consequence of estimation errors for the dead-zone break points decrease to zero, due to discrete observer approach and its correct designing. As expected, this convergence for dead-zone estimation is illustrated in Fig.4.23, where the UIO estimating signals  $\omega_i \to 0$  when the presence of dead-zone influence is mitigated from the inputs of the system.

In Fig.4.26 and Fig.4.27, the displacement and velocity with FSP and discretetime UIO adaptive scheme are depicted, respectively, for several dead-zone breakpoints initial values sets, where  $b_r = \{+0.8, +1.7, +2.5\}$  and  $b_l = \{-0.8, -1.7,$  $-2.5\}$ . Note that the steady-state responses are not affected by choosing the different dead-zone initial guess limits, considering the approach proposed, including time-delay presence, which is mitigated by FSP.

The time-domain response for displacement and velocity, considering a modeling error such as  $\alpha_M = -0.05$ ,  $\alpha_C = +0.07$   $\alpha_K = -0.05$ ,  $\alpha_r = -0.02$  and the presence of an additive noise at displacement and velocity measurements, similar to the test case I, is illustrated in Fig.4.28. The additive noise was configured as

follows: (i) noise power  $10^{-3}W$ ; (ii) sample time equals 0.1s and (iii) distinct seed parameter values for each signal, for representation of sensors with uncorrelated noises. As illustrated, the signals are minimally affected, compared with the dynamics shown in Fig.4.22. Besides, the dead-zone break-points estimations  $b_r$  and  $b_l$  illustrated in Fig.4.29 are also minimally affected under this condition, as expected, and the proposed approach has a relevant robustness margin.

#### 4.2.3 Test case III: a two-link robot arm

This example consisted of a two-link flexible robot arm illustrated in Fig. 4.30 and was employed in [2], [62] as a benchmark for vibration control analysis. The matrices of the model were obtained analytically and validated through an experimentally identified receptance in both works and can be considered a prototype of real-world engineering application, such as pick and place robotic task. This system has 2 DoFs, comprising the absolute rotations  $\theta_1$  and  $\theta_2$ , both in rad. The joint A is actuated through the torque  $T_m$  (N/m) by a DC motor, and joint B is passive, with a torsional spring  $k_s$ . The  $Simulink^{\mathbb{R}}$  default ode45 integration method was applied for this test case. Based on the experimental approach developed in [2], the M, C, K and B matrices are

$$\mathbf{M} = \begin{bmatrix} 0.047 & 0.0002767 \\ 0.0002767 & 0.000168 \end{bmatrix}, \quad \mathbf{C} = \begin{bmatrix} 0.012 & 0.0004 \\ 0.0004 & 0.0003 \end{bmatrix},$$
$$\mathbf{K} = \begin{bmatrix} 0.4624 & -0.1772 \\ -0.1772 & 0.1932 \end{bmatrix}, \quad \mathbf{B} = \begin{bmatrix} 1 \\ 0 \end{bmatrix}.$$

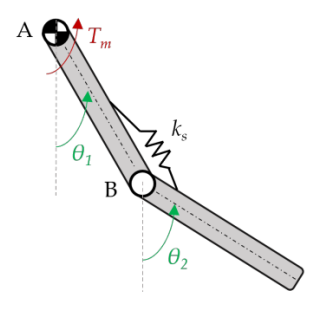


Figure 4.30: The two-link flexible robot arm and its kinematic scheme [2] for Test case III.

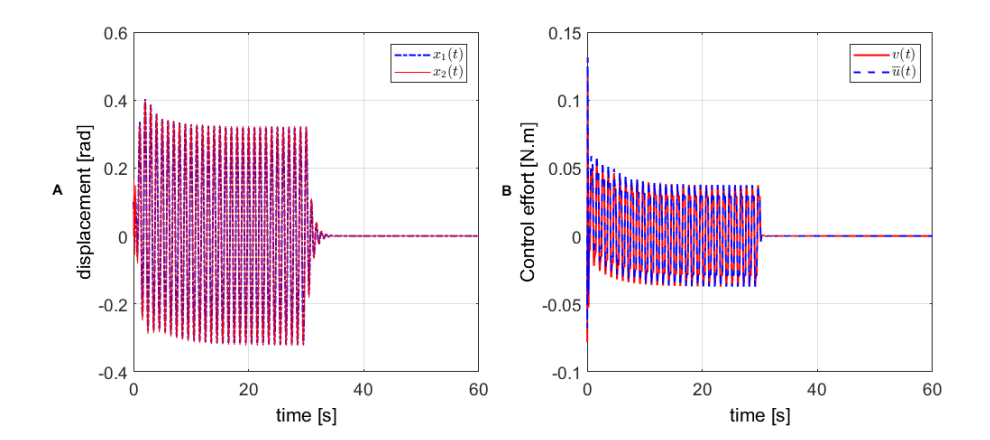


Figure 4.31: Time-domain responses with FSP and UIO discrete observer approach for the system in Test case III: (A) Displacement; (B) Closed-loop control effort.

where the first open-loop eigenpair is  $\lambda_{1,2} = -1.0382 \pm 38.2093i$  and the second eingepair is  $\lambda_{3,4} = -1.1966 \pm 7.3248i$ . The first eigenpair is reassigned to the position  $\mu_{1,2} = -10 \pm 20i$ , while the second eigenpair is not modified, where state feedback gains obtained are

$$\mathbf{F} = \begin{bmatrix} -0.0279 & 0.0297 \end{bmatrix}, \quad \mathbf{G} = \begin{bmatrix} 1.5767 & -1.5038 \end{bmatrix}$$

and the time delay is setting as  $\tau = 0.1s$ . The filter applied in FSP receptance-based method described on [5] was implemented for  $\tau_f = 0.02$  and considering resonant frequency  $\omega_r = 38.2093 rad/s$ , resulting in

$$\phi(s) = \frac{-0.0005130s^2 - 0.02523s + 1}{(0.02s + 1)^3}$$

Now, consider an existence of an asymmetrical dead zone on joint A actuator, where  $b_{r,1} = 0.04$  and  $b_{l,1} = -0.03$ , The sample time to discrete observer approach was defined as  $T_s = 0.001s$ , the initial value to adaptive dead-zone algorithm was defined as +0.05 to  $b_{r,1}$  and -0.02 to  $b_{l,1}$ , respectively, the adaptive constant gain  $K_{l,i} = K_{r,i} = 0.45$  and initial conditions  $\mathbf{x}(0) = \begin{bmatrix} 0.1 & 0 \end{bmatrix}^T rad$  and  $\dot{\mathbf{x}}(0) = \begin{bmatrix} 0 & 0 \end{bmatrix}^T rad/s$ .

In Fig. 4.31, the time-domain response and closed-loop effort control are depicted with a discrete observer approach. Note that occurs no switching during

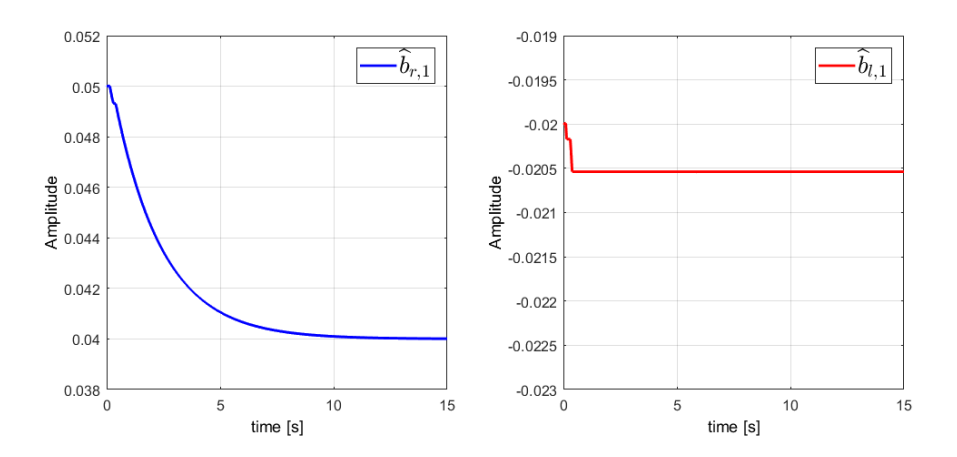


Figure 4.32: Dead-zone estimation parameters under the proposed approach for the system in Test case III.

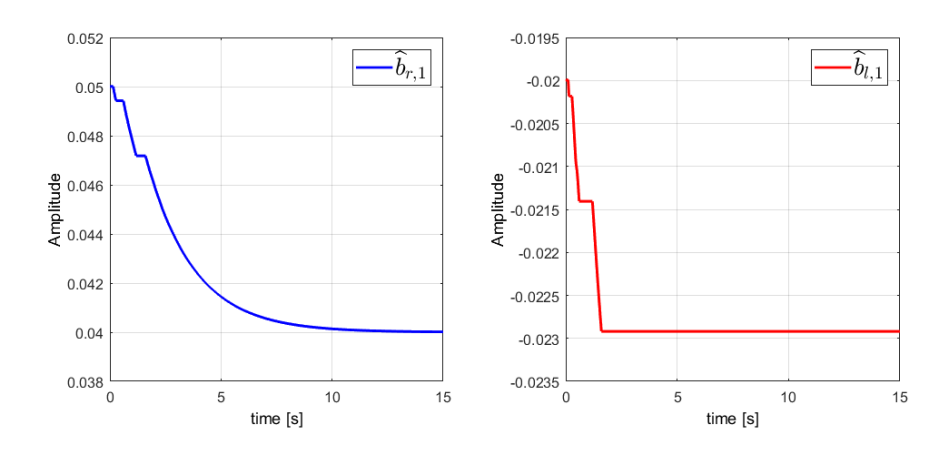


Figure 4.33: Dead-zone estimation parameters under the proposed approach and additive signal for the system in Test case III.

transient at the same time that the discrete observer approach calculates the  $b_{r,1}$  and  $b_{l,1}$  estimated values along the time. In this situation, occurs a polarization in the adaptive structure, which can also be visualized in Fig. 4.32, where  $b_{l,1}$  estimation converges to a value very close to the starting point of the observer, while  $b_{r,1}$  is successfully estimated.

For dealing with polarization, a square wave additive persistent signal is applied, of frequency 1Hz and amplitude of 0.01, at closed-loop control effort signal  $\mathbf{v}_i(t)$ , to establish a switching behavior. In Fig. 4.33 and Fig. 4.34, the dead-zone

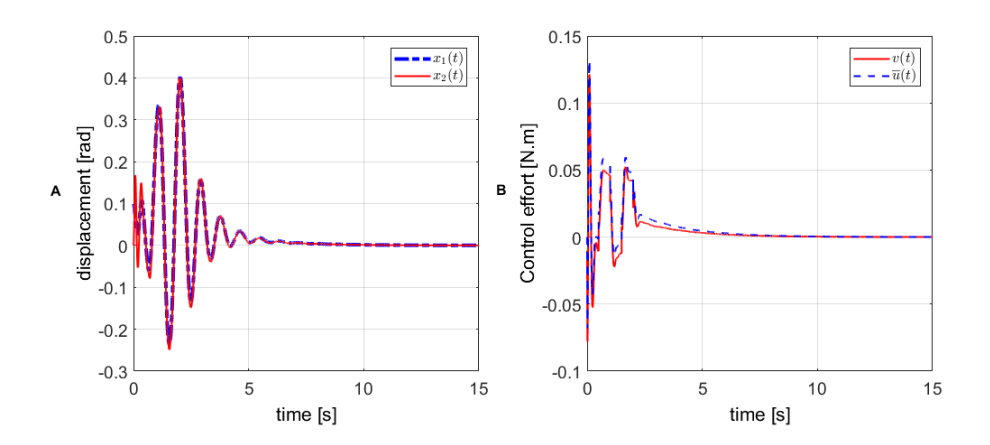


Figure 4.34: Time-domain responses with FSP and UIO discrete observer approach for the system in Test case III: (A) Displacement; (B) Closed-loop control effort.

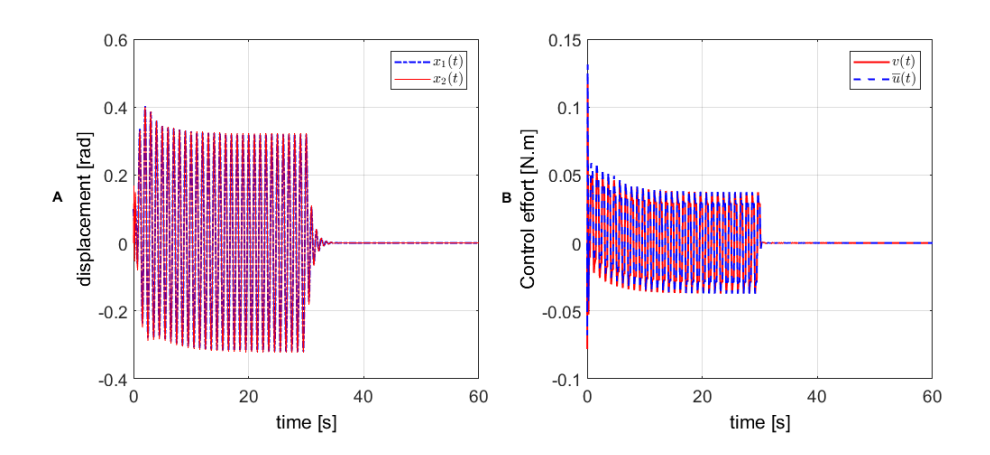


Figure 4.35: Time-domain responses with FSP and UIO discrete observer approach for the system in Test case III: (A) Displacement; (B) Closed-loop control effort.

break-points estimations and time-domain responses for displacement and closed-loop control effort are illustrated, where the additive signal applied for an interval of 2s provides a better estimation to  $b_{l,1}$  parameter, in comparison to Fig. 4.35, without affecting  $b_{r,1}$  estimation. Also, note that additive signal provides switching behavior on state vector  $\xi(t)$  and control effort.

Thus, to improve an accurate estimation of dead-zone break-points, the additive signal is applied for 30s over control effort and then turned off, as depicted

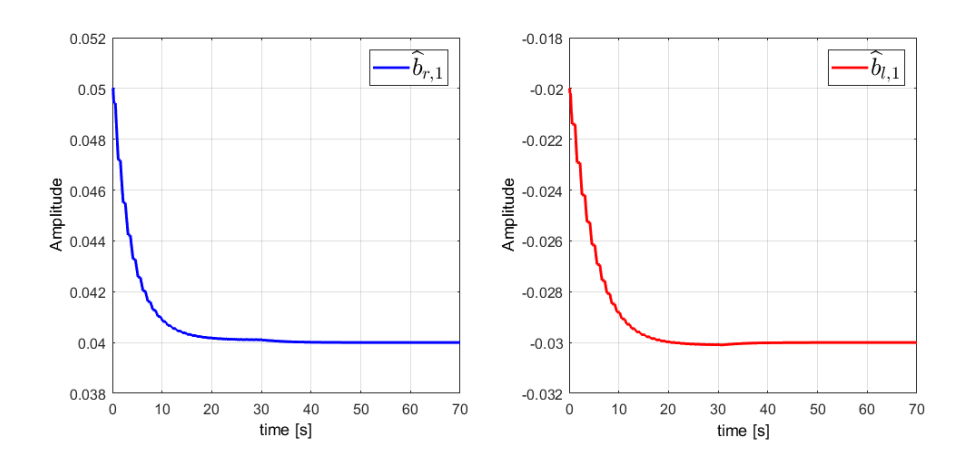


Figure 4.36: Dead-zone estimation parameters under the proposed approach for the system in test case III.

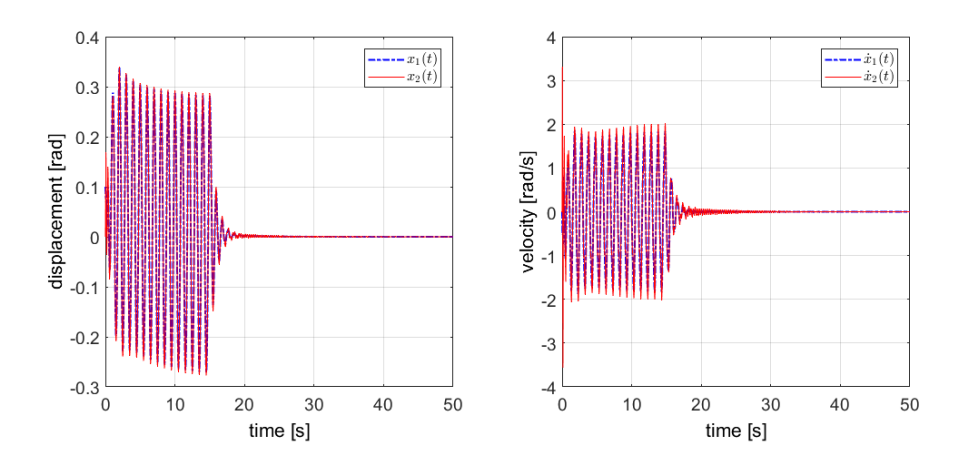


Figure 4.37: Time-domain responses with FSP and UIO discrete observer approach and modeling error for the system in test case III.

in Fig. 4.35, aiming to obtain  $\hat{b}_{r,1} \to b_{r,1}$  and mitigating the dead-zone influence over the system. In Fig. 4.36, the dead-zone break-points estimation is depicted as accurate.

For evaluating the robustness under modeling error, it were considered  $\alpha_M = \alpha_C = \alpha_K = +0.07$  and  $\alpha_r = +0.10$ , such as additive signal was applied for 15s over control effort and then turned off, dealing with polarization and robustness using the proposed approach. The time-domain responses for displacement and velocity are depicted in Fig. 4.37, illustrating that steady-state convergence ob-

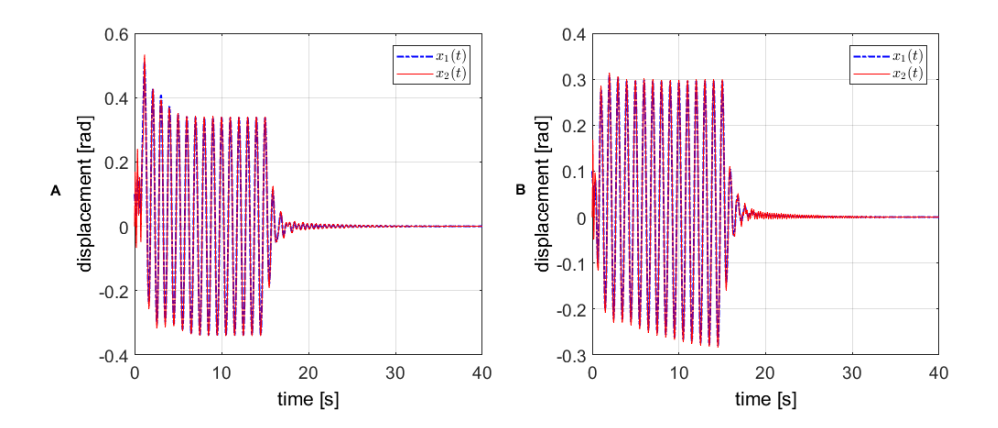


Figure 4.38: Displacement responses with FSP and UIO discrete observer approach and modeling error in the test case III: (A)  $\alpha_M = \alpha_C = \alpha_K = -0.25$  and  $\alpha_r = 0$ ; (B)  $\alpha_M = \alpha_C = \alpha_K = +0.25$  and  $\alpha_r = 0$ ;

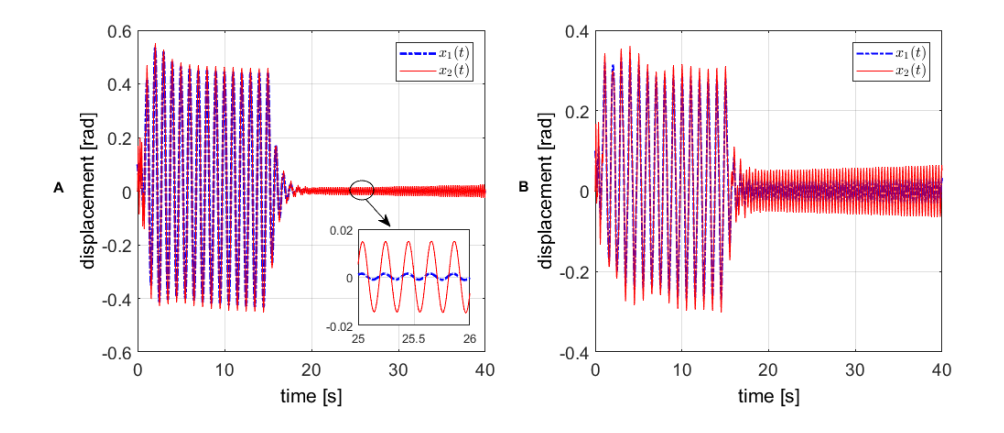


Figure 4.39: Displacement responses with FSP and UIO discrete observer approach and modeling error in the test case III: (A)  $\alpha_M = \alpha_C = \alpha_K = 0.0$  and  $\alpha_r = -0.19$ ; (B)  $\alpha_M = \alpha_C = \alpha_K = +0.0$  and  $\alpha_r = +0.20$ ;

tained is similar to time-domain curves obtained for the absence of modeling error in Fig 4.35(A). Besides, the sensitivity also was evaluated considering the following premises: (i) modeling error relative to time delay ( $\alpha_r = 0$ ) for a limit values of -0.25 and +0.25 for  $\alpha_M$ ,  $\alpha_C$  and  $\alpha_K$ , with the aim of illustrating the modeling error for **M**, **C** and **K** matrices, which the results are illustrated in Fig.4.38; (ii) only the modeling error relative to time delay for  $\alpha_r = -0.19$  and  $\alpha_r = +0.20$  and  $\alpha_M = \alpha_C = \alpha_K = 0.0$ , which the results are illustrated in Fig.4.39. In Fig.4.38, the convergence obtained is similar to time-domain curves obtained for the absence

of modeling error in Fig 4.35(A) and in 4.37 (for displacement time responses). In Fig.4.39, observe that the modeling error limits imposed to the approach can lead to an unstable condition, which in turn can define a sensitivity range for evaluating the robustness for closed-loop stability.

## **4.2.4** Test case IV: the 3-DoF asymmetric system flutter suppression case

In this standard benchmark [58], the system matrices of a 3-DoF model for a wing in an airstream are given as

$$\mathbf{M} = \begin{bmatrix} 17.6 & 1.28 & 2.89 \\ 1.28 & 0.824 & 0.413 \\ 2.89 & 0.413 & 0.725 \end{bmatrix}, \quad \mathbf{C} = \begin{bmatrix} 7.66 & 2.45 & 2.1 \\ 0.23 & 1.04 & 0.223 \\ 0.60 & 0.756 & 0.658 \end{bmatrix},$$

$$\mathbf{K} = \begin{bmatrix} 121 & 18.9 & 15.9 \\ 0 & 2.7 & 0.145 \\ 11.9 & 3.64 & 15.5 \end{bmatrix}, \quad \mathbf{B} = \begin{bmatrix} 1 \\ 0 \\ 0 \end{bmatrix}.$$

where the eigenvalues are  $\lambda_{1,2} = -0.8848 \pm 8.4415i$ ,  $\lambda_{3,4} = 0.0947 \pm 2.5229i$  and  $\lambda_{5,6} = -0.9180 \pm 1.7660i$ , with the second one being unstable, from where it is observed that **C** and **K** matrices contain asymmetrical components. Flutter instability is a relevant issue for aerospace and building engineering and can cause the collapse of flexible structures if not duly treated. Well-known cases of flutter damages are the 1952 Farnborough Airshow crash [63] and (possible) Tacoma Narrows Bridge collapse [64], [65]. The internal delay is  $\tau = 1s$ . A no-spillover design is carried out to reassign this unstable eigenpair to  $\mu_{3,4} = -1 \pm 2.5229i$  and thus suppress flutter vibrations. Also, in this test case, the *Simulink*® default ode45 integration method was applied. The feedback matrices obtained for no spillover design, considering no delay, are

$$\mathbf{F} = \left[ \begin{array}{ccc} -40.025 & -3.9307 & -7.0637 \end{array} \right], \quad \mathbf{G} = \left[ \begin{array}{ccc} -3.8827 & 7.1916 & 0.5330 \end{array} \right].$$

A discrete filtered Smith predictor approach proposed in [6] was designed to deal with delay effects and ensure internal stability. Thus, the FSP filter, in this case, considering sample time  $T_s = 0.1s$  and free filter parameter a = 0.6065, is given by:

$$\phi(z) = \frac{z^3 - 1.273z^2 - 0.6766z + 1.011}{z^3 - 1.82z^2 + 1.104z - 0.2231}$$

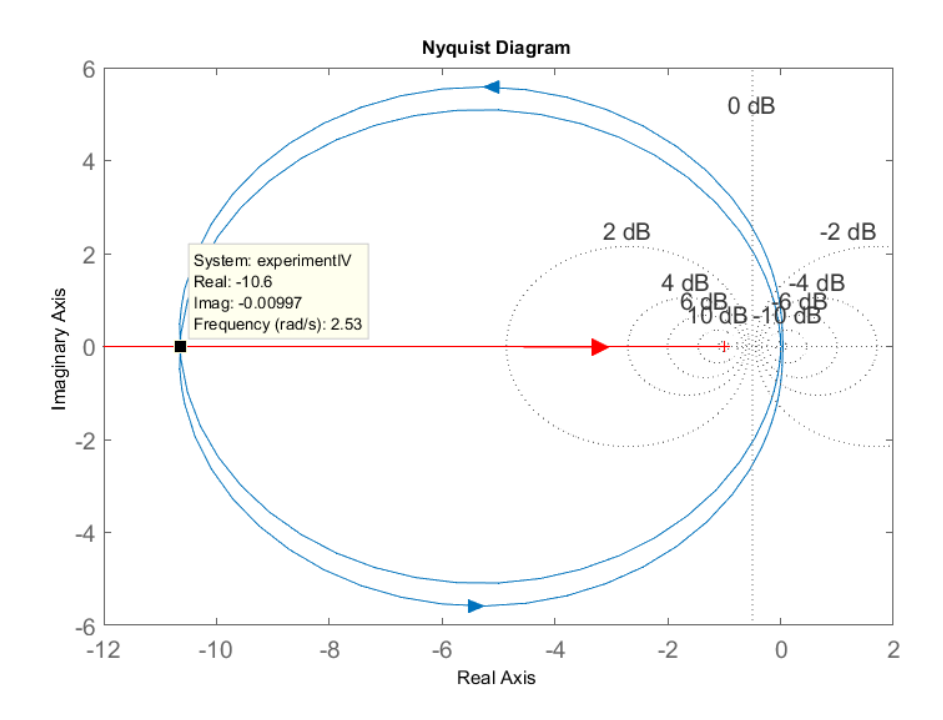


Figure 4.40: Nyquist diagram for the system in Test case IV.

Besides, to evaluate the effects of dead-zone nonlinearity over the system, a symmetrical dead zone is considered, whose break-points are  $b_{r,1} = 0.5$ ,  $b_{l,1} = -0.5$ ,  $\beta = 10^6$ , the adaptive constant gains  $K_{l,i} = K_{r,i} = 0.3$  and initial conditions: (i) for displacement vector:  $x_1(0) = 0.1$  in,  $x_2(0) = 0$  rad and  $x_3(0) = 0$  rad; (ii) for velocity vector:  $\dot{x}_1(0) = 0$  in/s,  $\dot{x}_2(0) = 0$  rad/s and  $\dot{x}_3(0) = 0$  rad/s. The metric units for the effort control is the poundal [pdl].

Based on describing functions method, it is possible to predict the oscillation frequency originating from the dead zone using the Nyquist diagram and consider that, due to the imparity of the dead-zone symmetrical curve, the amplitude of oscillation does not depend on frequency [49], [50], [53]. Thus, in Fig. 4.40, the Nyquist curve of linear part  $\mathbf{L}(s) = [-(s\mathbf{F} + \mathbf{G})\mathbf{H}(s)\mathbf{B}]$  together with the negative reciprocal describing function of dead-zone nonlinearity -1/N(A) is displayed. On the two curves intersection, -1/N(A) curve along into direction of amplitude increasing from instability area to stable area, and the frequency characteristic will make two circles in the positive direction around the point (-1,0). This case is stable based on the Nyquist criterion since the number of turns in the

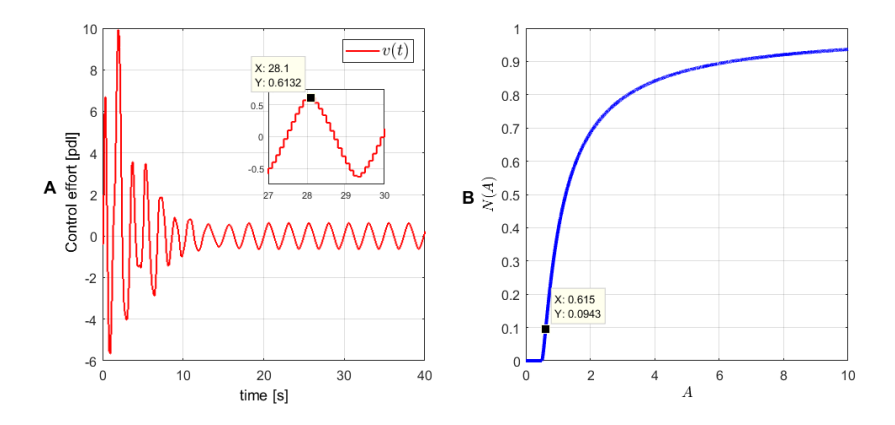


Figure 4.41: Dead-zone amplitude analysis for the Test case IV. (A) Control effort  $\mathbf{v}(t)$ . (B) Describing function dead-zone curve N(A)

positive direction coincides with the number of open-loop unstable poles. Thus, the frequency of system limit cycles oscillation can be obtained at this intersection in Fig. 4.40 and its value is  $\omega_r = 2.53 rad/s$ . Note that oscillation frequency is an important definition, in the sense that the sampling time for discrete observer designing can be defined based on the Nyquist criteria  $2f_s > f_r$ , where  $f_r$  is the oscillation due to dead-zone nonlinearity and  $f_s$  is the sampling frequency, in Hz. For this test case,  $T_s = 0.1s$  fulfills the criteria above and is the same defined value for the discrete FSP approach above. Besides, by the same intersection, is possible for estimating the amplitude relative to the output signal system. Considering that this signal corresponds to the  $\mathbf{v}(t)$  (control effort based on displacement and velocity states signals of receptance-based systems), then, based on the numerical value obtained from its intersection (on the Nyquist diagram, -10.6), N(A) =0.094. By the  $N(A) \times (A)$  plotted, considering that  $b_r = b_l = \delta = 0.5$ , then the estimated amplitude for A is about 0.615, as displayed in Fig.(4.41)B. Note that it is about the same amplitude displayed in Fig.(4.41)A for the  $\mathbf{v}(t)$  signal at steadystate condition. Thus, this method, for the Test case on analysis, gives an accurate result for frequency and amplitude for limit cycles oscillation due to dead-zone influence.

In Figs.4.42 and 4.43,  $\hat{b}_{r,1}$ ,  $\hat{b}_{l,1}$  and the time-domain response are displayed, respectively. Note that, through the discrete FSP approach, is possible to cancel the unstable open-loop modes from disturbance to displacement and velocity,

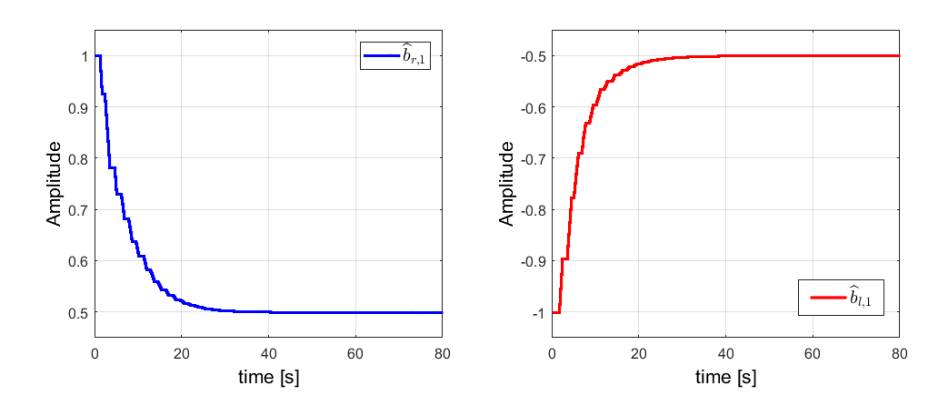


Figure 4.42: Dead-zone estimation parameters under the proposed approach for the system in test case IV.

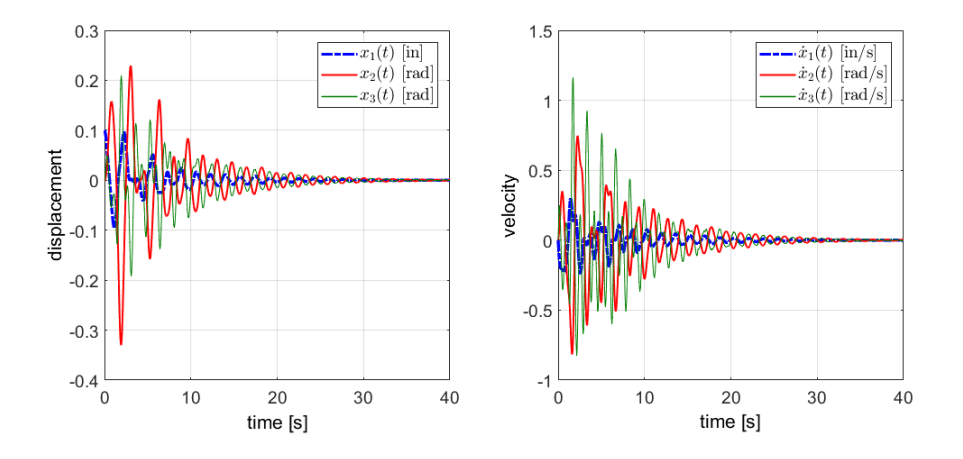


Figure 4.43: Displacement and velocity responses with the proposed approach for the system in test case IV.

obtaining stable predictions for  $\mathbf{X}(s)$  and  $\dot{\mathbf{X}}(s)$  to guarantee internal stability [6]. The discrete observer approach performs very well, as expected, with an accurate estimation for  $b_{r,1}$  and  $b_{l,1}$ , mitigating its effects on time-domain response.

The time-domain responses for displacement and velocity considering a modeling error of 0.08 for  $\alpha_M$ ,  $\alpha_C$ , and  $\alpha_K$  are illustrated in Fig.4.44. The proposed approach has a good robustness margin to allow the convergence of states to the origin even with some modeling error and open-loop unstable poles. This same conclusion is valid for the results obtained for control effort signals  $\mathbf{v}(t)$  and  $\overline{\mathbf{u}}(t)$ , such as the UIO estimation signal  $\omega(t)$  displayed in Fig.4.45. In Fig.4.46 are

illustrated the control effort signals  $\mathbf{v}(t)$  and  $\overline{\mathbf{u}}(t)$ , considering the modeling error only over the  $\mathbf{M}$  matrix, for  $\alpha_M = -0.10$  and  $\alpha_M = +0.20$ , where the proposed approach has a good robustness margin and convergence in steady-state. In Fig.4.47, only the modeling error for  $\mathbf{C}$  matrix was applied, for  $\alpha_C = -0.25$  and  $\alpha_C = +0.25$ , which the displacement time responses converge in a steady-state, in a similar behavior to the velocity time responses depicted in Fig.4.48 for modeling error limits in for  $\mathbf{K}$  matrix ( $\alpha_K = -0.15$  and  $\alpha_K = +0.15$ ).

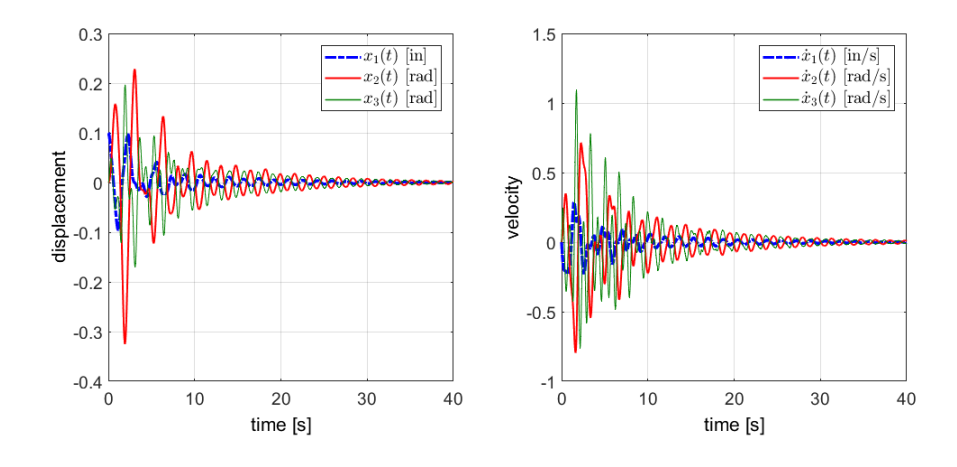


Figure 4.44: Displacement and velocity responses with the proposed approach and modeling error in the test case IV.

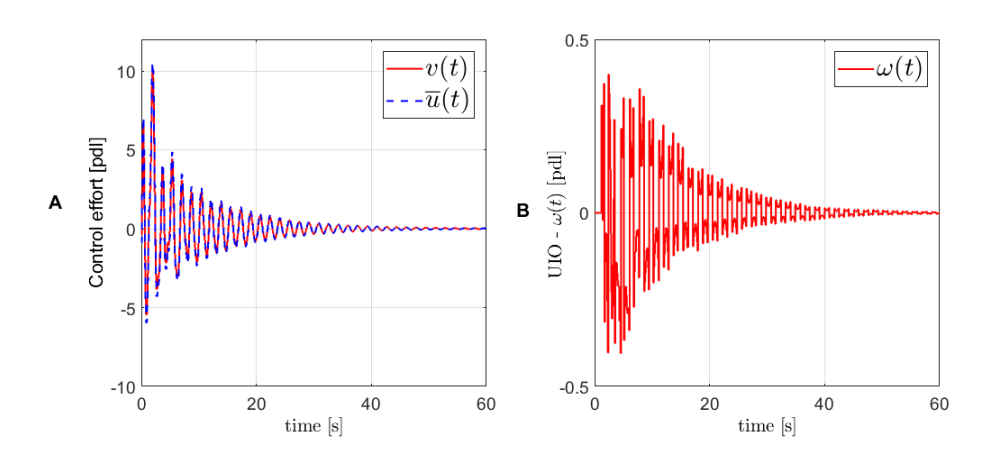


Figure 4.45: Time-domain responses with FSP and UIO discrete observer approach for the system with modeling error in Test case IV: (A) Closed-loop control effort; (B) UIO dead-zone estimation signal.

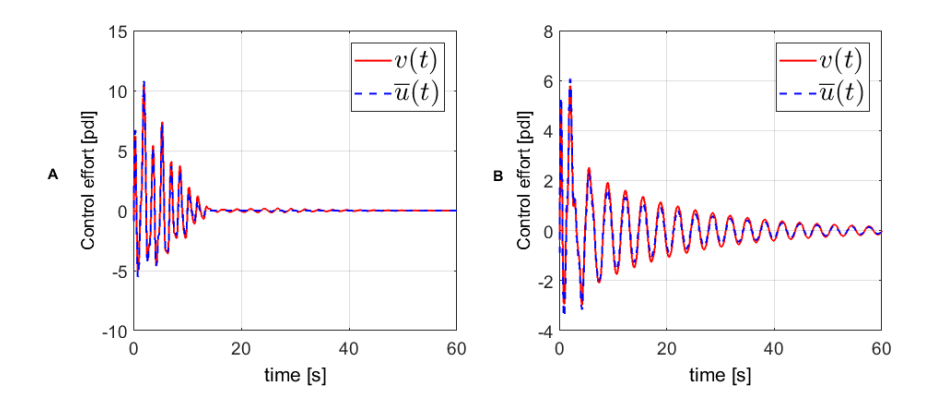


Figure 4.46: Closed-loop control effort responses with FSP and UIO discrete observer approach for the system with modeling error in Test case IV: (A)  $\alpha_M = -0.10$  (B)  $\alpha_M = +0.20$ .

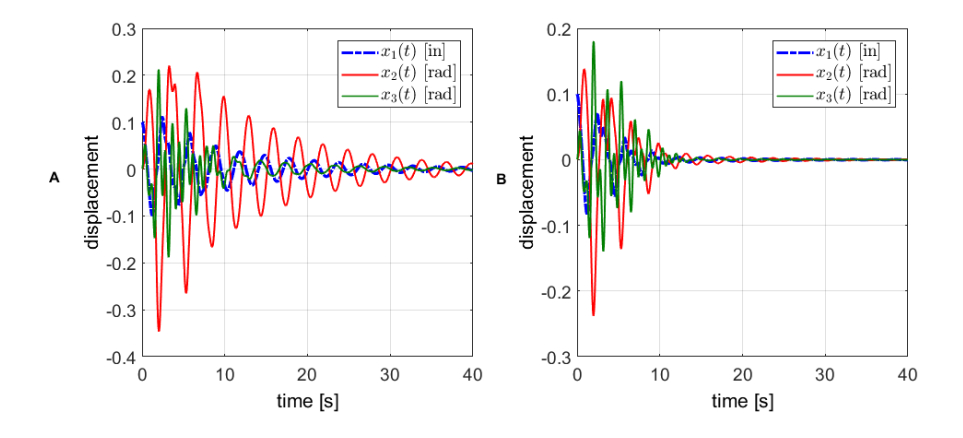


Figure 4.47: Displacement responses with FSP and UIO discrete observer approach for the system with modeling error in Test case IV: (A)  $\alpha_C = -0.25$  (B)  $\alpha_C = +0.25$ .

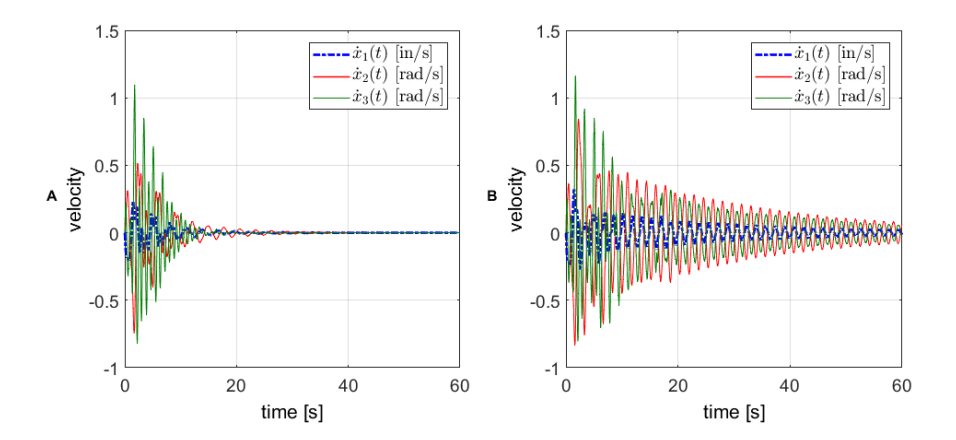


Figure 4.48: Displacement responses with FSP and UIO discrete observer approach for the system with modeling error in Test case IV: (A)  $\alpha_K = -0.15$  (B)  $\alpha_K = +0.15$ .

### **Chapter 5**

## **Concluding remarks and future works**

This dissertation proposed a new approach to tackle dead-zone nonlinearity and time delay for receptance-based second-order systems. The approach brings together two outstanding tools: the filtered Smith predictor and dead-zone compensation strategy, concerning an adaptive mechanism based on discrete state observer to track the unknown asymmetrical dead-zone break-points parameters.

This approach was applied to several examples based on benchmarks from the literature, aiming to illustrate the approach's effectiveness, involving both stable and unstable open-loop poles and multi-input second-order systems. In the Test Case I, the unknown input-output observer approach has been compared with the adaptive schema proposed in [15] with no time delay, with the UIO giving a good estimating for the unknown dead zone, based on state vector  $\xi(t)$  and  $\mathbf{v}(t)$  control signal, both accessible for measuring, which can be considered an advantage in terms of practical applications. Besides, the overall approach was tested under time delay, for several initial guesses for unknown dead zone, under modeling errors, and additive noise for displacement and velocity measurements. The time responses illustrated that the overall approach ran as expected. In Test Case II, the partial pole placement for multiple inputs was applied, where the complete approach was tested for similar conditions as illustrated in Test Case I. The time responses and phase portrait planes illustrated the effectiveness of the proposed schema. For Test Case III, a link-robot arm was tested under time delay and an unknown dead zone, where it was applied a persistent signal on  $\mathbf{v}(t)$  to deal with polarization. Similar to later examples, it illustrated the effectiveness of the

proposed schema. In Test Case IV, based on a system modeled by an asymmetrical receptance matrix that results in unstable poles, the discrete-time FSP was applied to deal with time delay, as proposed in [6]. Describing function method was applied to verify the existence of self-sustained oscillations (by Nyquist diagram) and estimate their amplitude and frequency. The frequency value is essential to determine the sampling time for the discrete observer UIO.

Based on these results, the following contributions could be verified:

- (i) The time-delay influence was mitigated by the continuous and discretetime receptance-based FSP approach, which considers the active vibration control designing of its structure;
- (ii) The proposed dead-zone inverse compensation strategy provided chattering mitigation, and its unknown parameters were dynamically estimated through a discrete-time unknown input observer UIO based on the state vector from the system (displacement and velocity) and the feedback control law signal;
- (*iii*) The BIBO stability was addressed in this thesis, which the approximated dead-zone nonlinear compensation can be described for an equivalent linear bounded signal disturbance can.
- (*iv*) The closed-loop control law can be designed based on a receptance model without delay or dead zone, and the FSP mitigates the effects of the input delay. Uncertain input dead-zone effects were mitigated by UIO adaptive schema.

Any receptance-based design strategy for delay-free models can be used for second-order systems with input delay and an uncertain dead zone.

Based on this thesis, two technical papers were written:

 André Juarez Jaime Duarte, Tito Luís Maia Santos, José Mário Araújo, Preditor de Smith Baseado em Receptâncias para Sistemas de Segunda Ordem com Atraso e Compensação de Zona Morta, Proceedings of SBAI 2021, doi: 10.20906/sbai.v1i1.2569. André Juarez Jaime Duarte, Tito Luís Maia Santos, José Mário Araújo, A receptance-based vibration control with dead-zone compensation for systems with input delay, Mechanical Systems and Signal Processing, Accepted May 9, 2022.

For future works, based on the proposed approach for receptance-based systems for continuous and discrete-time representations, some suggestions can be summarized:

- (i) Extend the analysis and design of adaptive scheme for inclusion and adaptive estimating of other nonlinearities together with dead zone, such as asymmetric saturation and backslash, commonly found in mechanical systems.
- (*ii*) Extend the adaptive method for time-variant dead-zone nonlinearity, where the unknown parameters will vary over time, analyzing the adaptive mechanism performance for parametric variations.
- (*iii*) Extend the analysis for a time-variant delay at the system's input, considering the filtered Smith predictor for dealing with time delay, where the stability and convergence criteria, considering the influence of adaptive schema on closed-loop control, could be detailed.
- (*iv*) For the overall approach, emphasizing the adaptive schema, the treatment for disturbance rejection at the system's input in closed-loop control aims to minimize its effect.

#### **Bibliography**

- [1] D. Lisitano, S. Jiffri, E. Bonisoli, and J. E. Mottershead, "Experimental feedback linearisation of a non-smooth nonlinear system by the method of receptances," *Mathematics and Mechanics of Solids*, vol. 24, no. 2, pp. 465–482, Jan. 2018.
- [2] J. M. Araújo, J. Bettega, N. J. B. Dantas, C. E. T. Dórea, D. Richiedei, and I. Tamellin, "Vibration control of a two-link flexible robot arm with time delay through the robust receptance method," *Applied Sciences*, vol. 11, no. 21, p. 9907, 2021.
- [3] J. E. Mottershead and Y. M. Ram, "Receptance method in active vibration control," *AIAA Journal*, vol. 45, no. 3, pp. 562–567, Mar. 2007.
- [4] —, "Inverse eigenvalue problems in vibration absorption: Passive modification and active control," *Mechanical Systems and Signal Processing*, vol. 20, no. 1, pp. 5–44, 2006.
- [5] J. M. Araújo and T. L. M. Santos, "Control of a class of second-order linear vibrating systems with time-delay: Smith predictor approach," *Mechanical Systems and Signal Processing*, vol. 108, pp. 173–187, 2018.
- [6] J. M. Araujo and T. L. Santos, "Control of second-order asymmetric systems with time delay: Smith predictor approach," *Mechanical Systems and Signal Processing*, vol. 137, p. 106 355, 2020.
- [7] Y. Ram and J. Mottershead, "Multiple-input active vibration control by partial pole placement using the method of receptances," *Mechanical Systems and Signal Processing*, vol. 40, no. 2, pp. 727–735, Nov. 2013.
- [8] J. M. Araújo, "Discussion on 'state feedback control with time delay'," *Mechanical Systems and Signal Processing*, vol. 98, pp. 368–370, 2018.
- [9] Z. Palmor, "Time delay compensation smith predictor and its modifications," in *The Control handbook*, W. S. Levine, Ed., 1st ed., Boca Raton, Fl. New York, NY: CRC Press IEEE Press, 1996, pp. 224–237.
- [10] L. Mirkin and Z. J. Palmor, "Control issues in systems with loop delays," in *Handbook of Networked and Embedded Control Systems*, D. Hristu-Varsakelis, Ed., 1st ed., Birkhäuser Boston, 2005, pp. 627–648.
- [11] O. Smith, "Closer control of loops with dead time," *Chemistry Engineering Progress*, vol. 53, no. 5, pp. 217–219, 1957.

- [12] J. Normey-Rico, C. Bordons, and E. Camacho, "Improving the robustness of dead-time compensating PI controllers," *Control Engineering Practice*, vol. 5, no. 6, pp. 801–810, 1997.
- [13] J. E. Normey-Rico and E. F. Camacho, *Control of Dead-time Processes*, 1st. Springer London, 2007, ISBN: 978-1-84628-829-6.
- [14] D. M. Lima, T. L. M. Santos, and J. E. Normey-Rico, "Robust nonlinear predictor for dead-time systems with input nonlinearities," *Journal of Process Control*, vol. 27, pp. 1–14, 2015.
- [15] E.-W. Bai, "Adaptive dead zone inverses for possibly nonlinear control systems," in *Adaptive Control of Nonsmooth Dynamic Systems*, G. Tao and F. L. Lewis, Eds., 1st ed., Springer-Verlag London Ltd., 2001, pp. 31–47.
- [16] C.-C. Hsu and I.-K. Fong, "Ultimate boundedness control of linear systems with band-bounded nonlinear actuators and additive measurement noise," *Systems and Control Letters*, vol. 43, no. 5, pp. 329–336, 2001.
- [17] Y. Zhang, C. Hua, and J. Qian, "Adaptive robust visual servoing/force control for robot manipulator with dead-zone input," *IEEE Access*, vol. 7, pp. 129 627–129 636, 2019.
- [18] P. Liu, Y. Song, P. Yan, and Y. Sun, "Actuator saturation compensation for fast tool servo systems with time delays," *IEEE Access*, vol. 9, pp. 6633–6641, 2021.
- [19] V. Dilda, M. Jungers, and E. B. Castelan, "Uniform ultimate boundedness analysis and synthesis for linear systems with dead-zone in the actuators," *International Journal of Robust and Nonlinear Control*, vol. 25, no. 14, pp. 2502–2514, 2014.
- [20] A. Mannarino, "An adaptive compensation strategy of control surfaces free-play," in AIAA Guidance, Navigation, and Control Conference, 2015, pp. 1–20
- [21] G. Tao and P. Kokotovic, "Discrete-time adaptive control of plants with unknown output dead-zones," *Automatica*, vol. 31, no. 2, pp. 287–291, 1995.
- [22] —, "Adaptive control of plants with unknown dead-zones," *IEEE Transactions on Automatic Control*, vol. 39, no. 1, pp. 59–68, 1994.
- [23] Z. Zhang, J. H. Park, K. Zhang, and J. Lu, "Adaptive control for a class of nonlinear time-delay systems with dead-zone input," *Journal of The Frankiln Institute*, vol. 353, no. 17, pp. 4400–4421, 2016.
- [24] Z. Zhang, S. Xu, and B. Zhang, "Exact tracking control of nonlinear systems with time delays and dead-zone input," *Automatica*, vol. 52, pp. 272–276, Feb. 2015.

- [25] J. Zhang, J. Ye, and H. Ouyang, "Static output feedback for partial eigenstructure assignment of undamped vibration systems," *Mechanical Systems and Signal Processing*, vol. 68-69, no. Complete, pp. 555–561, 2016.
- [26] K. He, C. Dong, and Q. Wang, "Active disturbance rejection adaptive control for uncertain nonlinear systems with unknown time-varying dead-zone input," *Asian J Control*, pp. 1–14, 2021.
- [27] D. X. Phu and V. Mien, "Robust control for vibration control systems with dead-zone band and time delay under severe disturbance using adaptive fuzzy neural network," *Journal of the Franklin Institute*, vol. 357, no. 17, pp. 12281–12307, Nov. 2020.
- [28] H. Wu, "Robust output tracking of uncertain nonlinear systems with completely unknown dead-zone input: A self-tuning design approach," *International Journal of Adaptive Control and Signal Processing*, vol. 30, no. 11, pp. 1627–1642, 2016.
- [29] Y. Liang, H. J. Ouyang, and H. Yamaura, "Active partial eigenvalue assignment for friction-induced vibration using receptance method," *Journal of Physics: Conference Series*, vol. 744, no. 1, p. 012 008, 2016.
- [30] H. Ouyang, D. Richiedei, and A. Trevisani, "Pole assignment for control of flexible link mechanisms," *Journal of Sound and Vibration*, vol. 332, no. 12, pp. 2884–2899, 2013.
- [31] Y. Ram, A. Singh, and J. E. Mottershead, "State feedback control with time delay," *Mechanical Systems and Signal Processing*, vol. 23, no. 6, pp. 1940–1945, 2009.
- [32] Y. Ram, J. Mottershead, and M. Tehrani, "Partial pole placement with time delay in structures using the receptance and the system matrices," *Linear Algebra and Its Applications*, vol. 434, no. 7, pp. 1689–1696, 2011.
- [33] M. G. Tehrani, R. N. Elliott, and J. E. Mottershead, "Partial pole placement in structures by the method of receptances: Theory and experiments," *Journal of Sound and Vibration*, vol. 329, no. 24, pp. 5017–5035, 2010.
- [34] J. Xiang, C. Zhen, and D. Li, "Partial pole assignment with time delay by the receptance method using multi-input control from measurement output feedback," *Mechanical Systems and Signal Processing*, vol. 66-67, no. Supplement C, pp. 743–755, 2016.
- [35] H. Ouyang, "Pole assignment of friction-induced vibration for stabilisation through state-feedback control," *Journal of Sound and Vibration*, vol. 329, no. 11, pp. 1985–1991, 2010.
- [36] K. V. Singh and H. Ouyang, "Pole assignment using state feedback with time delay in friction-induced vibration problems," *Acta Mechanica*, vol. 224, no. 3, pp. 645–656, 2013.

- [37] C. Zhen, S. Jiffri, D. Li, J. Xiang, and J. E. Mottershead, "Feedback linearisation of nonlinear vibration problems: A new formulation by the method of receptances," *Mechanical Systems and Signal Processing*, vol. 98, pp. 1056–1068, 2018.
- [38] M. G. Tehrani, L. Wilmshurst, and S. J. Elliott, "Receptance method for active vibration control of a nonlinear system," *Journal of Sound and Vibration*, vol. 332, no. 19, pp. 4440–4449, 2013.
- [39] D. Lisitano, S. Jiffri, E. Bonisoli, and J. Mottershead, "Experimental feedback linearisation of a vibrating system with a non-smooth nonlinearity," *Journal of Sound and Vibration*, vol. 416, pp. 192–212, Mar. 2018.
- [40] H. Xie, "A receptance method for robust and minimum norm partial quadratic eigenvalue assignment," *Mechanical Systems and Signal Processing*, vol. 160, p. 107 838, 2021.
- [41] Y. Liang, H. Yamaura, and H. Ouyang, "Active assignment of eigenvalues and eigen-sensitivities for robust stabilization of friction-induced vibration," *Mechanical Systems and Signal Processing*, vol. 90, pp. 254–267, 2017.
- [42] J. M. Araújo, C. E. T. Dórea, L. M. G. Gonçalves, J. B. P. Carvalho, and B. N. Datta, "Robustness of the quadratic partial eigenvalue assignment using spectrum sensitivities for state and derivative feedback designs," *Journal of Low Frequency Noise, Vibration & Active Control*, vol. 37, no. 2, pp. 253–268, 2018.
- [43] R. M. Saback, A. G. S. Conceicao, T. L. M. Santos, J. Albiez, and M. Reis, "Nonlinear model predictive control applied to an autonomous underwater vehicle," *IEEE Journal of Oceanic Engineering*, vol. 45, no. 3, pp. 799–812, 2020.
- [44] D. M. Lima, J. E. Normey-Rico, and T. L. M. Santos, "Temperature control in a solar collector field using filtered dynamic matrix control," *ISA Transactions*, vol. 62, pp. 39–49, 2016.
- [45] B. C. Torrico, R. D. Pereira, A. K. Sombra, and F. G. Nogueira, "Simplified filtered smith predictor for high-order dead-time processes," *ISA Transactions*, vol. 109, pp. 11–21, 2021.
- [46] R. Haruyama, R. Tanaka, and Y. Ishida, "Simplified design method of a filtered smith predictor for unstable and integrative plants with dead-time," in *TENCON 2016 2016 IEEE Region 10 Conference*, IEEE, 2016, pp. 3402–3405.
- [47] C.-Y. Kao and B. Lincoln, "Simple stability criteria for systems with time-varying delays," *Automatica*, vol. 40, no. 8, pp. 1429–1434, 2004.

- [48] T. L. Santos, P. E. Botura, and J. E. Normey-Rico, "Dealing with noise in unstable dead-time process control," *Journal of Process Control*, vol. 20, no. 7, pp. 840–847, 2010.
- [49] A. Gelb and W. E. V. Velde, *Multiple-Input Describing Functions and Non-linear System Design*, 1st. New York: McGraw Hill, 1968.
- [50] J.-J. E. Slotine and W. Li, *Applied Nonlinear Control*. Prentice Hall, New Jersey, 1991.
- [51] A. R. Bergen and R. L. Franks, "Justification of the describing function method," *SIAM Journal on Control*, vol. 9, no. 4, pp. 568–589, 1971.
- [52] M. B. Özer, H. N. Özgüven, and T. J. Royston, "Identification of structural non-linearities using describing functions and the sherman–morrison method," *Mechanical Systems and Signal Processing*, vol. 23, no. 1, pp. 30–44, 2009.
- [53] X. Wei and J. E. Mottershead, "Limit cycle assignment in nonlinear aeroelastic systems using describing functions and the receptance method," in *Topics in Modal Analysis, Volume 7*, Springer New York, 2013, pp. 701–713.
- [54] H. Khalil, *Nonlinear systems*. Upper Saddle River, New Jersey: Prentice Hall, 2002.
- [55] W. M. Bessa, M. S. Dutra, and E. Kreuzer, "Sliding mode control with adaptive fuzzy dead-zone compensation of an electro-hydraulic servo-system," *J Intell Robot Syst*, vol. 58, no. 1, pp. 3–16, 2009.
- [56] Z. Yang and H. Zhang, "A fuzzy adaptive tracking control for a class of uncertain strick-feedback nonlinear systems with dead-zone input," *Neuro-computing*, vol. 272, pp. 130–135, 2018.
- [57] Y. Ram, A. Singh, and J. E. Mottershead, "State feedback control with time delay," *Mechanical Systems and Signal Processing*, vol. 23, no. 6, pp. 1940–1945, 2009, Special Issue: Inverse Problems.
- [58] A. R. Collar, "The second lanchester memorial lecture: Aeroelasticity—retrospect and prospect," *Journal of the Royal Aeronautical Society*, vol. 63, pp. 1–15, 1959.
- [59] R. Ariyatanapol, Y. Xiong, and H. Ouyang, "Partial pole assignment with time delays for asymmetric systems," *Acta Mechanica*, vol. 229, no. 6, pp. 2619–2629, 2018.
- [60] C. Fuller, "Active vibration control," in *Handbook of Noise and Vibration Control*. John Wiley & Sons, Ltd, 2008, ch. 64, pp. 770–784.
- [61] M. G. Tehrani and J. Mottershead, "An overview of the receptance method in active vibration control," *IFAC Proceedings Volumes*, vol. 45, no. 2, pp. 1174–1178, 2012.

- [62] D. Richiedei and A. Trevisani, "Simultaneous active and passive control for eigenstructure assignment in lightly damped systems," *Mechanical Systems and Signal Processing*, vol. 85, pp. 556–566, Feb. 2017.
- [63] F. P. Miller, A. F. Vandome, and J. McBrewster, *1952 Farnborough Airshow Dh.110 Crash*. Alphascript Publishing, Nov. 2010.
- [64] R. Plaut, "Snap loads and torsional oscillations of the original tacoma narrows bridge," *Journal of Sound and Vibration*, vol. 309, no. 3–5, pp. 613–636, 2008.
- [65] G. Arioli and F. Gazzola, "A new mathematical explanation of what triggered the catastrophic torsional mode of the tacoma narrows bridge," *Applied Mathematical Modelling*, vol. 39, no. 2, pp. 901–912, 2015.

#### Appendix A

#### **Describing function representation**

To represent a nonlinear component by a describing function, consider a sinusoidal input  $\hat{\mathbf{u}}(t) = Asin(\omega t)$ , amplitude A and frequency  $\omega$  and its output signal  $\overline{\mathbf{u}}(t)$ , represented by its Fourier representation:

$$\overline{\mathbf{u}}(t) = \frac{a_0}{2} + \sum_{n=1}^{\infty} \left[ a_n cos(n\omega t) \right] + \left[ b_n sin(n\omega t) \right]$$
(A.1)

where the Fourier coefficients are usually functions of  $A \in \omega$ , given by:

$$a_0 = \frac{1}{\pi} \int_{-\pi}^{\pi} \gamma(t) d(\omega t) \tag{A.2}$$

$$a_n = \frac{1}{\pi} \int_{-\pi}^{\pi} \widehat{\mathbf{u}}(t) cos(n\omega t) d(\omega t)$$
 (A.3)

$$b_n = \frac{1}{\pi} \int_{-\pi}^{\pi} \widehat{\mathbf{u}}(t) \sin(n\omega t) d(\omega t)$$
 (A.4)

Due to imparity property, that implies in  $a_0 = 0$ , and considering that only the fundamental Fourier component is considered,  $\hat{\mathbf{u}}(t)$  is given by:

$$\overline{\mathbf{u}}(t) = \overline{\mathbf{u}}_1(t) \approx a_1 cos(\omega t) + b_1 sin(\omega t) = M sin(\omega t + \phi)$$
 (A.5)

where:

$$M(A, \omega) = \sqrt{a_1^2 + b_1^2}, \quad \phi(A, \omega) = \arctan(\frac{a_1}{b_1})$$
 (A.6)

and, in complex representation:

$$\overline{\mathbf{u}}_1(t) = Me^{i(\omega t + \phi)} = (b_1 + ia_1)e^{i\omega t}$$
(A.7)

Similarly to the concept of frequency response function, which is the frequency domain ratio of the sinusoidal input and the sinusoidal output of a system, the describing function of the nonlinear element is defined by complex ratio of the fundamental component of the nonlinear element by the sinusoidal input:

$$N(A, \mathbf{\omega}) = \frac{Me^{i(\mathbf{\omega}t + \mathbf{\phi})}}{Ae^{j\mathbf{\omega}t}} = \frac{1}{A}(b_1 + ia_1)$$
 (A.8)

Thus, with a describing function representing the nonlinear component, the nonlinear element, in the presence of sinusoidal input, can be treated as if it were a linear element with a frequency response function  $N(A, \omega)$ .

### Appendix B

# Continuous and discrete-time FSP filters design

In this appendix, the filter design for filtered Smith predictor, considering continuous [5] and discrete time [6] representations, will be explained.

#### **B.1** Continuous-time FSP filter design

The low-pass filter considered for continuous-time FSP approach, is given by:

$$\phi(s) = \frac{1 + a_1 s + a_2 s^2 + \dots + a_k s^k}{(\tau_f s + 1)^{k+1}}$$
(B.1)

where: (i)  $\tau_f > 0$  is a free tuning parameter; (ii)  $a_l$ , l = 1, ..., k are defined in order to guarantee  $[1 - \phi(s)e^{-s\tau}]|_{s=j\omega_i} = 0$ ; (iii) i = 1, ..., v, v is the total number of undesirable resonance peaks, avoiding high frequency noise amplification. The main tuning condition for FSP is defined by:

$$1 + a_1 s + a_2 s^2 + \ldots + a_k s^k|_{s=j\omega_i} = (\tau_f s + 1)^{k+1} e^{s\tau}|_{s=j\omega_i}$$
 (B.2)

For a given  $\tau_f$ , note that  $(\tau_f s + 1)^{k+1} e^{s\tau}|_{s=j\omega_i}$  can be decomposed into real and imaginary parts:

$$\sigma_1 = Re(j\tau_f \omega_1 + 1)^{k+1} e^{j\omega_i \tau}$$
(B.3)

$$\beta_1 = Imag(j\tau_f \omega_1 + 1)^{k+1} e^{j\omega_i \tau}$$
 (B.4)

and

$$(\tau_f s + 1)^{k+1} e^{s\tau}|_{s=j\omega_i} = \sigma_i + j\beta_i$$
(B.5)

Based on equation above, is possible to define the following set of linear equations:

$$\begin{bmatrix} \omega_{1} & 0 & -\omega_{1}^{3} & 0 & \dots \\ 0 & -\omega_{1}^{2} & 0 & -\omega_{1}^{4} & \dots \\ \vdots & \vdots & \vdots & \vdots & \vdots \\ \omega_{v} & 0 & -\omega_{v}^{3} & 0 & \dots \\ 0 & -\omega_{v}^{2} & 0 & -\omega_{v}^{4} & \dots \end{bmatrix} \begin{bmatrix} a_{1} \\ a_{2} \\ a_{3} \\ a_{4} \\ \vdots \\ a_{k-1} \\ a_{k} \end{bmatrix} = \begin{bmatrix} \beta_{1} \\ \sigma_{1} - 1 \\ \beta_{2} \\ \sigma_{2} - 1 \\ \vdots \\ \beta_{v} \\ \sigma_{v} - 1 \end{bmatrix}$$
(B.6)

where the  $2\nu \times k$  matrix on the left-nad side of Eq.(B.6) has  $2\nu$  independent rows if  $\omega_i = \omega_l$ ,  $\forall i \neq l$  and  $k = 2\nu$ .

#### **B.2** Discrete-time FSP filter design

In a similar way for continuous-time prediction error filter design, the filter structure for digital implementation is given by:

$$\phi(z) = \frac{z^m + b_1 z^{m-1} + \dots + b_{m-1} z + b_m}{(z - a^m)}$$
(B.7)

where the free parameter a, 0 < a < 1, is used to tuning the trade-off between transient performance and robustness. For preservation of the steady-state characteristics in the presence of constant disturbances. Thus, applying the constraint  $\lim_{z\to 1} \phi(z) = 1$ :

$$b_1 + \ldots + b_{m-1} + b_m = (1-a)^m$$
 (B.8)

If the system have a set of l unstable poles  $p_1, \ldots, p_l$  to be cancelled, then the following identities must to be matched for  $k = 1, \ldots, l$ :

$$[1 - z^{-\ell}\phi(z)]|_{z=p_k} = 0$$
(B.9)

$$[b_1 p_k^{m-1} + \ldots + b_{m-1} p_k + b_m = p_k^{\ell} (p_k - a)^m$$
 (B.10)

Then, combining the Eq.(B.8), Eq.(B.9) and Eq.(B.10), the linear equations to define the  $b_1, \ldots, b_m$  coefficients of the filter is given by:

$$\begin{bmatrix} 1 & \dots & 1 & 1 \\ p_1^{m-1} & \dots & p_1 & 1 \\ \vdots & \ddots & \vdots & \vdots \\ p_l^{m-1} & 0 & p_l & 1 \end{bmatrix} \begin{bmatrix} b_1 \\ \vdots \\ b_{m-1} \\ b_m \end{bmatrix} = \begin{bmatrix} (1-a)^m - 1 \\ p_1^{\ell}(p_1 - a)^m - p_1^m \\ \vdots \\ p_l^{\ell}(p_l - a)^m - p_l^m \end{bmatrix}$$
(B.11)

where m = l + 1 is the order that gives an unique solution for the equation above.

### **Appendix C**

#### **UIO** convergence analysis

Consider the nominal problem without disturbance and assume that  $\beta$  is sufficiently high such that  $\mathbf{q}(t)$  is negligible. In this case,  $\mathbf{\omega}[k-d-1]$  is defined such that

$$\omega_{i}[k-d-1] = \rho(\gamma(v_{i}[k-d-1])) - v_{i}[k-d-1] 
= \rho(sat_{i}(\beta v_{i}[k-d-1]) + v_{i}[k-d-1]) - \mathbf{v}[k-d-1].(C.1)$$

Hence, if  $v_i[k-d-1] > 0$ , then

$$\omega_i[k-d-1] = \hat{b}_{r,i}[k-d-1] - b_{r,i}, \tag{C.2}$$

where  $b_{r,i}$  comes from the dead-zone and  $\hat{b}_{r,i}[k]$  is the expected compensation. Moreover, if  $v_i[k-d-1] < 0$ , then

$$\omega_i[k-d-1] = -\hat{b}_{l,i}[k-d-1] + b_{l,i}.$$
 (C.3)

Now, for notation simplicity, consider  $\theta_{r,i}[k] = \hat{b}_{r,i}[k]$  and  $\theta_{l,i}[k] = -\hat{b}_{l,i}[k]$ . Notice that both  $\theta_{r,i}[k]$  and  $\theta_{l,i}[k]$  can be classified into adaptation instant and non-adaptation instants. If k is an adaptation instant for  $\hat{b}_{r,i}[k]$ , then

$$\theta_{r,i}[k] = \theta_{r,i}[k-1] - K_{r,i}T_s(\theta_{r,i}[k-d-1] - b_{r,i}).$$
 (C.4)

Obviously,  $\theta_{r,i}[k] = \theta_{r,i}[k-1]$  whenever k is not an adaptation instant. With respect to the adaptation of  $\theta_{l,i}[k] = -\hat{b}_{l,i}[k]$ 

$$\theta_{l,i}[k] = \theta_{l,i}[k-1] - K_{l,i}T_s(\theta_{l,i}[k-d-1] - b_{r,i}). \tag{C.5}$$

The convergence analysis of  $\theta_{r,i}[k]$  (or  $\theta_{l,i}[k]$ ) with respect to  $K_{r,i}$  (or  $K_{l,i}$ ) is not so direct because the adaptation is not regularly performed. In this case, linear

time-invariant results do not hold. However, this analysis can be simplified considering the convergence of the envelope of the evolution which means that the non-adaptation instants are neglected from the convergence analysis.

The analysis of the envelope departs from the fact that  $\theta_{r,i}[k-1] = \theta_{r,i}[k-2]$ = .... =  $\theta_{r,i}[k-\check{d}_{r,i}[k]]$ . Now, assume without loss of generality that  $\check{d}_{r,i}[k] \leq d+1$ .

Then, the adaptation law can be shifted as follows

$$\theta_{r,i}[k] = \theta_{r,i}[k - \check{d}_{r,i}[k]] - K_{r,i}T_s(\theta_{r,i}[k - d - 1] - b_{r,i}). \tag{C.6}$$

To complete the convergence analysis with the small-gain theorem, consider that  $\eta_i[k-1] = \theta_{r,i}[k-\check{d}_{r,i}[k]] - \theta_{r,i}[k-1]$  and  $b_{r,i} = 0$  due to the superposition principle as follows

$$\theta_{r,i}[k] = \theta_{r,i}[k-1] - K_{r,i}T_s\theta_{r,i}[k-d-1] + \eta_i[k-1]. \tag{C.7}$$

The transfer function from  $\eta_i[k]$  to  $\theta_{r,i}[k]$  is defined for each i=1,2,...,m by  $\mathcal{P}_{r,i}(z)=\frac{z^{-1}}{1-z^{-1}+K_{r,i}T_sz^{-d-1}}$ . Finally, the envelope of  $\theta_{r,i}[k]$  is bounded if  $K_{r,i}$  is defined such that  $\mathcal{P}_{r,i}(z)$  is a stable transfer function and the following norm condition is respected  $||\mathcal{P}_{r,i}(z)(1-z^{-1})||_{\infty}d<1$  as discussed in [47]. The same result holds for  $\mathcal{P}_{l,i}(z)=\frac{z^{-1}}{1-z^{-1}+K_{l,i}T_sz^{-d-1}}$  where  $K_{l,i}$  should be defined such that  $\mathcal{P}_{l,i}(z)$  is a stable transfer function and  $||\mathcal{P}_{l,i}(z)(1-z^{-1})||_{\infty}d<1$ .

It should be remarked that this is a sufficient condition that guarantees BIBO stability of the envelope of  $\theta_{r,i}[k]$  and  $\theta_{l,i}[k]$  convergence is achieved due to the integral action in the nominal case in the presence of a persistent transient. Anyway, this type of sufficient condition may be significantly conservative because arbitrarily fast time-varying delays can be considered. In practice, convergence is verified even if the small-gain criterion is not respected.

If  $\check{d}_{r,i}[k] > d+1$ , the same result holds with  $\theta_{r,i}[k-1] = \theta_{r,i}[k-d-1]$ .